AN ABSTRACT OF THE THESIS OF

Daniela Zima for the degree of Master of Science in Oceanography presented on November 29, 2006

Title: Reconstructing Salinity Conditions in Nares Strait (Canadian Archipelago) from Stable Isotope Profiles in Bivalve Shells

Abstract approved:_____
Marta E. Torres, Kelly K. Falkner

Nares Strait is one of three main passages of the Canadian Archipelago that channels freshwater from the Arctic Ocean to the North Atlantic. There are very few observations regarding the role of this region on the present day Arctic freshwater budget, and even less regarding the changes in freshwater fluxes through time. Larger scale Arctic Ocean circulation features have recently been observed to shift. Such changes will likely be manifest in Nares Strait before propagating into Baffin Bay and Labrador Sea. The $\delta^{18}O$ of the water in Nares Strait strongly co varies with salinity. We analyzed the isotopic composition of bivalve shells collected live from the Greenland and Ellesmere Island sides of the Strait in an effort to reconstruct salinity changes with time along this passage over the 5-30 m depth range where these organisms live.

Specimens of *Hiatella arctica* and *Astarte borealis* collected at the northernmost station show a strong shift towards lighter $\delta^{18}O$ values in the most recently accreted sections of their shells, which corresponds to significant freshening with salinity as low as 23. These specimens at the northern end of Nares Strait began experiencing an increase in freshwater input as far back as 20 years ago. Similar freshwater pulses occur with diminishing frequency and magnitude through the 30 and 40 year timeslices. Lesser signals occur further south, probably reflecting significant along channel mixing.

Reconstructing Salinity Conditions in Nares Strait (Canadian Archipelago) from Stable Isotope Profiles in Bivalve Shells

by
Daniela Zima

A THESIS

submitted to

Oregon State University

in partial fulfillment of
the requirements for the
degree of

Master of Science

Presented November 29, 2006

Commencement June 2007

Master of Science thesis of Daniela Zima presented on November 29, 2006

APPROVED:

Co-major professor, representing Oceanography

Co-major professor, representing Oceanography

Dean of the College of Oceanic and Atmospheric Sciences

Dean of the Graduate School

I understand that my thesis will become part of the permanent collection of Oregon State University libraries. My signature below authorizes release of my thesis to any reader upon request.

Daniela Zima, Author

ACKNOWLEDGEMENTS

My major professors, Marta Torres and Kelly Falkner, have challenged me, helped me to grow as a scientist, and strengthened my ability to handle diverse situations professionally with colleagues. They pushed me and guided me when my thought processes or writing went astray, and provided me with unique travel experiences. I thank Marta and Kelly for allowing me to come and learn from them, and for giving me the opportunity to work with other influential scientists in my field that I would not have otherwise met.

I would also like to thank Jason Dunham at the US Geological Survey, Forest and Rangeland Ecosystem Science Center (FRESC), Corvallis Research Group for stepping in as a third member on my committee, and for providing partial funding towards the end of my thesis. Jason has been an unwavering source of support and positivity, and provided me with opportunities to hike, camp, and explore the rivers of Oregon and Idaho through involvement with the freshwater mussel project. I have enjoyed my time working with Jason and look forward to more work with him in the future.

I am grateful to PD Bernd R. Schone, head of the INCREMENTS research group at the University of Frankfurt, Frankfurt/Main, Germany, for instructing me on bivalve shell preparation and aging analysis, consulting with me on the implications of isotope data, and for making me feel welcome in his research group along with post-doc David Rodland.

The isotope data in my thesis was made possible by the assistance of Bill Rugh and Andy Ross. Bivalve species identification and abundance, collection site descriptions, and length and weight measurements were provided by Robie

Macdonald and Mary O'Brien from the Institute of Ocean Sciences in British Columbia, Canada, and Tim Siferd, Manager of the Resolute Marine Laboratory, Fisheries and Oceans Freshwater Institute in Winnipeg, Manitoba, Canada. Data for salinity, temperature, and $\delta^{18}O$ of the water were provided by Kelly Falkner. I would also like to acknowledge the National Science Foundation for funding the Canadian Archipelago Throughflow Study that included Marta Torres and Kelly Falkner, which funded this research through grant OPP-0230354.

Carrie Jackson, Kristen Splinter, Rebecca Poulson, and Dorothy Roholt have been good friends, sources of support, and distraction to me during my time in Corvallis. They were always the perfect people to bounce ideas off of, and seemed to know exactly the right times for coffee or walk breaks. I would also like to thank my boyfriend, Royal Kropf, for believing in me and encouraging me at the times when I needed it the most, and helping me to remember that I was never alone. My fellow students, faculty and staff have also made my time at COAS enjoyable.

Finally, I would like to thank my friends from New Jersey, Ruth Keck, Heather Johnson, Melissa Topol, and Erin Healy for supporting me all the way from my choice to come to OSU to where I am now. Most of all I want to thank my parents, John and Daniela Zima, for being able to let their only child grow up, and for supporting me through experiences good and bad from nearly 4,000 miles away. Last but not least, I want to acknowledge Edward Paul from the Richard Stockton College of New Jersey for believing in me and encouraging me to apply to OSU, because if it was not for him, I would not be where I am now.

TABLE OF CONTENTS

	Page
1. Introduction……...	1
1.1 The Arctic Ocean as a Freshwater Reservoir……..	1
1.2 Circulation in the Eastern Canadian Archipelago and Northern Baffin Bay……	3
1.3 Bivalves as Environmental Recorders…….	7
2. MATERIALS AND METHODS……..	13
2.1 Bivalve Collection……...	13
2.2 Water Sampling and Analyses…….	16
2.3 Site Descriptions……..	17
2.4 Bivalve Shell Preparation……	22
2.5 Sclerochronology……	24
2.6 Characterization of Stable Isotope Composition of Carbonates……	27
3. RESULTS…….	30
3.1 Temperature, Salinity, and Isotopic Composition of the Water……	30
3.2 Bivalve Species Distribution and Abundance……	42
3.3 Age and Depth Distribution of Bivalves……	45
3.4 Arctic Bivalve Growth and Production……..	48
3.5 Isotope Data……	53
3.6 Carbon Isotopic Signatures…….	58
4. DISCUSSION……...	61
4.1 Arctic Bivalve Distribution and Abundance……...	61

TABLE OF CONTENTS (Continued)

	Page
4.2 Arctic Bivalve Growth and Production……...	62
4.3 Bivalve Reliability as Hydrographic Indicators……..	70
5. CONCLUSIONS……...	85
BIBLIOGRAPHY……..	88
APPENDICES…….....	98

LIST OF FIGURES

Figure		Page
1.	Surface circulation patterns south of the Canadian Arctic Archipelago and Baffin Bay……..	5
2.	View of the Nares Strait general study area between Northern Greenland and Canada……..	10
3.	Methods employed at the bivalve collection sites…….	14
4.	Images from bivalve collection efforts at Station 1 near Littelton Island……..	18
5.	Images from bivalve collection efforts at Station 2 near Bellot Island……..	19
6.	Images from bivalve collection efforts at Station 3 across Nares Strait from Bellot Island near Offley Island……	20
7.	Images from bivalve collection efforts at Station 4 in Scoresby Bay…….	21
8.	Image near Station 5 in Alexandra Fjord one week before bivalve collection efforts southwest of Cairn Island showing the abundant sea ice at this station, as well as the steep walled cliffs of the peninsulas of Ellesmere Island near the sampling site..……...	22
9.	Bivalve specimen coated in J-B® KWIK Weld™ quick drying metal epoxy from the umbo to the ventral margin, perpendicular to the growth lines along the axis of maximum growth……...	23
10.	Composite cross-section of *Hiatella arctica* stained with Mutvei's solution, where (A) represents the prismatic layer (outer shell layer) and (B) represents the nacreous layer (inner shell layer)……	26
11.	Sampling of shell carbonate for isotope analysis using a 1 mm diameter diamond drill bit…….	29
12.	Temperature and salinity contour maps generated from a 50 km west-east transect of Robeson Channel, the northernmost point of Nares Strait……..	31

LIST OF FIGURES (Continued)

Figure		Page
13.	Temperature and salinity contour maps generated from a 60 km west-east transect of Kennedy Channel North……..	32
14.	Temperature and salinity contour maps generated from a 60 km west-east transect of Kennedy Channel South, the approximate mid-point of Nares Strait……..	33
15.	Temperature and salinity contour maps generated from a 100 km west-east transect of Smith sound, the southernmost point of Nares Strait……..	34
16.	Temperature (blue lines) and salinity (red lines) profiles in the upper 30 meters of the water column for the bivalve collection sites at A) Littelton Island, B) Bellot Island, C) Offley Island, D) Scoresby Bay, and E) Alexandra Fjord.……...	36
17.	Salinity-$\delta^{18}O$ diagrams at each of the bivalve collection sites…….	40
18.	Temperature-salinity diagrams for each of the bivalve collection sites (pink circles)…….	41
19.	Photographs of the eight bivalve species that were collected in Nares Strait……...	43
20.	Age and depth distributions of Arctic bivalves……	47
21.	Distribution of organic tissue mass as shell free wet weight (pink squares) and shell length (blue circles) with depth for the 8 bivalve species collected…….	49
22.	Length-at-age distribution for species of live-collected Arctic bivalves……..	52
23.	Results of $\delta^{13}C$ (blue symbols) and $\delta^{18}O$ (pink symbols) analysis on *Hiatella arctica* and *Astarte borealis* shells from Bellot Island as a function of age.……	54
24.	Results of $\delta^{13}C$ (blue symbols) and $\delta^{18}O$ (pink symbols) analysis on *Hiatella arctica* and *Astarte borealis* shells from Scoresby Bay…….....	56

LIST OF FIGURES (Continued)

Figure — Page

25. Results of $\delta^{13}C$ (blue symbols) and $\delta^{18}O$ (pink symbols) analysis on *Hiatella arctica* and *Astarte borealis* shells from Alexandra Fjord……..... 57

26. Relationship between $\delta^{13}C$ and $\delta^{18}O$ for *Hiatella Arctica* and *Astarte borealis* from all stations in Nares Strait……..... 59

27. Von-Bertalanffy growth curve fitted to length-at-age data for specimens of *Hiatella arctica*…….. 66

28. Cross-section of the shell of an individual specimen of *Hiatella arctica* (NS-49) showing the total length (L) measured from the umbo to the tip of the ventral margin (red line)…… 68

29. Cross-section of an individual specimen of *Astarte borealis* (NS-95) showing the total length (L) measured from the umbo to the tip of the ventral margin**.**…….. 69

30. Relationship between salinity and $\delta^{18}O_{water}$ for the Nares Strait region…… 71

31. Measured $\delta^{18}O$ shell composition in the youngest sections of bivalve shells collected from all stations in Nares Strait as a function of temperature (A) and salinity (B) for this region using the empirical relationship of Bohm (2000).…… 75

32. Measured $\delta^{18}O$ shell composition of A) 10 year shell sections, B) 20 year shell sections, C) 30 year shell sections, and D) 40 year shell sections from bivalve shells collected from all stations in Nares Strait.……. 81

33. Frequency distribution and ranges of deviation from expected ^{18}O shell values to lighter measured values in shell sections corresponding to the most recent year of growth (Age 0), 10, 20, 30 and 40 years.…….. 84

LIST OF TABLES

Table		Page
1.	Sources from which the data on bivalves throughout the Arctic were compiled…….	11
2.	Most common bivalves occurring in marine Arctic environments……..	12
3.	Summary of bivalve collection sites……..	15
4.	Hydrography of the clam collection sites……..	38
5.	Location and deployment dates of the CTD-rosette casts used to estimate temperature at the bivalve collection sites.…….	39
6.	Total number of each of the eight bivalve species collected at the five Arctic bivalve collection sites..…….....	44
7.	Length ranges and typical maximum lengths for adult individuals of the bivalve species collected in this study, and from previous studies in the Arctic.…….	64
8.	Measured $\delta^{18}O_{water}$ values for freshwater sources to the Arctic, including the ranges of variability for six major rivers, mean values for ice and rivers near bivalve collection sites from this study, and mean salinity Arctic Ocean water……...	72

LIST OF APPENDICES

Appendix		Page
I	Summary of species collected and age for live-collected Arctic bivalves organized by station and depth of collection……	99
II	Summary of live-collected Arctic bivalve sizes and weights……	104
III	Measured $\delta^{18}O$ and $\delta^{13}C$ isotopic composition in the youngest sections of shells collected from all stations in Nares Strait……	109
IV	Measured $\delta^{18}O$ and $\delta^{13}C$ isotopic composition in whole shells of *Hiatella arctica* and *Astarte borealis* from Bellot Island (Station 2), Scoresby Bay (Station 4), and Alexandra Fjord (Station 5)…….	111

Dedicated to

my parents, John and Daniela,

who let me follow a dream to keep learning and be happy

and supported me every step of the journey

no matter how far away.

Reconstructing Salinity Conditions in Nares Strait (Canadian Archipelago) from Stable Isotope Profiles in Bivalve Shells

1. INTRODUCTION

1.1 The Arctic Ocean as a Freshwater Reservoir

The Arctic Ocean plays a pivotal role in the global hydrologic cycle by returning waters evaporated and transported from the surface of the subtropical Atlantic Ocean to the North Pacific and circum-Arctic watersheds (Aagaard and Carmack, 1989). The upper Arctic Ocean stores nearly 100,000 km^3 of freshwater (including ice), which is about 15 times the annual throughput into or out of the system (Aagaard and Carmack, 1989). The principal sources of Arctic Ocean surface water include 10% of the global riverine input from large rivers in Russia and Canada amounting to about 3,000 km^3/yr. It receives again half as much fresh water from relatively fresh seawater of Pacific origin through Bering Strait (Aagaard and Carmack, 1989). Direct precipitation to the ocean surface exceeds evaporation and some freshening occurs in the Norwegian coastal current before it enters the Barents Sea (Aagaard and Carmack, 1989; Steele et al., 1996; Serreze, 2000). Freeze-melt cycles and mixing overprint the freshwater sources in the Arctic (Rudels, 1986; Collin, 1962; Muench, 1971). The products of these freshwater sources and mixing processes are exported back to the North Atlantic in the form of ice and freshened seawater through the eastern side of Fram Strait and the passages of the Canadian Archipelago (Aagaard and Carmack, 1989).

The reservoir of freshwater stored in the Arctic Ocean provides the means for the system to export large pulses of freshwater to the North Atlantic, as well as buffer short-

term variability in its freshwater budget (Aagaard and Carmack, 1989). However, the freshwater is unevenly distributed across the system, with the Canadian Basin containing a majority of it (45%), followed by the continental shelves, ice cover, and the Eurasian Basin (Aagaard and Carmack, 1989). Poorly understood processes affect the freshwater distribution, and determine the amount, location, and timing of freshwater return to the North Atlantic (Melling, 2000). Over the past few decades, a number of factors have been observed to undergo marked changes that influence Arctic freshwater (including ice) distribution and storage. These include altered positioning of the Eurasian-Canadian Basin water mass boundaries (McLaughlin, 1996); subsurface penetration of significantly warmer Atlantic waters (Carmack, 1995; Morison, 1998; Quadfasel, 1991); shifts in the average position of the transpolar drift stream (Rigor, 2002) and Eurasian cold halocline layer (Boyd, 2002; Steele, 1998); diminishing ice cover (Maslanik, 1996; Rothrock, 1999; Smith, 1998; Serreze et al., 2003); altered precipitation patterns (Dickson, 2000; Serreze, 2000); permafrost warming in Siberia and Alaska (Lachenbruch, 1986; Osterkamp, 1999; Pavlov, 1994; Walter et al., 2006); and increased runoff in the Eurasian sector (Peterson, 2002). Many of these changes in the Arctic appear to be associated with changing atmospheric pressure patterns (Dickson, 200; Serreze, 2000; Thompson, 1998), and potentially global warming trends (Peterson, 2002).

Globally significant and variable freshwater export from the Arctic has been observed (Belkin, 1998; Dickson, 1988, 1996, 2000, 2002; Weaver, 1994; Wohlleben, 1995; Delworth, 2000; Rahmstorf, 1999). These observations include propagation of a "Great Salinity Anomaly" throughout the North Atlantic (Belkin, 1998; Dickson, 1988), and a freshening trend over deep North Atlantic water masses (Dickson, 2002). Arctic

freshwater is output adjacent to the formation regions of deep waters in the Nordic Sea through Fram Strait and to the Labrador Sea through the passages of the Canadian Archipelago and Baffin Bay.

If enough freshwater spreads to the deep water formation regions, it may prevent waters from attaining sufficient density to sink and ventilate the deep ocean. In this way, Arctic freshwater export can play a governing role in global thermohaline circulation (Aagaard and Carmack, 1989; Melling, 2000). Some have hypothesized that freshwater inputs and warming will slow the global meridional overturning (Delworth, 2000; Rahmstorf, 1999). Such changes in circulation could negatively impact the climate of the northern hemisphere (Renssen et al., 2001; Ottera et al., 2003; Saenko et al., 2003). A quantitative assessment of the variability and forcing of freshwater fluxes to/from the Arctic Ocean is essential for assessing possible sensitivity to natural and anthropogenic climate perturbations. Of the Arctic-global ocean fresh water exchanges, those through the Canadian Archipelago remain by far the least well characterized but potentially rival that of sea ice and freshened seawater output through Fram Strait. Hence, we have chosen to focus our study on better characterizing variability in these fluxes in the Canadian Arctic Archipelago (Rudels, 1986; Barry and Serreze, 2000).

1.2 Circulation in the Eastern Canadian Archipelago and Northern Baffin Bay

Baffin Bay connects to the Canadian Arctic Archipelago through Nares Strait at Smith Sound in the north, and in the east through Jones and Lancaster Sounds (Fig. 1). Exchange through these connections is limited by shallow sills upstream of the respective sounds at Barrow Strait (≈ 150 m deep, 55 km wide), and Wellington Channel (≈ 175 m

deep, 30 km wide), Cardigan Strait (180 m deep, 8 km wide), and Hell Gate (125 m deep, 5 km wide), and the southern end of Kane Basin (220 m deep, 100 km wide) (Melling, 2000). In the south, Labrador Sea and Baffin Bay waters are exchanged through Davis Strait, which is situated between Baffin Island and Greenland. Davis Strait is about 300 km wide at the narrowest point, and the sill depth is 650 m.

Surface circulation in this region has been derived from observations of ship and ice drift, hydrographic sections, satellite data, mooring deployment, and modeling (Muench, 1971; Kleim, 2003; Tang, 2004; Fig. 1). At eastern Davis Strait, a small portion of the relatively warm and salty West Greenland current composed of waters originating from the Irminger and East Greenland currents flows northward along the west Greenland shelf, while the dominant fraction veers westward into the Labrador Sea (Falkner et al., 2006; Zweng and Muenchow, 2006; and references therein). As it travels northward into Baffin Bay, the extension of the West Greenland Current is cooled and freshened. A portion of this current veers southward at about 72ºN (Tang, 2004). The remainder that continues northward rounds northern Baffin Bay, and is joined by the even fresher, colder throughputs from the Canadian Archipelago passages to form the southward moving Baffin Current, also called the Baffin Island or Canadian Current. The core of this current is topographically steered along 500-1000 m at the shelf slope break. Eventually, the Baffin Island Current exits via Davis Strait into the Labrador Sea to become the Labrador Current. Circulation at depth in Baffin Bay is less well-characterized, but is generally thought to be cyclonic over the slope as for the surface waters (Tang, 2004).

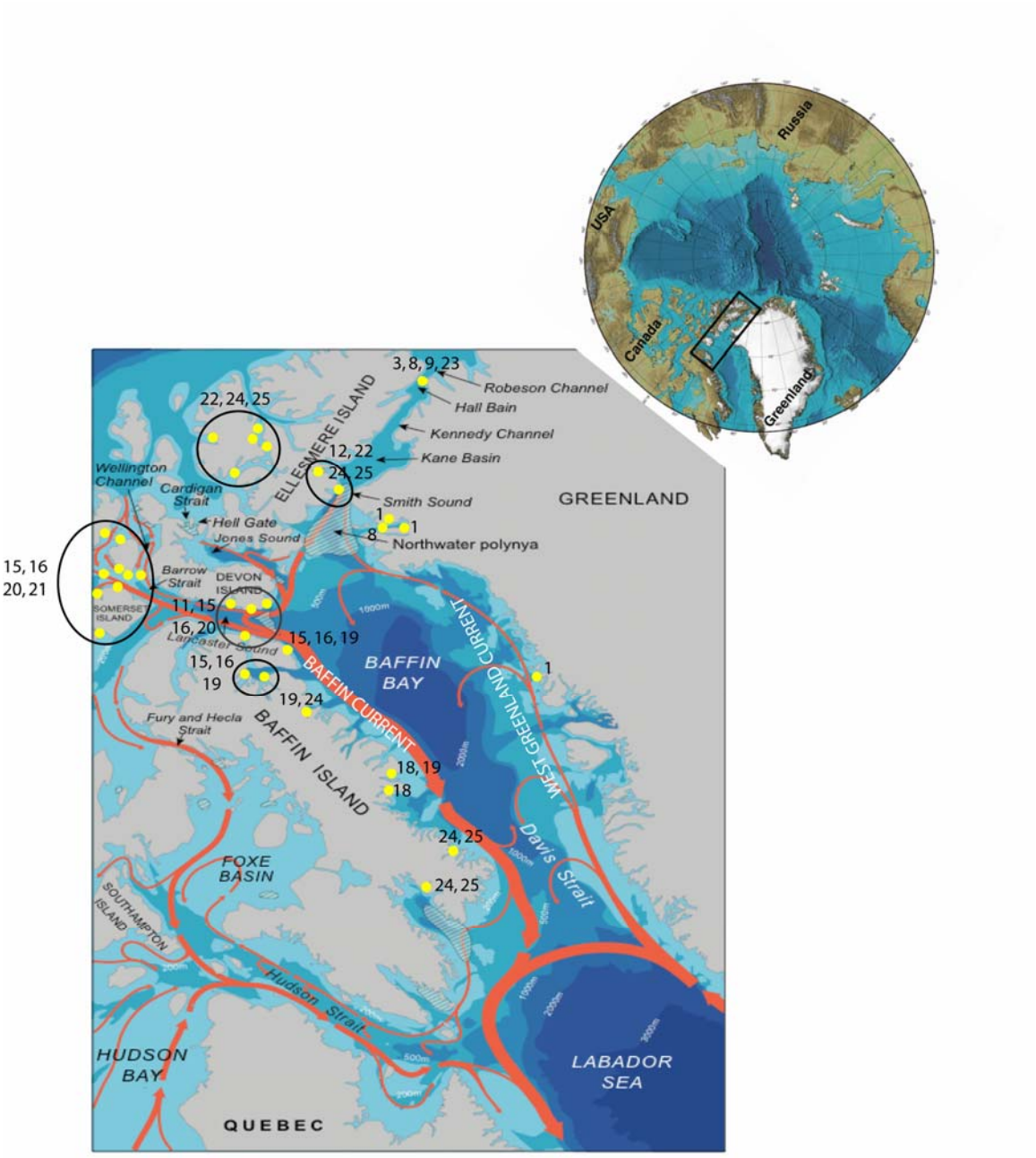

Figure 1: Surface circulation patterns south of the Canadian Arctic Archipelago and Baffin Bay. The red arrows indicate the direction of current flows, and the width indicates the relative magnitude of water that is transported with the currents. Yellow dots and the corresponding numbers indicate regions where previous bivalve studies have been conducted as referenced in Table 1.

Baffin Bay hydrography is characterized as follows. An upper (100-300 m) cold fresh layer called Arctic or Polar water ($S < 33.7$) includes throughflow from the Arctic Ocean and upper West Greenland current waters. This surface layer can be influenced by seasonal heating, sea-ice melt/formation, glacial melt (icebergs and runoff), non-glacial runoff, precipitation, and mixing processes. Below the Polar water (300-800 m) is the saltier West Greenland Intermediate water ($33.7 < S < 34.55$) that includes a temperature maximum (approaching 2ºC) from the Davis Strait inflow. Underlying this are Baffin Deep ($-0.45 < T < 0.7$ºC, $S < 34.5$) and bottom waters (depth $\geq$ 1800 m, $T \approx -0.458$ºC, and $S \geq 34.495$). These depth trends appear to be fairly homogeneously distributed throughout the basin (Falkner et al., 2006). Recently, a statistically significant decadal warming trend (0.2ºC per decade) in the core of West Greenland Intermediate water and extending with depth to the bottom water was reported (Zweng and Muenchow, 2006). This is thought to reflect a warming of Davis Strait source waters over time. Furthermore, a decadal freshening trend of the Arctic surface layer (-0.08/decade) was observed that is most pronounced near Baffin Island.

Flow within the passages of the Canadian Archipelago is not simply unidirectional. Facing Baffin Bay, waters tend to flow into the channels from Baffin Bay on the left and out to Baffin Bay on the right (Fissel, 1988; Falkner et al., 2006; Coote and Jones, 1982). Tidal components of flow can be significant (30-300 cm/sec), and combined with winds, friction from bottom topography and ice cover can induce significant along channel mixing (Melling, 1984; Muenchow, 2006; Falkner et al., 2006). Thus, mixtures of Baffin Bay water with Arctic Ocean water are found within the passages.

Nares Strait is one of three main passages connecting the Arctic Ocean to Baffin Bay and the North Atlantic Ocean (Fig. 2). The head of Nares Strait is situated just downstream of the confluence of the Transpolar Drift and Beaufort Gyre, where Atlantic and Pacific water mass assemblies meet (Steele et al., 2004; Karcher and Oberhuber, 2002). These water mass boundaries have recently been observed to shift (McLaughlin et al., 1996; Steele and Boyd 1998), possibly in response to changed atmospheric pressure patterns and global warming (Dickson, 2000; Serreze, 2000; Thompson, 1998; Peterson et al., 2002). It has been proposed that seasonal and interannual variability of the positioning and properties of these larger scale Arctic Ocean circulation features will be manifest in Nares Strait before propagating into Baffin Bay, across Davis Strait, and into the Labrador Sea (Steele, 1996).

1.3 Bivalves as environmental recorders

Historic hydrographic data are limited for the Arctic (Mueller-Lupp et al., 2003, 2004), as it is difficult to orchestrate monitoring programs for hydrological changes in this dynamic region, especially during periods of ice formation and break-up (Simstich et al., 2005). In addition to this strong seasonal variability, fresh water inventories and fluxes are subject to inter-annual and longer timescale variations, and may be highly susceptible to global warming trends (Peterson et al., 2002; Hakkinen and Proshutinsky, 2004). The use of isotopic data from bivalve shells as hydrographic proxies is gaining significant attention as a valuable tool to generate the much needed retrospective time series data (Khim et al., 2001, 2003; Mueller-Lupp et al., 2004; Dettman et al., 2004).

Bivalves are a convenient tool from which to obtain proxy data, as they have been found distributed throughout the Canadian Arctic and Archipelago (Table 1), and are ubiquitous over a wide range of environments and depths (Table 2).

Bivalves grow by accreting new shell material at the outer edge of their shells throughout the year, but growth is accentuated in the spring/summer. This process leads to the formation of annual growth rings throughout the bivalves' lives, which may extend from 10 years to 100 years or more (Rhoads and Lutz, 1980). Shells are composed primarily of calcium carbonate ($CaCO_3$), which contains oxygen and carbon atoms derived from inorganic carbonate dissolved in seawater (Khim et al., 2003). When the dissolved carbonate is in equilibrium with the seawater, the $\delta^{18}O$ of the accreting shell reflects the temperature and isotopic composition of the ambient seawater (Epstein et al., 1953; Grossman and Ku, 1986). In our study region, the oxygen isotopic composition of seawater is primarily influenced by the amount of freshwater from glacier melt and runoff sources (Khim et al., 2003). Our work shows bivalve shells may provide proxy records of ambient hydrographic conditions for time periods on the order of 10 to 100 years or more, provided the temperatures are low enough and do not vary greatly.

Here we present the results of sclerochronolgy and isotopic composition for bivalve shells recovered during USCGC Healy cruise 031 in 2003 from Nares Strait in the Canadian Archipelago. Bivalve shells were analyzed for $\delta^{18}O$ to determine whether they serve as reliable proxies for natural variability in salinity in Nares Strait over the past several decades. Our results have proven bivalve shells to be useful recorders of the ambient hydrographic conditions in which they live.

The isotope records have revealed significant variations in the magnitude of freshwater fluxes through Nares Strait that have become more pronounced over the past two decades, particularly at the northern end of the Strait. Greater variability in isotopic signatures at northern stations in Nares Strait over this time period are indicative of the proximal influence of fresh Arctic source waters in the north, a signal that is attenuated by mixing as waters transit south through the Strait.

Figure 2: View of the Nares Strait general study area between northern Greenland and Canada. Solid white lines represent transects for water sampling at Smith Sound, Kennedy Channel South, Kennedy Channel North, and Robeson Channel. Numbers in white represent stations of bivalve collection that are listed in Table 3.

Table 1: Sources from which the data on bivalves throughout the Arctic were compiled. The localities indicate the regions in which previous studies were conducted by each author, and are illustrated as yellow dots in Fig. 1.

Locality:	Greenland and fjords	Baffin Islands and fjords	Canadian High Arctic and Archipelago
Source:	(1) Vibe, 1939; 1950 (2) Curtis, 1975 (3) Petersen, 1978 (4) Stewart et al., 1985 (5) Thomson et al., 1986 (6) Thorson, 1957 (7) Ockelmann, 1958 (8) Lubinsky, 1980 (9) Schmid and Pipenburg, 1993 (10) Sejr et al., 2000; 2002	(11) Ellis, 1960 (12) Curtis, 1975 (13) Petersen, 1978 (14) Lubinsky, 1980 (15) Thomson, 1982 (16) Thomson et al., 1986 (17) Dale et al., 1989 (18) Syvitski et al., 1989 (19) Aitken and Fournier, 1993	(20) Lubinsky, 1980 (21) Thomson et al., 1986 (22) Dale et al., 1989 (23) Welch et al., 1992 (24) Aitken and Gilbert, 1996 (25) Gordillo and Aitken, 2000 (26) Khim et al., 2001; 2003 (27) Sejr et al., 2002 (28) Mueller-Lupp et al., 2003; 2004 (29) Mueller-Lupp and Bauch, 2005 (30) Simstich et al., 2005 (31) Ambrose et al., 2006 (32) Peck and Bullough, 1993 (33) Piepenburg and Schmid, 1996

Table 2: Most common bivalves occurring in marine Arctic environments. The data come from the references in Table 1.

Environment:	Shallow water near glacier margins and deltas in fjords	Deep water in fjords	Shallow nearshore marine environments on the continental shelf (including intertidal flats)	Deep water marine environments on the continental shelf
Species:	*Astarte borealis* *Hiatella arctica* *Macoma calcarea* *Mya truncata* *Portlandia arctica* *Nuculana pernula* *Nucula bellotti* *Serripes groenlandicus*	*Astarte borealis* *Hiatella arctica* *Nucula bellotti* *Nuculana pernula* *Portlandia arctica*	*Astarte borealis* *Hiatella arctica* *Macoma calcarea* *Mya truncata* *Serripes groenlandicus*	*Astarte borealis* *Macoma calcarea* *Nucula bellotti*
Substrate:	Loosely consolidated mud and sand	Poorly sorted mixtures of mud, sand, and gravel	Sandy mud to mud	Mud, including clay and silt
References:	1 to 33	1 to10 11 to 16 20 to 25 32 and 33	1 to 33	1 to 9 11 to 19 20 to 30 32 and 33

2. MATERIALS AND METHODS

2.1 Bivalve Collection

Bivalves were collected during Healy cruise 031 from 2-14 August 2003 at 5 locations on the Greenland and Ellesmere Island sides of Nares Strait (Fig. 2). The sampling sites were selected after helicopter reconnaissance surveys. Criteria included the absence of nearby freshwater streams and exposure to the main flow through Nares Strait. A relatively steeply sloping bottom was also sought so as to permit safe diver-based sampling over the 5-30 m depth range. A small motorized boat was deployed from the ship to the sampling area. On site, the location was surveyed with a submersible color camera, which revealed the siphons and closed shells of living bivalves on a benthic habitat consisting of soft sediment mixtures of sand, gravel and clay, protected from ice scour or grounded ice. The majority of the bivalve samples were hand-collected; but in a few cases the divers used a small grab sampler and a hydraulic excavator (stinger) composed of a pump driven by a two-stroke engine and enough hosing to reach the seabed from the small surface boat (Fig. 3). A total of 198 bivalves of 8 different species were collected over the depth range of 6 to 30 meters. Details of sample location and total specimens recovered at each station are listed in Table 3.

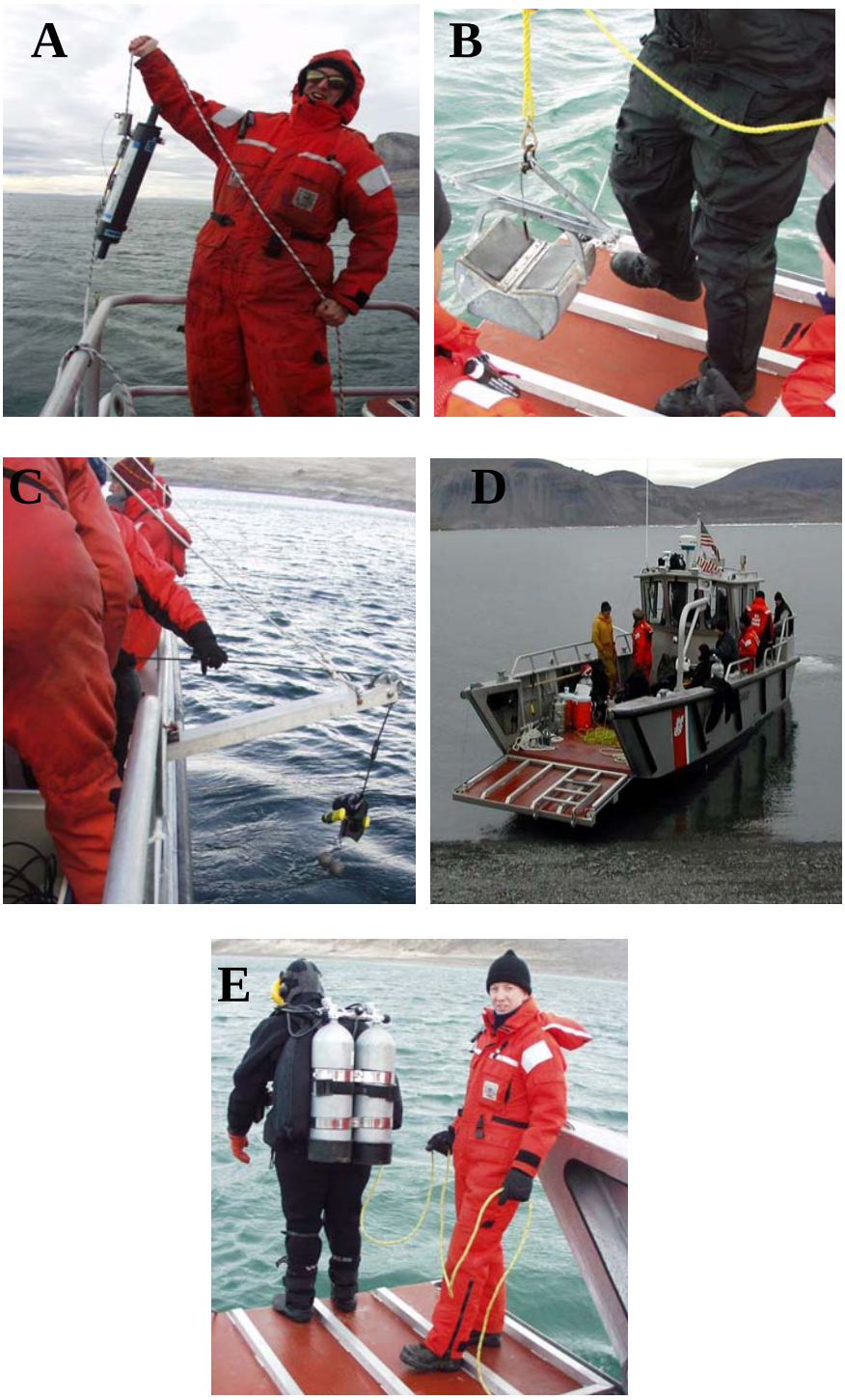

Figure 3: Methods employed at the bivalve collection sites. A) Niskin bottle used to collect water samples for salinity and $\delta^{18}O$ analysis, B) Grab device used to collect bivalves at some locations, C) The color camera used to survey the substrate, D) The dive boat prepared to launch from the shore, and E) A diver preparing to submerge.

Table 3: Summary of bivalve collection sites. Site locations are illustrated in Figure 2.

Date	Site Name	Lat N	Long W	Station	Depths (m)	Total Number of Clams
08/02/2003	Littelton Island	78° 22.20′	72° 51.0′	CL 1	6	1
08/07/2003	Bellot Island	81° 42.81′	64° * 55.0′	CL 2	13-27	56
08/10/2003	Offley Island	81° 17.91′	61° 43.93′	CL 3	10-20	1
08/12/2003	Scoresby Bay	79° 55.80′	71° 7.0′	CL 4	10-20	11
08/14/2003	Alexandra Fjord, Cairn Island	78° 54.35′	75° 47.16′	CL 5	6-22	91

* This was listed in the cruise report as 54º 55.0′ in error (Research Cruise Report: Mission HLY 031, 2003).

The bivalves were preliminarily identified on board by Robie Macdonald and Mary O'Brien from the Institute of Ocean Sciences in British Columbia, Canada. Total length, width, and wet weight (shell + body) were measured on board after collection. The soft tissue was removed from the shell to determine a body wet weight, and preserved for later analysis. A total weight of the shell after the body was removed was recorded as well. The shells of some specimens were dried and the shell dry weight was determined. The soft tissues and shells were sent to Tim Siferd, Manager of the Resolute Marine Laboratory, Fisheries and Oceans Freshwater Institute in Winnipeg, Manitoba, Canada for final species identification, and carbon and contaminant analysis of the soft tissues. The species collected, sizes, and weights are listed in Appendices I and II.

2.2 Water Sampling and Analyses

Water column samples and hydrographic data were collected from hydrocasts in Nares Strait using the USCGC Healy CTD-Rosette from 26 July 2003 to 14 August 2003, along 4 transects at Smith Sound, southern and northern Kennedy Channel, and at its northern inlet at Robeson Channel (Fig. 2). The rosette package consisted of 24 twelve-liter Niskin bottles, with a SeaBird SBE9Plus for pressure, temperature, and conductivity determinations. Additional sensors included an SBE43 dissolved oxygen probe, Wetlabs Cstar transmissometer, Chelsea AquaTrackaIII fluorometer, and a Benthos 916D Altimeter. Water column samples were not taken from all bottles at all casts, however, every time a Niskin was sampled, a bottle salinity was drawn and run on board in a temperature controlled room using an Autosal by Guildline, Model 8400B (#65-715), with a precision of 0.002 on the practical salinity scale. Samples for salinity and $\delta^{18}O$ were collected at the bivalve sites through deployment of a 1.7-L Niskin bottle at the depths of bivalve collection. Salinities were measured with the autosal on board. Oxygen isotopes were analyzed at Oregon State University (OSU) by the CO_2 equilibration method (Kroopnick et al., 1972; Ortiz et al., 2000; Graber and Aharon, 1991; Salata et al., 2000) using the Finnegan Mat 251 mass spectrometer at the College of Oceanic and Atmospheric Sciences (COAS). Results are reported in del units relative to Vienna Standard Mean Ocean Water (VSMOW) and 1-sigma precision is estimated to be +/- 0.05δ.

2.3 Site Descriptions

Sampling at Station 1 took place on the western side of Littelton Island in a small, protected channel (Fig. 2). The site was approximately 6 meters deep and productive, with abundant kelp, brittle stars, and prevalent siphons and clam shells (Fig. 4). However, the excessive turbidity generated by divers in contact with the muddy substrate made clam collection by hand and by hydraulic excavation difficult. As a result, only one single large *Serripes groenlandicus* was collected at a depth of 13.4 meters.

Bivalve collection at Station 2 was made near Discovery Harbor on the Ellesmere Island side of the Strait (Fig. 2; Fig. 5). The site was over a relatively gently sloping bottom on the east side of Bellot Island. The bottom sampled was muddy and free of macro algae. Bivalves were collected over a depth range from 13 to 27 meters predominantly by hand excavation, although a small dredge was deployed from the surface unsuccessfully. The sample collection at this site was dominated by large *Hiatella arctica* (4-5 cm) and *Astarte borealis* (3-5 cm). *Portlandia arctica* were also prevalent at this site, and a few live specimens of *Mya truncata, Nucula belloti,* and *Serripes groenlandicus* were also obtained. Station 3 was located across Nares Strait on the eastern side at Offley Island (Fig. 2), where a single, small specimen of *Hiatella arctica* (4 cm) was retrieved from 19 meters water depth using a small dredge (Fig. 6).

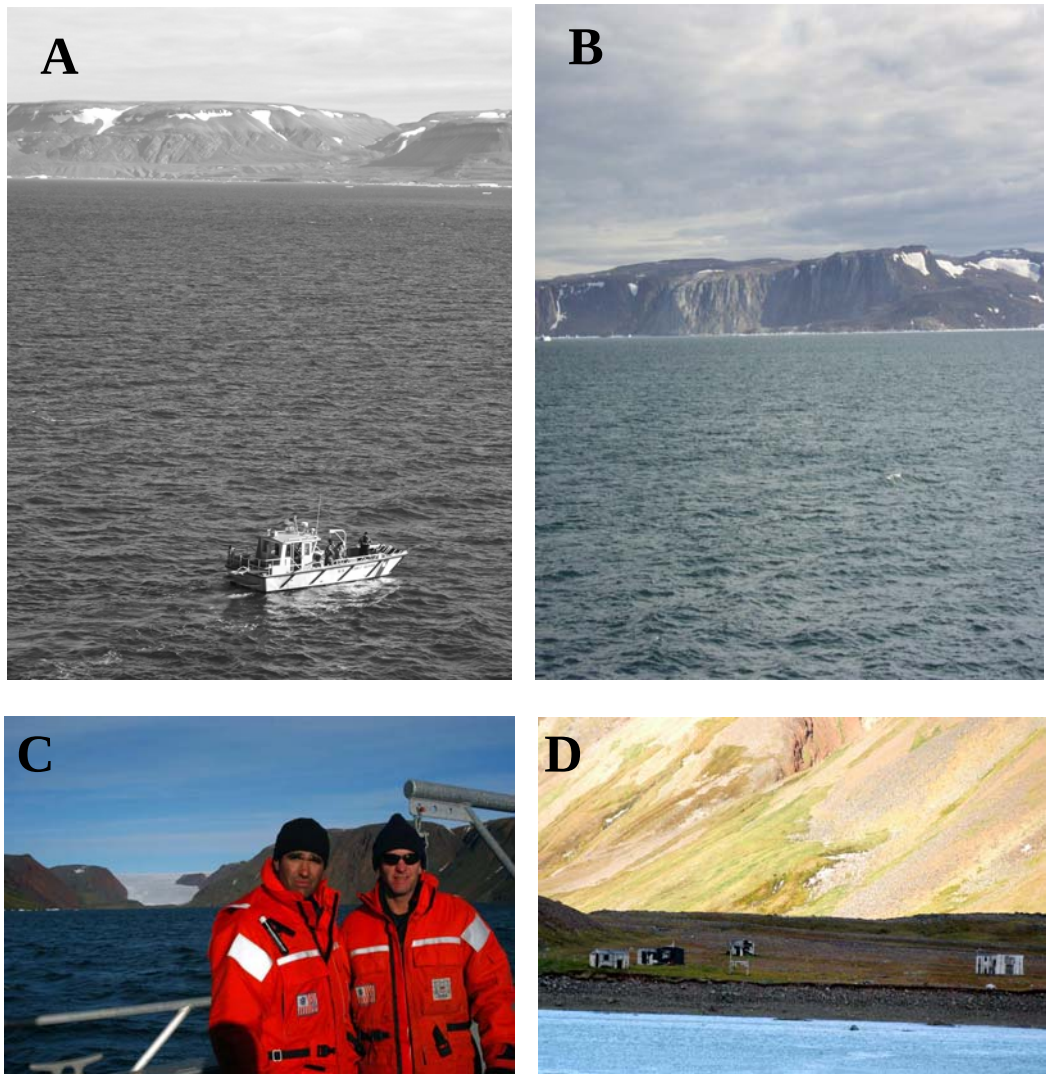

Figure 4: Images from bivalve collection efforts at Station 1 near Littelton Island. A) The dive boat with Greenland in the distance, B) A closer view of Greenland, C) A view towards Greenland from the diveboat at the collection site with a glacier evident and the Coast Guard Diving Team, and D) A close-up view towards the Cape Alexander, Greenland shoreline from the collection site.

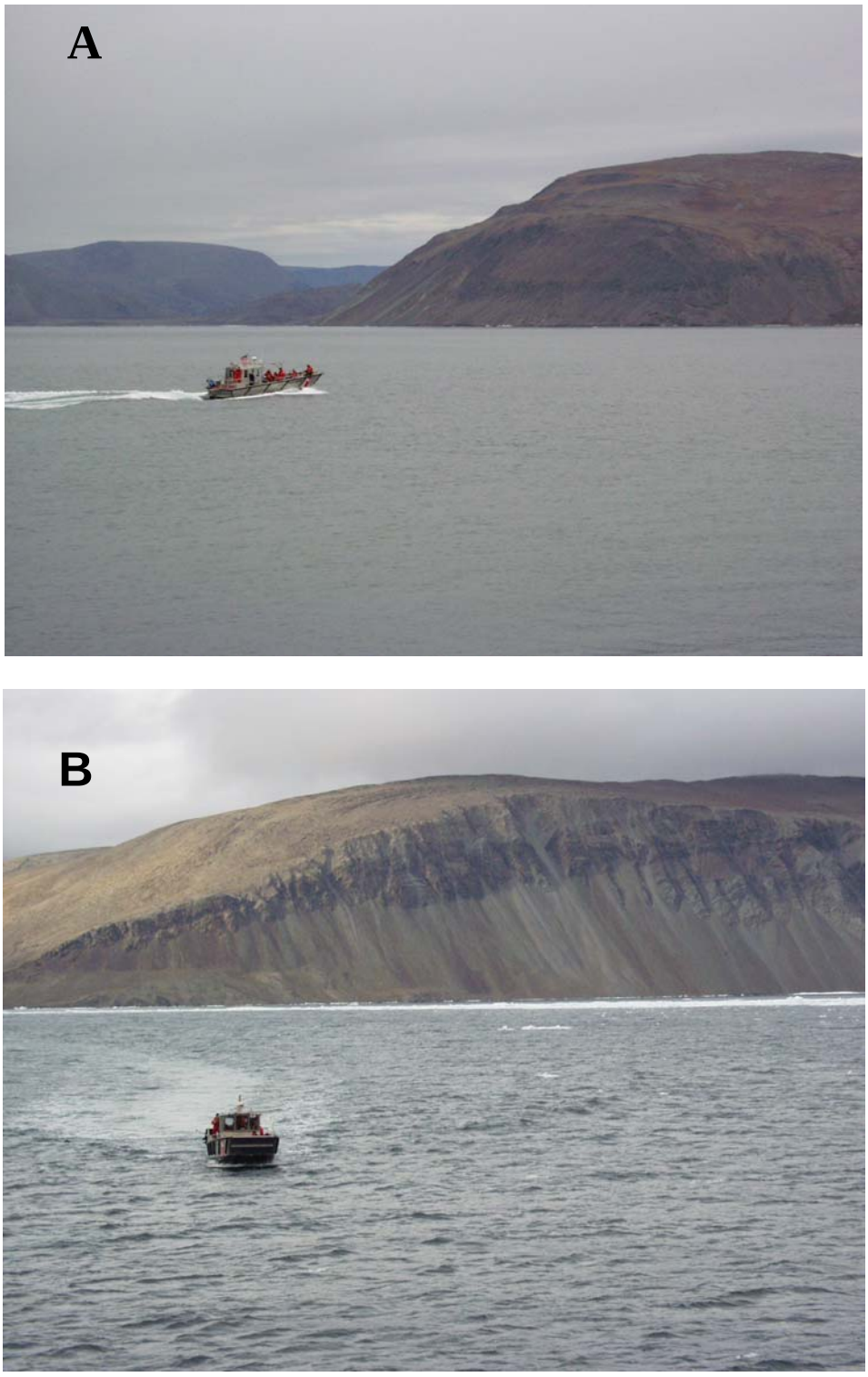

Figure 5: Images from bivalve collection efforts at Station 2 near Bellot Island. A) The diveboat traveling to the sampling site with the view of the mainland of Ellesmere Island in the distance, and B) The diveboat returning to the Healy with a close-up of Ellesmere Island in the background.

Figure 6: Images from bivalve collection efforts at Station 3 across Nares Strait from Bellot Island near Offley Island. The red hills of Greenland and Offley Island from a distance.

The area bordering Station 4 in Scoresby Bay (Fig. 7) consisted of exposed coastline with abundant grounded ice and regions of scour in the shallows. The western bay was dominated by large, inflowing rivers. The sampling location was near the northeastern mouth of the bay. The steeply sloping bottom appeared to be the continuation of a talus slope of a ridge that extended along the north side of the bay inside of Cape M'Clintock. The substrate was dominated by mud. The collection here was dominated by several *Astarte borealis* (up to 5 cm long) and some dead or fractured *Hiatella arctica*. A couple of live individuals of *Mya truncata, Nuculana pernula,* and *Serripes groenlandicus* were obtained as well.

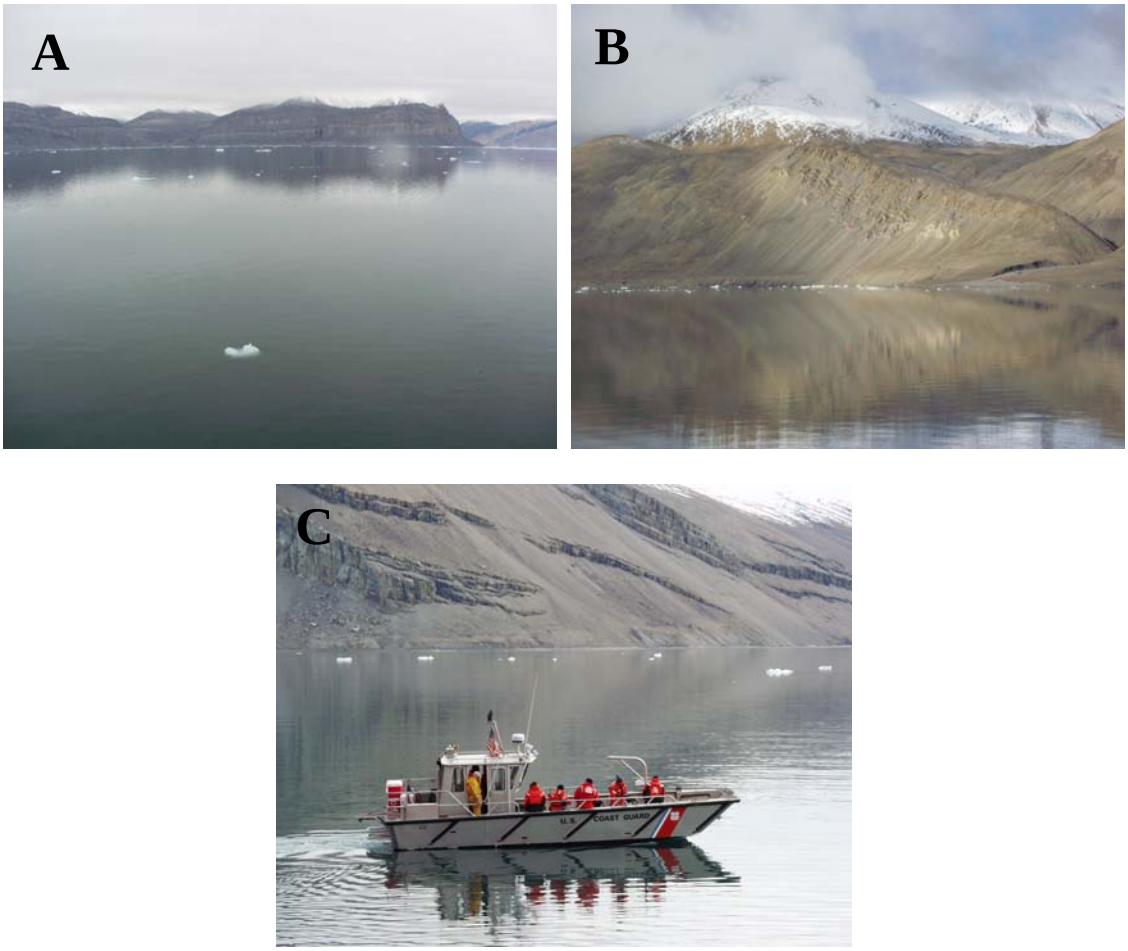

Figure 7: Images from bivalve collection efforts at Station 4 in Scoresby Bay. A) A view of the Scoresby Bay sampling site with some sea ice evident, B) The exposed coastline surrounding Scoresby Bay, and C) The dive boat near the sampling site showing an up close view of the coastline.

The collection at Station 5 was in Alexandra Fjord, just southwest of Cairn Island (Fig. 2), over a depth range of 6 to 22 meters. During the sampling time, the site was subject to strong currents, high winds and waves, and patches of ice were abundant (Fig. 8). Evidence of living bivalves was indicated by the presence of clam shells mixed into a sandy/rocky bottom, however, siphons were difficult to recognize. The sediment was organic-rich (Robie Macdonald, personal communication, 2006), and ice scour at the seafloor was prevalent. *Astarte borealis* dominated the bivalve community, but other

species at this site included *Mya truncata, Macoma calcarea, Nucula belloti, Nuculana pernula,* and *Serripes groenlandicus*.

Figure 8: Image near Station 5 in Alexandra Fjord one week before bivalve collection efforts southwest of Cairn Island showing the abundant sea ice at this station, as well as the steep walled cliffs of the peninsulas of Ellesmere Island near the sampling site. The ice moves in and out of the region rapidly as a function of the winds in the August timeframe.

2.4 Bivalve Shell Preparation

In order to date the specimens, bivalve shells were ultrasonically rinsed in water-free ethyl alcohol. They were then coated with J-B® KWIK Weld™ quick drying metal

epoxy to form a protective coating during cutting, grinding, and polishing (Fig. 9). Shells were coated from the umbo to the ventral margin, perpendicular to the growth lines along the axis of maximum growth. One- to three-millimeter thick mirror-image sections were cut from the shells perpendicular to the growth axis using a diamond band saw (Fig. 9). Mirror image sections were cut from the shells to ensure that any growth disturbances were similarly represented on the sections used for aging and isotope analysis. Sections were subsequently mounted on 3x1 glass microscope slides with J-B® KWIK Weld™ epoxy.

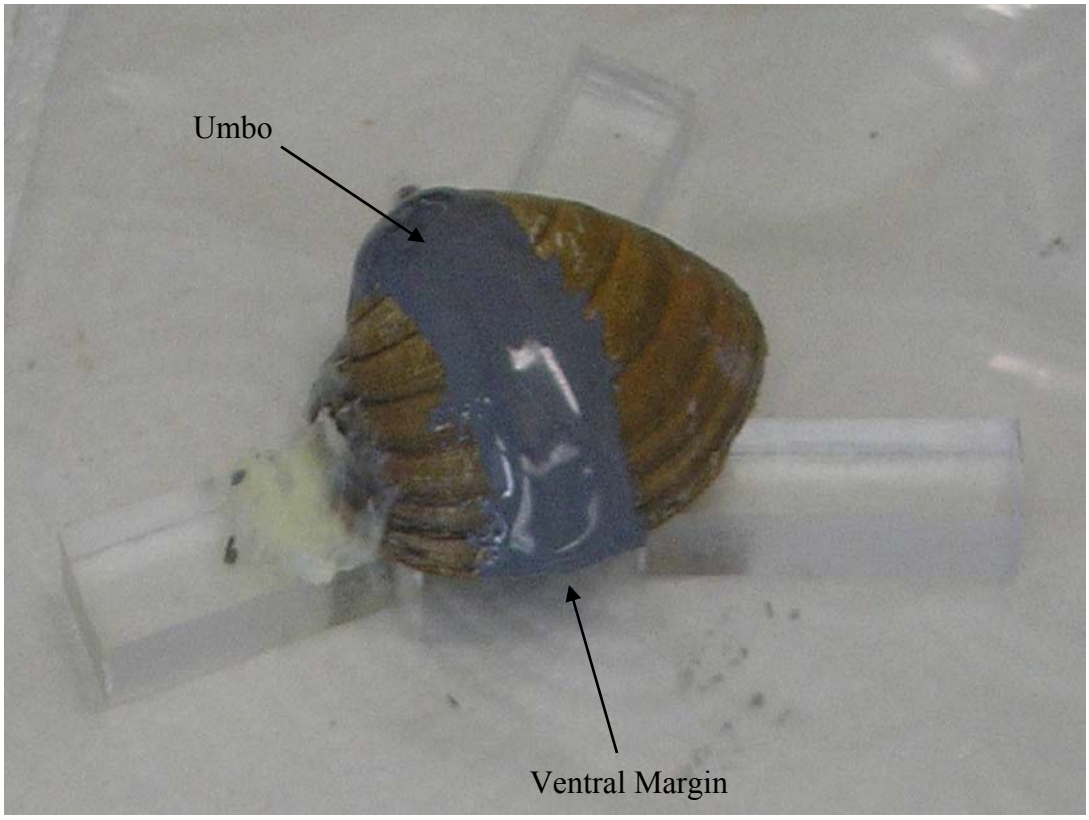

Figure 9: Bivalve specimen coated in J-B® KWIK Weld™ quick drying metal epoxy from the umbo to the ventral margin, perpendicular to the growth lines along the axis of maximum growth. The shells are mounted to plexiglass cubes with J-B® epoxy for ease of cutting through the center with a saw.

Shell sections were prepared both at Oregon State University (OSU) and the University of Frankfurt am Main in Frankfurt Germany. At OSU, shells were ground and polished sequentially on 320, 400, and 600 grit sand paper with a Buehler Handimet 2 Roll grinder, and 1.0 μm alpha alumina powder on a Buehler Ecomet III polisher. Sections of shells prepared at the University of Frankfurt am Main in Frankfurt, Germany were cut using a Beuhler Isomet low-speed saw with a 0.3 mm thick diamond wafering blade. These were then ground on glass plates with 800 and 1200 silicon-carbon (SiC) grid powder, and polished on 1 μm aluminum oxide (Al_2O_3) powder. All sections were ultrasonically cleaned following each grinding step, rinsed in 100% ethyl alcohol, and dried. Polished surfaces were kept free from dust by storing the shells in microscope slide boxes.

2.5 Sclerochronology

Growth layers were determined by microscopic examination of shells stained with Mutvei's solution (500 mL 1% acetic acid, 500 mL 25% glutaraldehyde, and 5 g of alcian blue powder), following published procedures of Schone and others (2004; 2005). Samples were immersed in Mutvei's solution under constant stirring at 37-40°C for 22 minutes. Immediately after removal from the solution, the etched sections were carefully rinsed with demineralized water and allowed to air-dry.

The components in Mutvei's solution function simultaneously to etch the carbonate, preserve the water-insoluble (structural framework molecules) and water-soluble (framework associated macromolecules) components of the organic matrix, and

differentially stain the soluble organics in a single preparation step (Schone et al., 2005). The acetic acid assists the glutaraldehyde in stabilizing the organic compounds, and removes the carbonate very gently (e.g.-etching). The acid reacts very slowly without producing large amounts of CO_2 bubbles that would carry away the soluble organics before they are fixed (Schone et al., 2005). Glutaraldehyde is used as a fixing agent for the water-soluble and water-insoluble organic components of the shell. Alcian blue in weak acetic acid forms reversible electrostatic bonds with anionic portions of polysaccharides. Glutaraldehyde and alcian blue work together to enhance preservation and contrast of cell coats and intercellular substances (Benhnke and Zelander, 1970; Schofield et al., 1975). The glutaraldehyde fixative traps proteins before staining (Gotliv et al., 2003). Treated samples were then viewed under a Leica DMLP reflected light binocular microscope with 16 or 25X magnification, and digitized with a Nikon Coolpix 995 camera. The growth lines were photographed, counted, and logged for every live-collected specimen. The results of the age analysis are given in Appendix I.

Cross-sections of the stained bivalves reveal crisp three-dimensional growth structures under oblique or axial light, which allows for identification of annual growth lines based on their sharp, darker-blue stained structures (Fig. 10). The annuli were composed of relatively wide, light blue stained etch-resistant ridges, and sharply defined, darker-blue stained narrow depressions. These correspond to summer and winter growth periods respectively. Bivalves grow faster and bands tend to be wider during the summer as a result of more favorable temperatures, food quantity and quality, and light conditions (Lutz and Rhoads, 1980; Schone et al., 2004). Winter growth retardations or cessations

result in reduced carbonate ($CaCO_3$) precipitation (Wada, 1961, 1980; Lutz and Rhoads, 1980; Schone et al., 2004).

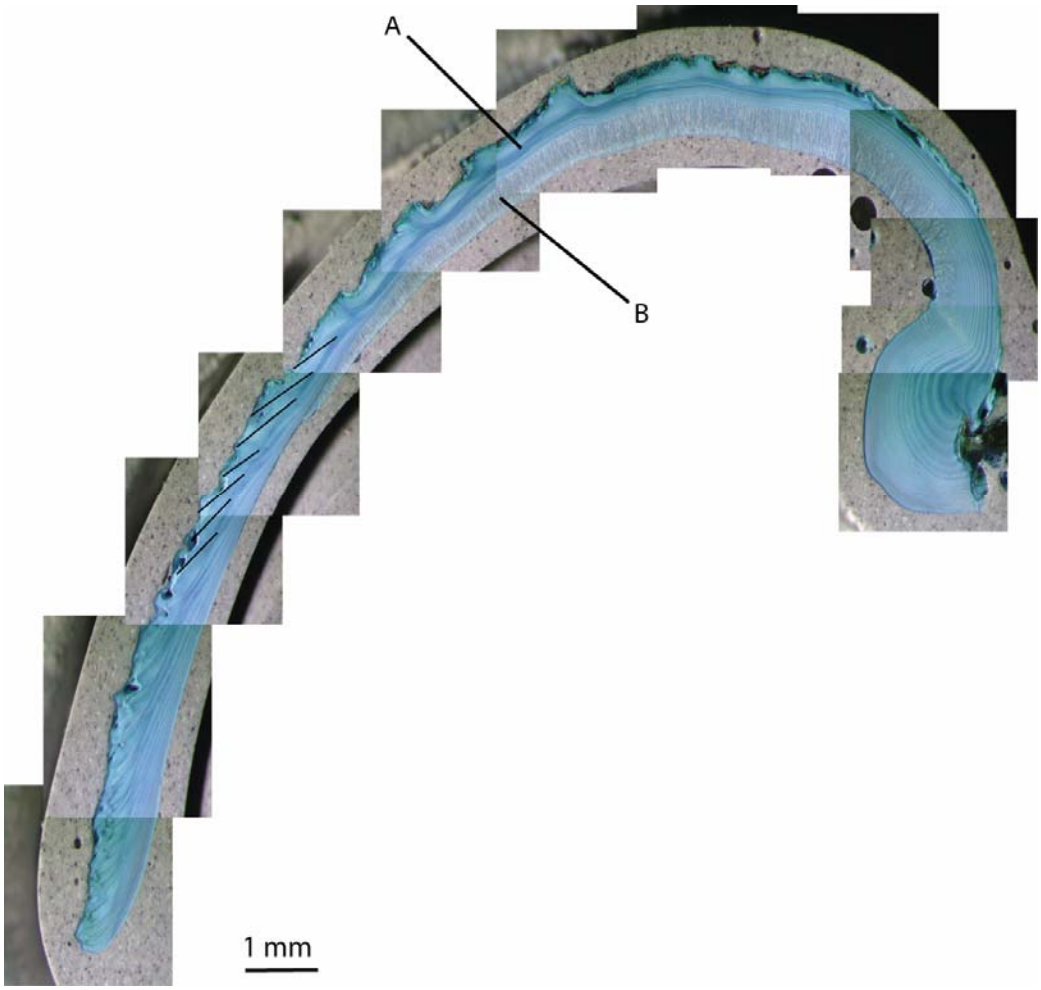

Figure 10: Composite cross-section of *Hiatella arctica* stained with Mutvei's solution, where (A) represents the prismatic layer (outer shell layer) and (B) represents the nacreous layer (inner shell layer). Spaces between black lines on the cross-sections represent annual growth increments. Darker stained portions of the shells indicate winter growth, while lighter-blue stained portions represent summer growth.

Annual growth variations due to environmental conditions can be complicated by the metabolic activity of the organism. As bivalves age, energy spent on shell secretion decreases, growth bands tend to become narrower, and are spaced closer together. The chemical composition of the summer and winter growth regions in annual bands is different, and therefore the components in Mutvei's solution react differently with them. The blue color indicates the presence of water-soluble macromolecules including aspartic and glutamic acids, and mucopolysaccharides (Marxen et al., 1998). The lines corresponding to winter growth retardation or cessation are more deeply stained because more polysaccharides and soluble organics are deposited or accumulated in the hard parts during periods of reduced $CaCO_3$ precipitation and skeletal growth (Wada, 1961, 1980; Rhoads and Lutz, 1980; Schone et al., 2004). The ontogenetic age for each individual is assigned by counting these banded pairs.

2.6 Characterization of Stable Isotope Composition of Carbonates

The mirror images of the cross-sections that were not stained with Mutvei's solution were drilled to obtain carbonate powders for $\delta^{18}O$ and $\delta^{13}C$ stable isotope analysis. Carbonate powder was drilled under a stereomicroscope at 10 to 20X magnification. Carbonate powders were collected from the outer shell layer along the growth axis in roughly annual increments after removal of the periostracum and excess metal epoxy (Fig. 11). The inner shell layer and periostracum were not included in isotope analysis as the chemistry of these layers are affected not only by variations in the

chemical composition of the water but also vital affects related to the metabolism of the bivalve (Rhoads and Lutz, 1980).

A 1 mm diameter cylindrical diamond drill bit (Brasseler USA) was used for drilling with either a Rexim Minimo microdrill, dentist drill (Brasseler USA UP500), or DREMEL® MultiPro™ rotary tool (Model 395T6). Each milling yielded approximately 50 μg or less of carbonate powder. The $\delta^{13}C$ and $\delta^{18}O$ in the carbonate powders were measured using a Finnigan/MAT 252 stable isotope mass spectrometer equipped with a dual-inlet and Kiel-III carbonate preparation device at OSU, with precisions of ± 0.02 ‰ and 0.06 ‰, respectively. Isotope values are reported relative to the PeeDeeBelemnite (PDB) scale established via NBS-18, 19, and 20 (National Bureau of Standards) and Wiley carbonate stable isotope standards.

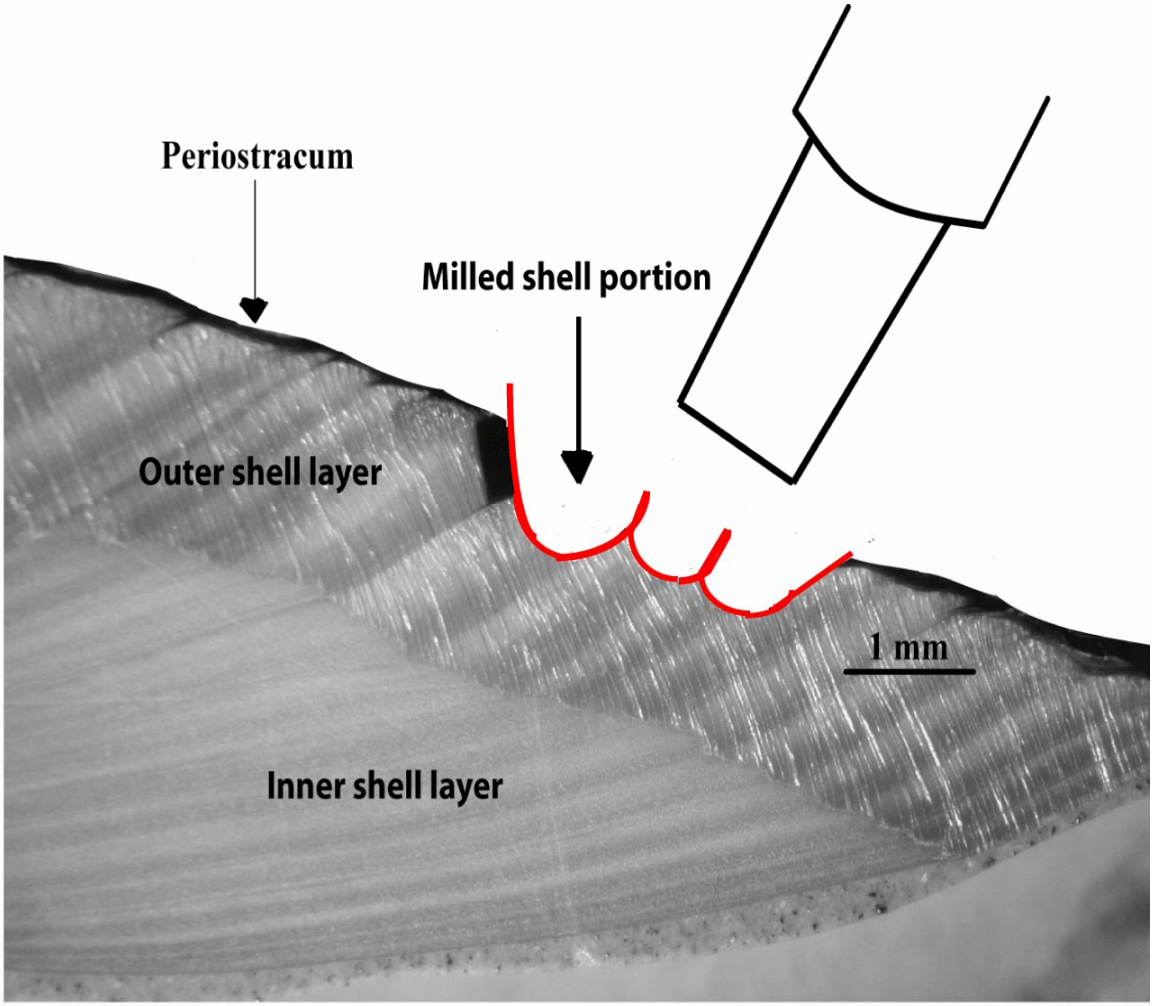

Figure 11: Sampling of shell carbonate for isotope analysis using a 1 mm diameter diamond drill bit. Carbonate powder was milled from the shell following the shape of the annual growth lines. The line segment represents a typical 1 mm wide annual growth increment that was milled at a time. The figure indicates the location of the outer shell layer, inner shell layer, and examples of milled shell portions. The periostracum is the thin black layer that forms the outer covering of the shell surface.

3. RESULTS

Currents through the Canadian Archipelago are multidirectional and complex (Falkner et al., 2006). They tap waters from both the Arctic Ocean and Baffin Bay. Superimposed on these are inputs from precipitation, both run-off and direct, sea-ice melt and formation, glacial melt, and variable mixing processes. Hence, temperature and salinity vary regionally and temporally (Figs. 12-15), particularly in the upper 100 to 200 meters of the water column where bivalves are most abundant. The oxygen isotopic composition of the seawater in cold Arctic regions is strongly correlated with salinity, since river waters and glacial ice melt tend to have highly negative ($\delta^{18}O$ = -18‰ to -25‰) values, and seawater is close to 0‰ (Khim et al., 2001, 2003; Mueller-Lupp et al., 2004, 2005; Simstich et al., 2005). Thus, variations in salinity and, to a much lesser extent temperature, can be expected to be recorded in the $\delta^{18}O$ of shell carbonates, which acquire their isotopic composition from the ambient water (Krantz et al., 1987).

3.1 Temperature, Salinity, and Isotopic Composition of the Water

In August 2003, temperatures in sections in Nares Strait from Robeson Channel to Kennedy Channel South ranged from -2ºC at 50 meters water depth to -1ºC at the surface, with the core of the cold water being centered just above 50 meters. Smith Sound exhibited a larger temperature range from near freezing to 2˚C. Salinity from Robeson Channel to Smith Sound ranged from 33 at 50 meters water depth to 31.5 at the surface (Figs. 12-15).

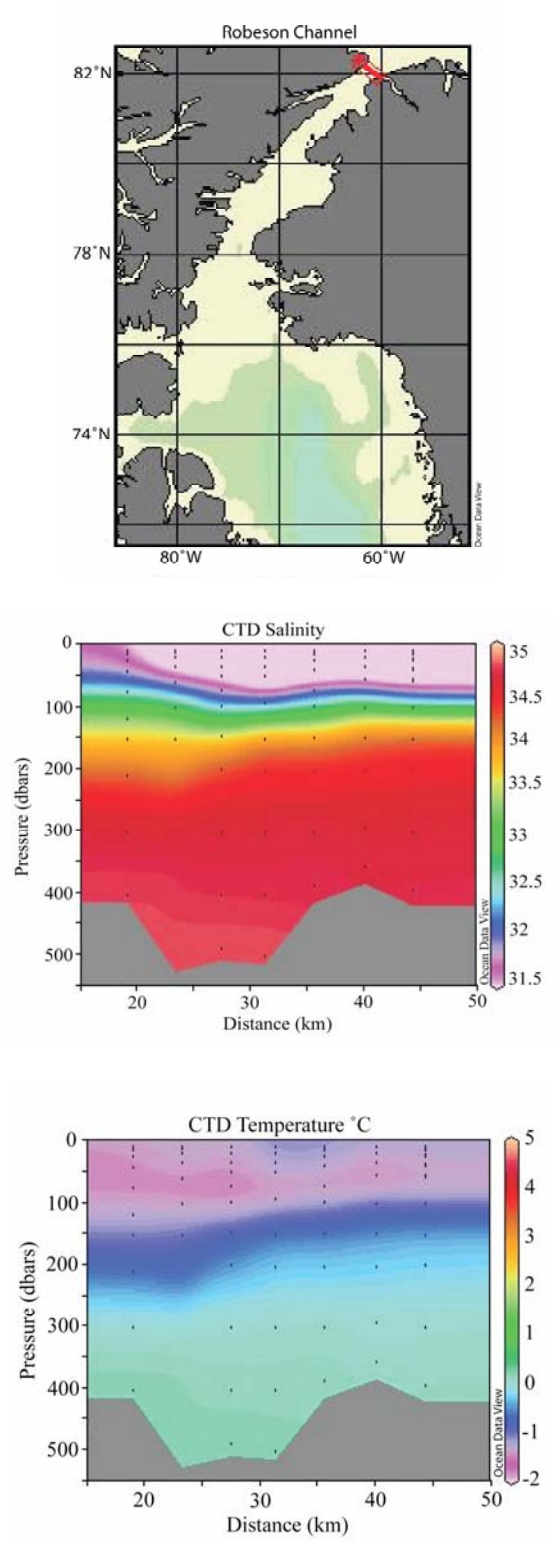

Figure 12: Temperature and salinity contour maps generated from a 50 km west-east transect of Robeson Channel, the northernmost point of Nares Strait.

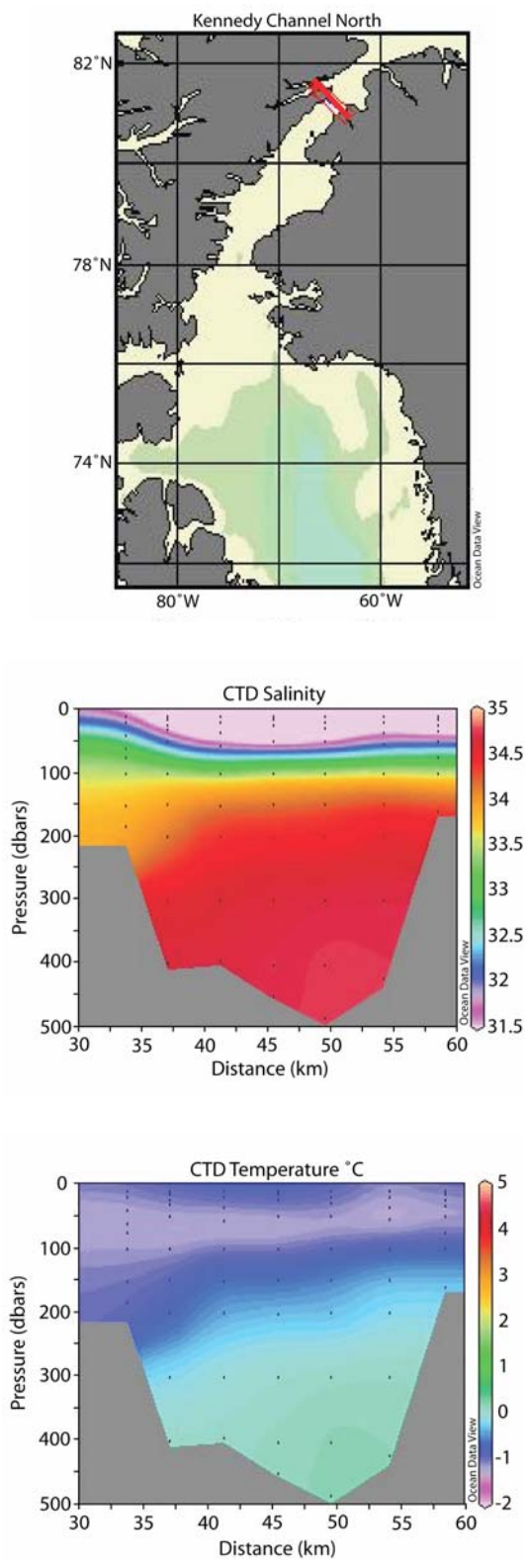

Figure 13: Temperature and salinity contour maps generated from a 60 km west-east transect of Kennedy Channel North.

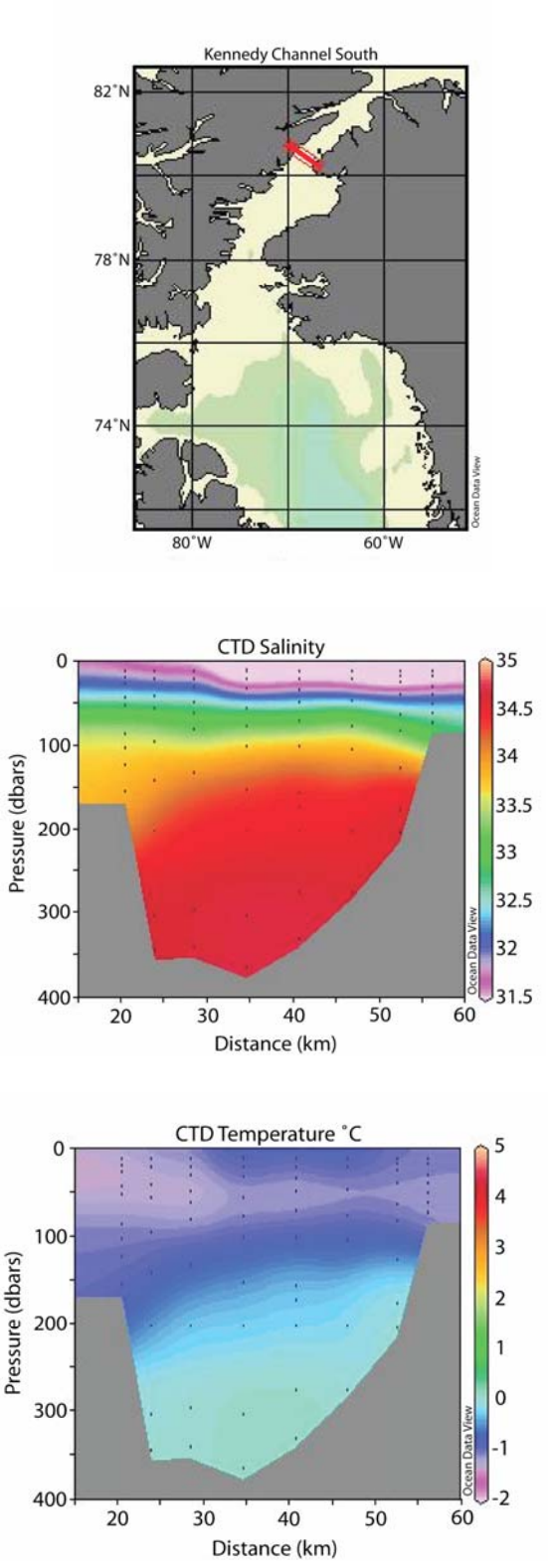

Figure 14: Temperature and salinity contour maps generated from a 60 km west-east transect of Kennedy Channel South, the approximate mid-point of Nares Strait.

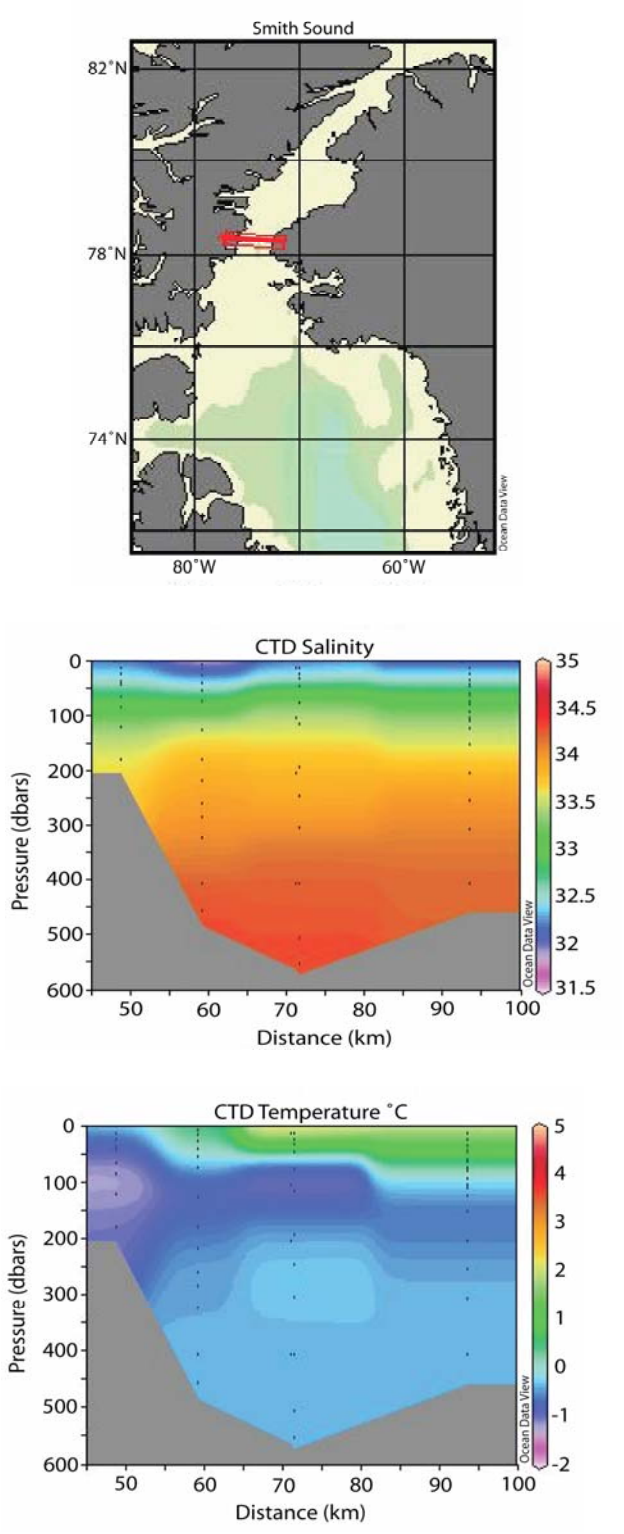

Figure 15: Temperature and salinity contour maps generated from a 100 km west-east transect of Smith Sound, the southernmost point of Nares Strait.

Salinity stratification appeared to be more pronounced in the western portions of the transects (Figs. 12-15). The relationship between temperature and salinity with depth is shown in Fig. 16. Salinity and $\delta^{18}O$ were directly measured at the clam collection sites, whereas temperature was not. Temperatures for the clam sites were estimated from CTD cast data on the Canadian Archipelago Throughflow Study (CATS) website (http://newark.cms.udel.edu/~cats/), by examining stations closest to the clam collection sites and matching depths and salinities (Tables 4 and 5).

The salinity and $\delta^{18}O$ at most of the clam collection sites fall on the linear S-$\delta^{18}O$ relationships of the nearest CTD-station, specifically at Littelton Island, Bellot Island, and Scoresby Bay (Figs. 17A, 17B, and R17D). Salinities measured near Alexandra Fjord and Offley Island were comparable to ones at nearby CTD stations; however, the $\delta^{18}O$ of the water at the clam sites were lighter than in the main channel of Nares Strait (Figs. 17C and 17E respectively). Since the $\delta^{18}O$ values of the water were lighter at these locations, bivalve shells collected from Alexandra Fjord and Offley Island are believed to exhibit the effects of local freshwater influences in their isotopic profiles. Temperature-salinity diagrams of these regions show very little relationship between these two parameters or with conditions at the bivalve collection sites (Fig. 18), and exhibit a great deal of variability between locations.

Figure 16: Temperature (blue lines) and salinity (red lines) profiles in the upper 30 meters of the water column for the bivalve collection sites at A) Littelton Island, B) Bellot Island, C) Offley Island, D) Scoresby Bay, and E) Alexandra Fjord. Salinity was directly measured at each collection site, while temperatures were estimated from CTD cast data by examining stations closest to the clam collection sites and matching depths and salinities (Tables 4 and 5).

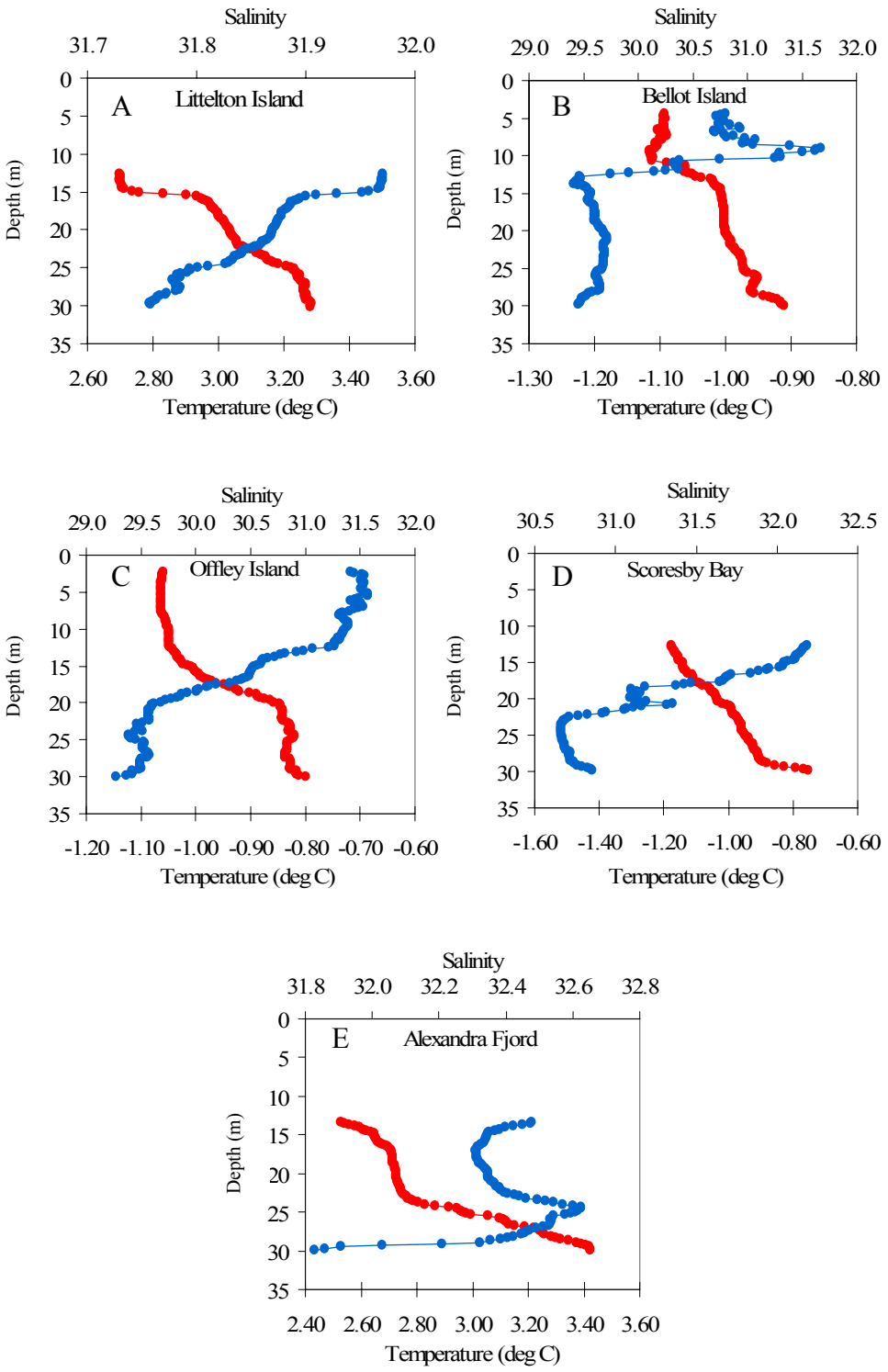
A
Littelton Island
Salinity
31.7 31.8 31.9 32.0
Depth (m)
0 5 10 15 20 25 30 35
2.60 2.80 3.00 3.20 3.40 3.60
Temperature (deg C)
B
Bellot Island
Salinity
29.0 29.5 30.0 30.5 31.0 31.5 32.0
Depth (m)
-1.30 -1.20 -1.10 -1.00 -0.90 -0.80
Temperature (deg C)
C
Offley Island
Salinity
29.0 29.5 30.0 30.5 31.0 31.5 32.0
Depth (m)
-1.20 -1.10 -1.00 -0.90 -0.80 -0.70 -0.60
Temperature (deg C)
D
Scoresby Bay
Salinity
30.5 31.0 31.5 32.0 32.5
Depth (m)
-1.60 -1.40 -1.20 -1.00 -0.80 -0.60
Temperature (deg C)
E
Alexandra Fjord
Salinity
31.8 32.0 32.2 32.4 32.6 32.8
Depth (m)
2.40 2.60 2.80 3.00 3.20 3.40 3.60
Temperature (deg C)

Figure 16

Table 4: Hydrography of the clam collection sites. Temperatures were estimated from CTD cast data on the Canadian Archipelago Throughflow Study (CATS) website (http://newark.cms.udel.edu/~cats/), by examining stations closest to the clam collection sites and matching depths and salinities. Salinity and $\delta^{18}O$ were directly measured at the clam collection sites from water samples collected in a 1.7-L Niskin bottle. The column labeled CTD Station indicates the CTD-rosette station from which data were used to estimate temperature. These stations are listed in Table 5.

Clam Collection Site (Station Number)	CTD Station	Depth (m)	Temperature (ºC)	Salinity	$\delta^{18}O_{water}$
Littelton Island	S01	1	3.48	31.8	-1.88
(1)	S01	5	3.48	31.8	-1.87
	S01	10	1.86	31.8	-1.78
	S01	20	1.57	31.9	-1.73
Bellot Island	RN1	1	-1.40	31.3	-2.67
(2)	RN1	5	-1.40	31.4	-2.68
	RN1	10	-1.40	31.4	-2.67
	RN1	20	-1.39	31.4	-2.61
	RN1	30	-1.46	31.6	-2.58
Offley Island	KN07	1	-0.85	30.0	-3.45
(3)	KN07	8	-0.85	30.1	-3.37
	KN07	17	-1.05	30.5	-3.17
Scoresby Bay	KS01	1	-1.16	30.8	-2.76
(4)	KS01	5	-1.16	31.5	-2.38
	KS01	10	-1.16	31.6	-2.27
	KS01	20	-1.45	31.9	-2.22
Alexandra Fjord	S04	1	0.49	31.3	-2.23
(5)	S04	5	0.49	31.3	-2.20
	S01	10	1.87	31.8	-2.02
	S05	18	-0.54	32.1	-1.85

Table 5: Location and deployment dates of the CTD-rosette casts used to estimate temperature at the bivalve collection sites. For information on the locations of the bivalve collection stations, refer to Table 3.

Date	CTD Station	Station Name	CTD Cast	Lat N	Long W
8/2/2003	S01	Smith Sound (1)	39	78° 19.89′	72° 54.85′
8/3/2003	S04	Smith Sound (2)	43	78° 19.99′	74° 26.19′
8/3/2003	S05	Smith Sound (5)	44	78° 19.89′	74° 53.87′
8/4/2003	KS01	Kennedy Channel South (1)	45	80° 33.55′	68° 55.54′
8/6/2003	KN07	Kennedy Channel North (7)	54	81° 08.61′	64° 06.95′
8/10/2003	RN1	Robeson Channel (1)	68	82° 07.54′	61° 36.65′

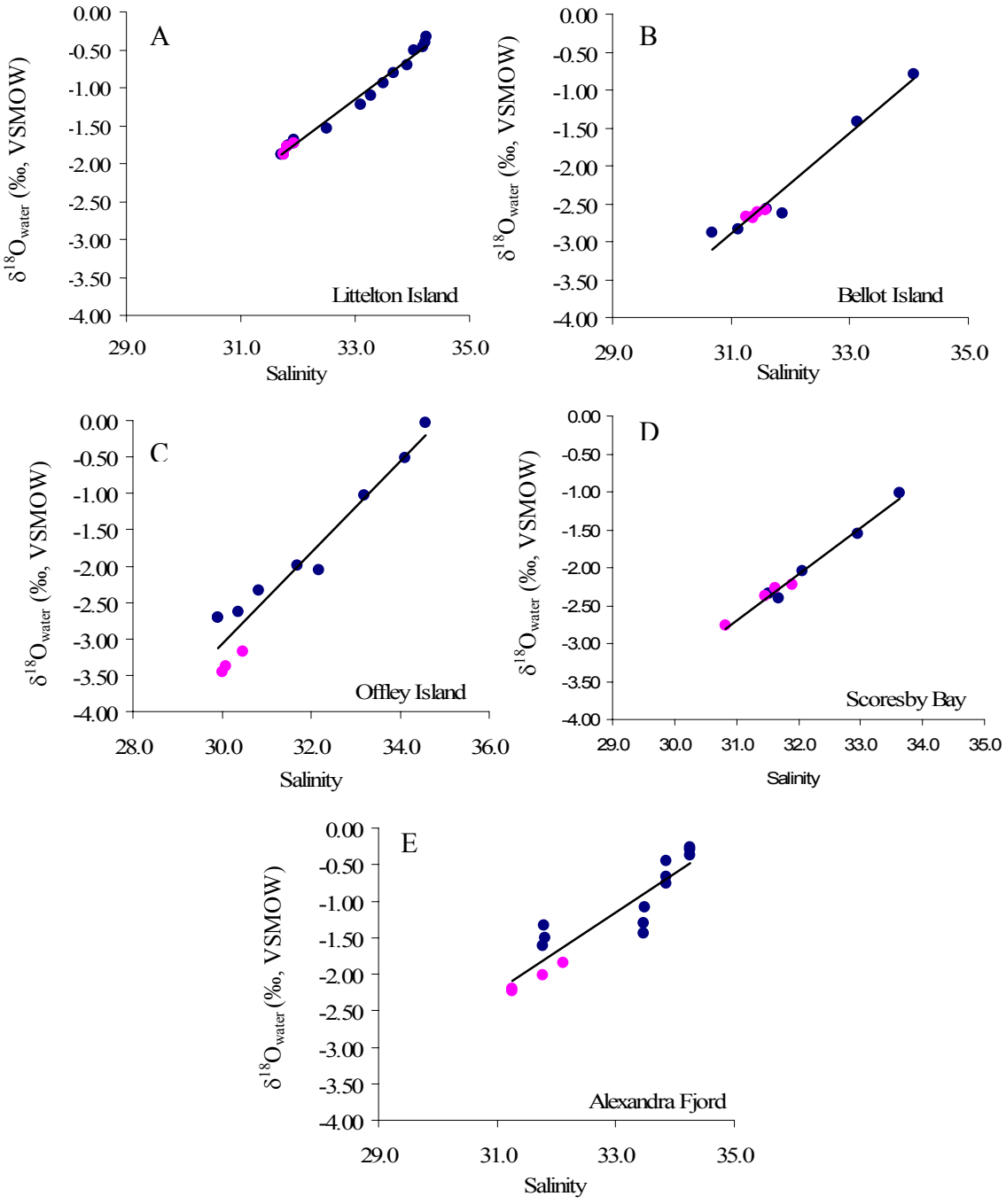

Figure 17: Salinity-$\delta^{18}O$ relationships at each of the bivalve collection sites. A) Littelton Island, B) Bellot Island, C) Offley Island, D) Scoresby Bay, and E) Alexandra Fjord. The blue circles represent the $\delta^{18}O$ and salinity of water samples collected during hydrographic sampling in the Strait closest to the bivalve collection sites, and the pink circles represent salinity and $\delta^{18}O$ water samples collected specifically at the locations of bivalve collection.

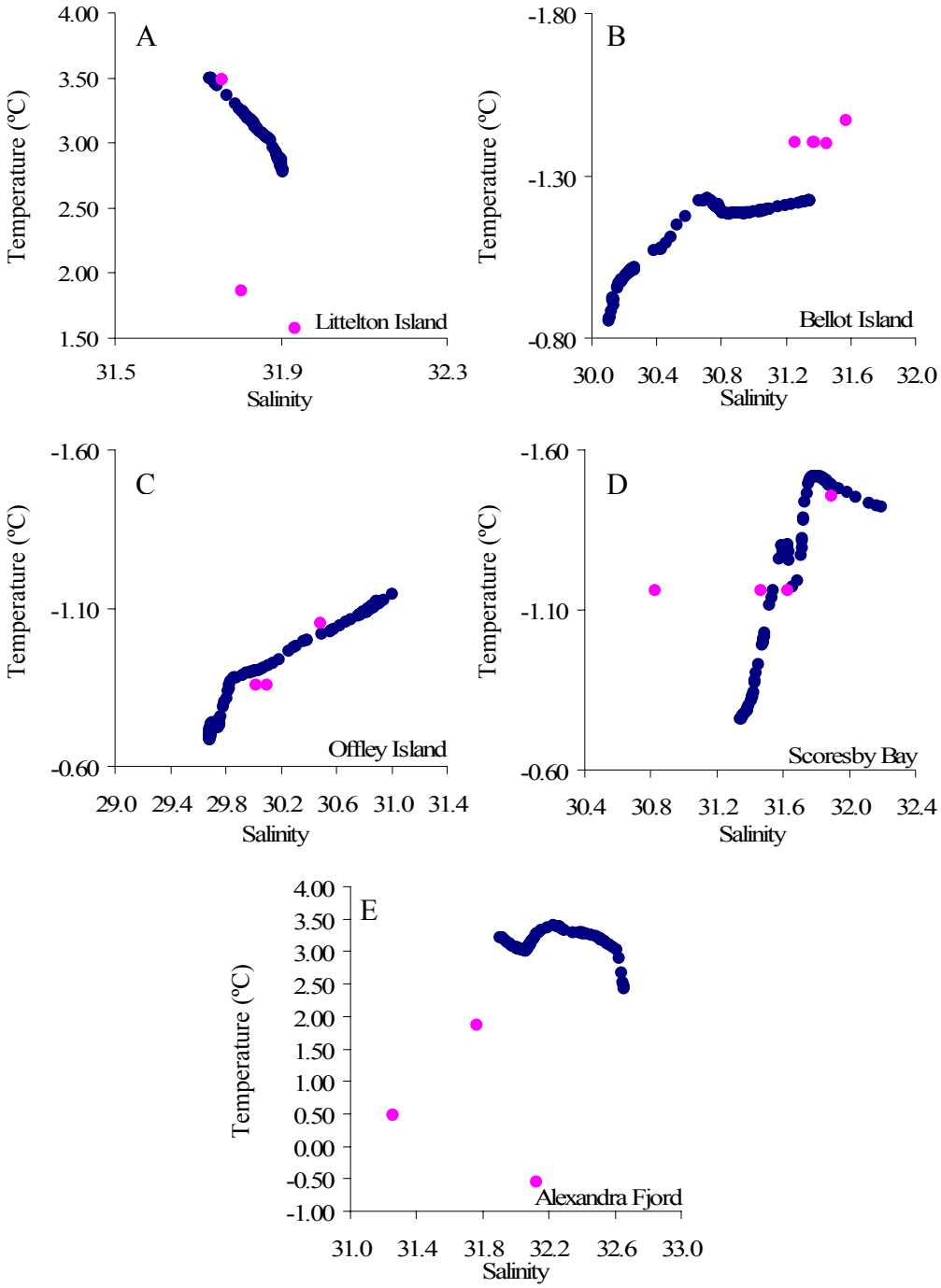

Figure 18: Temperature-salinity diagrams for each of the bivalve collection sites (pink circles). A) Littelton Island, B) Bellot Island, C) Offley Island, D) Scoresby Bay, and E) Alexandra Fjord. Salinity was directly measured, and temperature was estimated using temperature and salinity data from CTD-rosette casts closest to the collection sites (blue circles), and can be found in Tables 4 and 5.

The strong correlation between salinity and $\delta^{18}O$ both at the CTD stations and the bivalve collection sites, and the low temperature variability indicate that salinity variations are reflected in the $\delta^{18}O$ of the water. The more pronounced salinity stratification in the western regions of the hydrographic transects suggests that isotopic variability due to salinity variations in the shells will be more pronounced in these areas. Isotopic values can also be expected to become heavier with depth as salinity increases. Such variations in isotopic compositions can only be applied to an entire year of growth if the August data presented here is assumed to describe the full range of annual variability in salinity that can be experienced in this region. Interannual variability can cause the magnitude of these isotopic signatures to change dramatically with season if the isotopic composition of the freshwater contribution varies. Rivers emptying to the Arctic show seasonal $\delta^{18}O$ variations, but these tend to be small with respect to the difference between river water and seawater. Runoff from glaciers could lead to depletion in freshwater $\delta^{18}O$ values up to -50‰ or more (H. Melling, personal communication, 2006). This effect would presumably be more local, and furthermore, the total melt from glaciers is thought to be small relative to river water input.

3.2 Bivalve Species Distribution and Abundance

Eight species of bivalves were collected on the cruise (Fig. 19), and of the 198 bivalves collected, *Astarte borealis* constituted the most abundant of the species (Table 6).

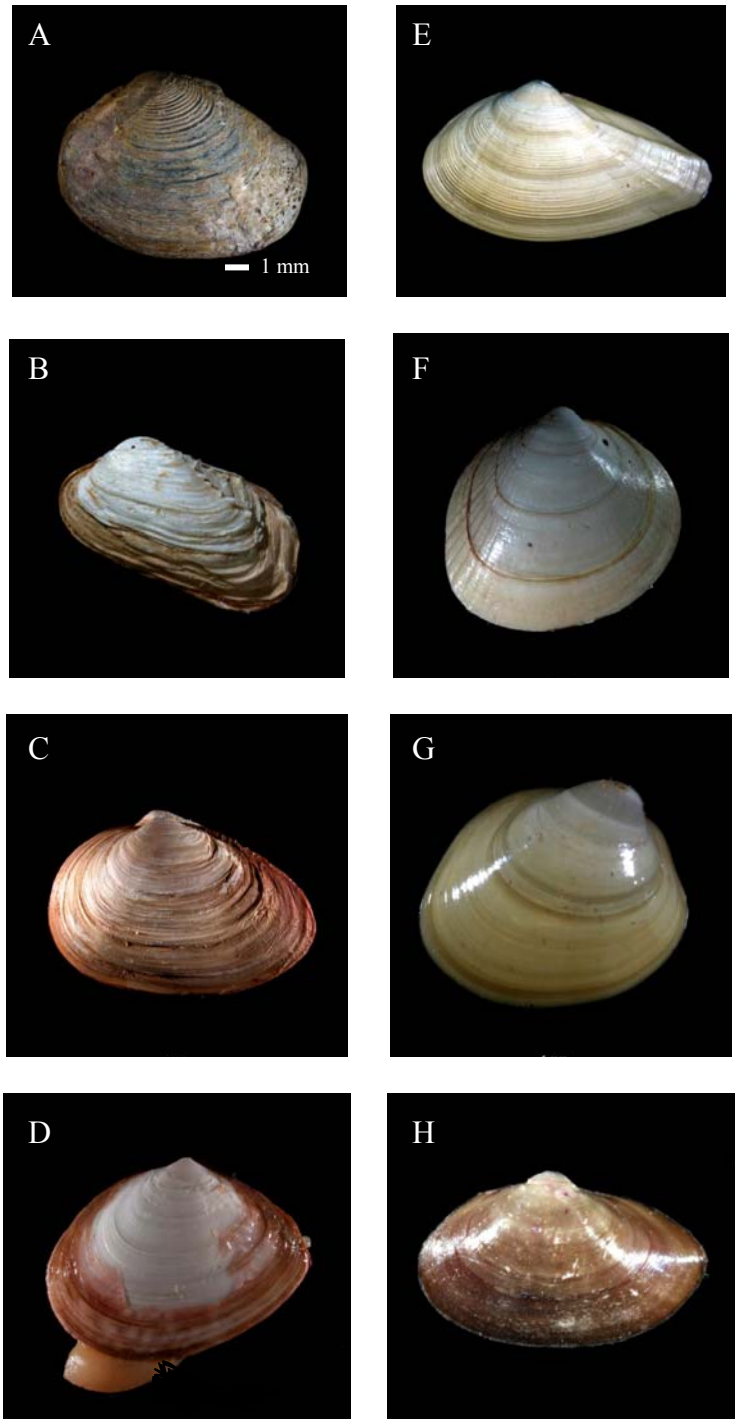

Figure 19: Photographs of the eight bivalve species that were collected in Nares Strait. A) *Astarte borealis*, B) *Hiatella arctica*, C) *Mya truncata,* D) *Macoma calcarea*, E) *Nuculana pernula*, F) *Serripes groenlandicus*, G) *Nucula bellotti*, and H) *Portlandia arctica*. The white line in A denotes the 1 mm size scale for all the photographs.

Table 6: Total number of each of the eight bivalve species collected at the five Arctic bivalve collection sites. Numbers in parentheses represent the number of each species that was dead upon collection.

Species	Alexandra Fjord	Scoresby Bay	Offley Island	Bellot Island	Littelton Island	Total
Astarte borealis	84 (7)	11 (3)	0	28 (2)	0	123
Hiatella arctica	2 (2)	3 (3)	1	15 (5)	1 (1)	22
Macoma calcarea	6	0	0	0	0	6
Mya truncata	5 (4)	6 (4)	0	4 (3)	0	15
Nucula bellotti	2	1	0	1	0	4
Nuculana pernula	2	1	0	0	0	3
Portlandia arctica	0	0	0	13	0	13
Serripes groenlandicus	5 (4)	3	0	3 (1)	1	12

Thirty-nine of the total bivalves collected were dead upon collection, and were not used for aging analysis. Population and species distribution varied with location. Divers were limited to depths shallower than 30 meters (80 feet) due to cold temperatures and poor visibility, so a systematic analysis of the distribution and abundance of the entire bivalve population spatially and with depth was not performed. The terms "distribution", "abundance", and "population" in the remainder of this work pertain only to the specimens collected during our study over the limited depth range that was accessible. Greater diversity of bivalves was collected at Bellot Island, Scoresby Bay, and Alexandra Fjord. Bivalves of all species were generally most abundant at Bellot Island followed closely by Alexandra Fjord, and then Scoresby Bay. Very low species diversity and abundance was observed at Littelton Island and Offley Island, which can most likely be attributed to the poorer benthic habitat (kelp, macrofauna, thick mud) and sampling conditions (turbidity, wind, wave action) observed at these sites. One dead *Hiatella arctica* and one live *Serripes groenlandicus* were collected at Littelton Island, and one live *Hiatella arctica* was collected at Offley Island.

3.3 Age and Depth Distribution of Bivalves

Distribution profiles of the live-collected bivalve ages and species composition with depth were generated for Bellot Island, Scoresby Bay, and Alexandra Fjord where bivalves were most abundant, and the species composition the most diverse (Fig. 20). Littelton Island and Offley Island were not included in these analyses, since only one live individual of *Serripes groenlandicus* was collected at Littelton Island (8 years old, 13.4

meters), and one live *Hiatella arctica* was collected at Offley Island (20 years old, 19.2 meters). *Astarte borealis* was found at all depths at all the other stations, and spanned the largest age range from about 30 to 150 years (+/- 5 years). Live *Hiatella arctica* were collected at Bellot Island over nearly the entire depth range up to approximately 30 meters, and spanned in age from 5 to 50 years (+/- 2 years). Error associated with the counting of growth rings in specimens of *Hiatella* are lower than those associated with *Astarte* because the growth rings of *Astarte* crowd together due to ontogenetic effects (slower metabolism and generation of new shell material with age), so discerning annuli became more of a challenge for these species.

Portlandia arctica was only found to be abundant at the shallower depths of Bellot Island, where they ranged in age from 5 to 106 years (+/-2 to +/-5 in the single, 106 year old individual). Living specimens were not found at any other sampling site. Also present at the shallower collection depths near Bellot Island were one young specimen each of *Nucula belloti* (6 years old), *Mya truncata* (20 years old), and *Serripes groenlandicus* (3 years old). The composition of these minor species varied with the station (Table 6), but in general specimens of *Nucula belloti, Nuculana pernula, Mya truncata, Serripes groenlandicus*, and *Macoma calcarea* were most prevalent in shallower waters (up to approximately 20 meters in the water column). These species were also predominantly either small, or young (10 to 20 years old or less) or both.

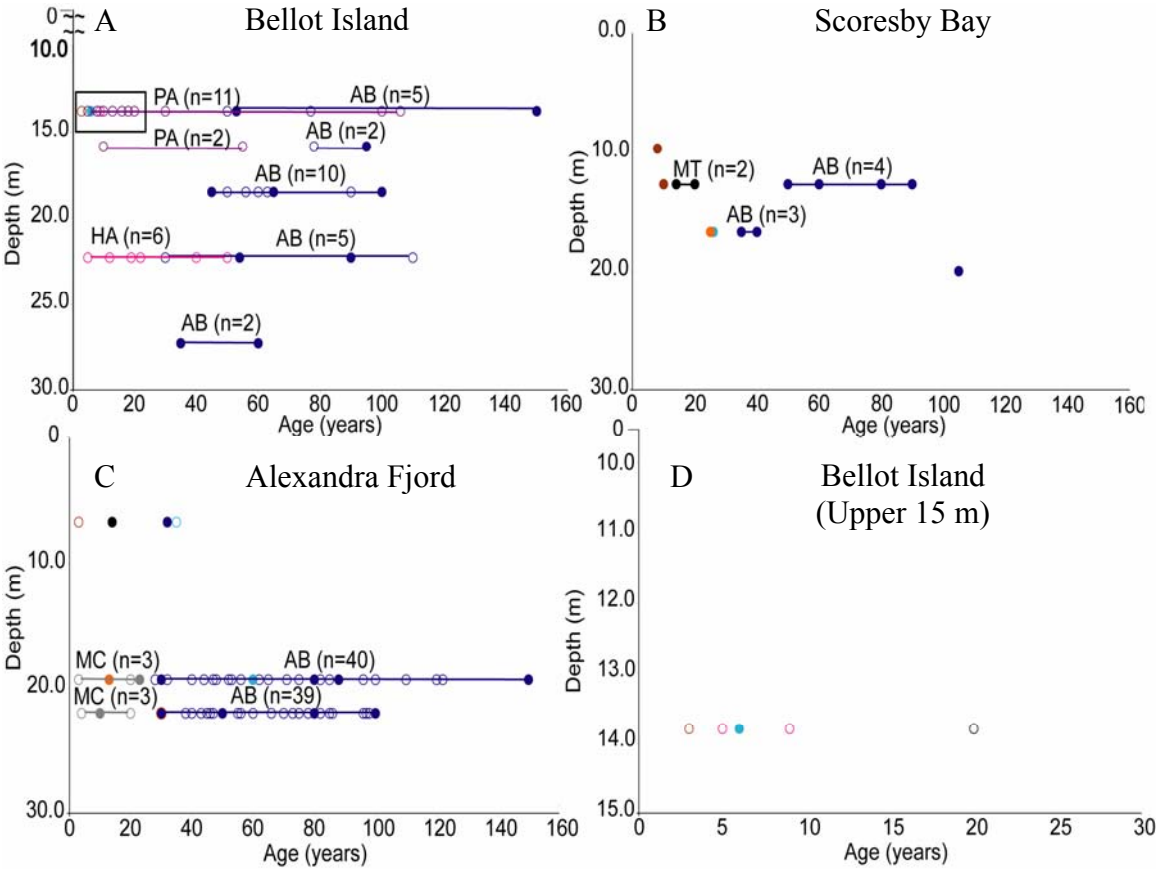

Figure 20: Age and depth distributions of Arctic bivalves. *Astarte borealis* (AB; blue circles), *Hiatella arctica* (HA; pink circles), *Mya truncata* (MT; black circles), *Nucual bellotti* (NB; turqoise circles), *Serripes groenlandicus* (SG; brown circles), *Portlandia arctica* (PA; purple circles), *Macoma calcarea* (MC; gray circles), and *Nuculana pernula* (NP; orange circles) collected from A) Bellot Island, B) Scoresby Bay, and C) Alexandra Fjord. Solid lines corresponding to the colors of the symbols for the different species represent the age range for that species at a particular depth of collection. The numbers in parentheses indicate the number of individuals of a species that were collected at a particular depth. Closed circles indicate individuals that were drilled for isotope analysis. Panel D is a blow up of the boxed area in panel A for the upper 15 m of the water column at Bellot Island, showing the depth and age distribution of species collected in lower abundance at this depth.

Older bivalves were represented by the species *Astarte borealis* and *Hiatella arctica,* and were found to be abundant at depths throughout the water column at all the sampling sites (particularly *Astarte borealis).* The oldest specimens of *Astarte borealis*

were found at Bellot Island and Alexandra Fjord. Given their longevity and ubiquitous distribution geographically and with depth, *Astarte borealis* may be the best candidate for providing longer-term proxy records for freshwater throughflow in the Nares Strait. The distribution profile for Bellot Island (Fig. 20A) represents similar findings for both Scoresby Bay and Alexandra Fjord. A complete size, age, weight and species summary for live collected Arctic bivalves organized by station and depth of collection can be found in Appendix I and Appendix II.

3.4 Arctic Bivalve Growth and Production

The total shell length and organic tissue mass measured as shell free wet weight (SFWW) were plotted as a function of depth for each of the species collected (Fig. 21). The size patterns discussed in this study pertain only to the specimens we collected, and are not representative of the bivalve population at these locations because a systematic size distribution survey was not performed. Biomass and size were variable among the species, however, the highest SFWW and largest shells were concentrated between 15 and 25 meters water depth, which is also where the greatest abundance and oldest individuals of all species were collected (Fig. 20). SFWW ranged from ~0.1g in smaller species like *N. bellotti* and *N. pernula*, up to 25 grams for *S. groenlandicus* and *M. truncata.* With the exception of a few outliers, the maximum SFWW attained by individuals of *Astarte borealis, Hiatella arctica, Mya truncata,* and *Macoma calcarea* ranged from 5.0g to 6.0g.

Figure 21: Distribution of organic tissue mass as shell free wet weight (pink squares) and shell length (blue circles) with depth for the 8 bivalve species collected. A) *Astarte borealis*, B) *Hiatella arctica*, C) *Mya truncata*, D) *Macoma calcarea*, E) *Nuculana pernula*, F) *Serripes groenlandicus*, G) *Nucula bellotti*, and H) *Portlandia arctica*.

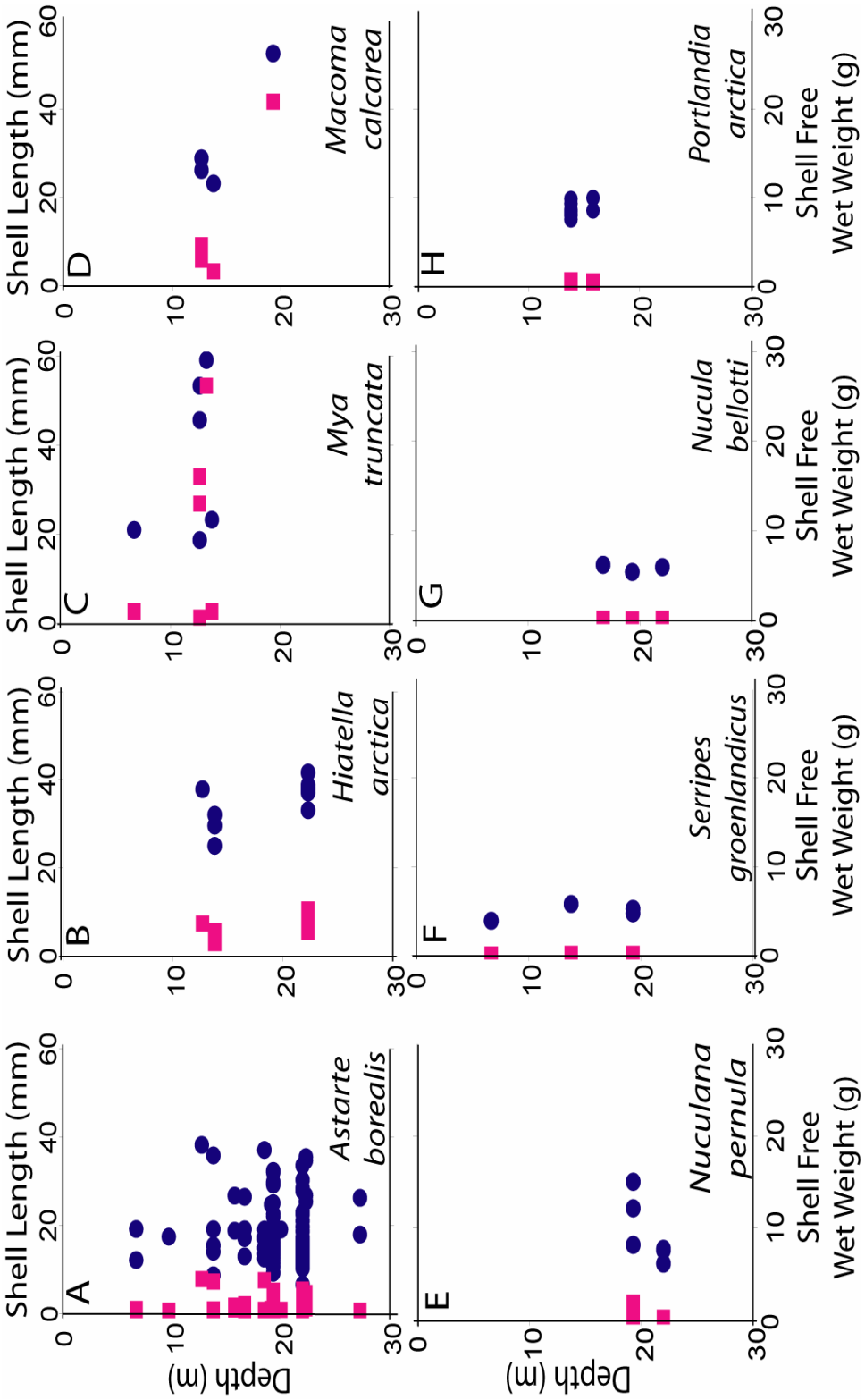
A
B
C
D
E
F
G
H
Depth (m)
Shell Length (mm)
Shell Free Wet Weight (g)
Astarte borealis
Hiatella arctica
Mya truncata
Macoma calcarea
Nuculana pernula
Serripes groenlandicus
Nucula bellotti
Portlandia arctica

Figure 21

Shell lengths ranged from a minimum of 10 mm to 40 mm for the species collected, with the exception of *S. groenlandicus* and *M. truncata*, which reached maximum lengths of near 60 mm (Fig. 21). In general, variability in size of individuals smaller than 30 mm in length is usually attributed to mortality, whereas variations in the characteristic maximum length and shell shape attained by each species controls the size distribution in individuals greater than 30 mm (Sejr et al., 2002). The uniform maximum length attained by the species collected in this study, with the exception of the smaller species *Nucula bellotti, Nuculana pernula*, and *Portlandia arctica,* suggests that they are all essentially affected similarly by the growth conditions in this region.

Length measurements were plotted as a function of age for all the live-collected bivalve species (Fig. 22). *Hiatella arctica* and *Astarte borealis* attained maximum lengths near 40 mm, although the majority of the *A. borealis* population attained lesser lengths (Fig. 22A). The sizes ranged from a minimum of 10 mm to 60 mm for individuals of *Serripes groenlandicus*. Individuals of *Nucula bellotti, Nuculana pernula, Portlandia arctica*, and *Macoma calcarea* reached maximum lengths of 12 mm, 20 mm, and 30 mm respectively, even in the case of the oldest individuals collected (Fig. 22B). The small maximum size of these species regardless of their age made them unsuitable for isotopic analysis beyond the youngest shell section due to poor resolution between growth lines. The lack of individuals of some species below 10 mm (Figs. 21 and 22) may imply high mortality rates in juvenile bivalves (< 10 or 20 mm), due to consumption by brittle stars, walrus, and eider duck, which has been indicated in previous studies in Arctic regions.

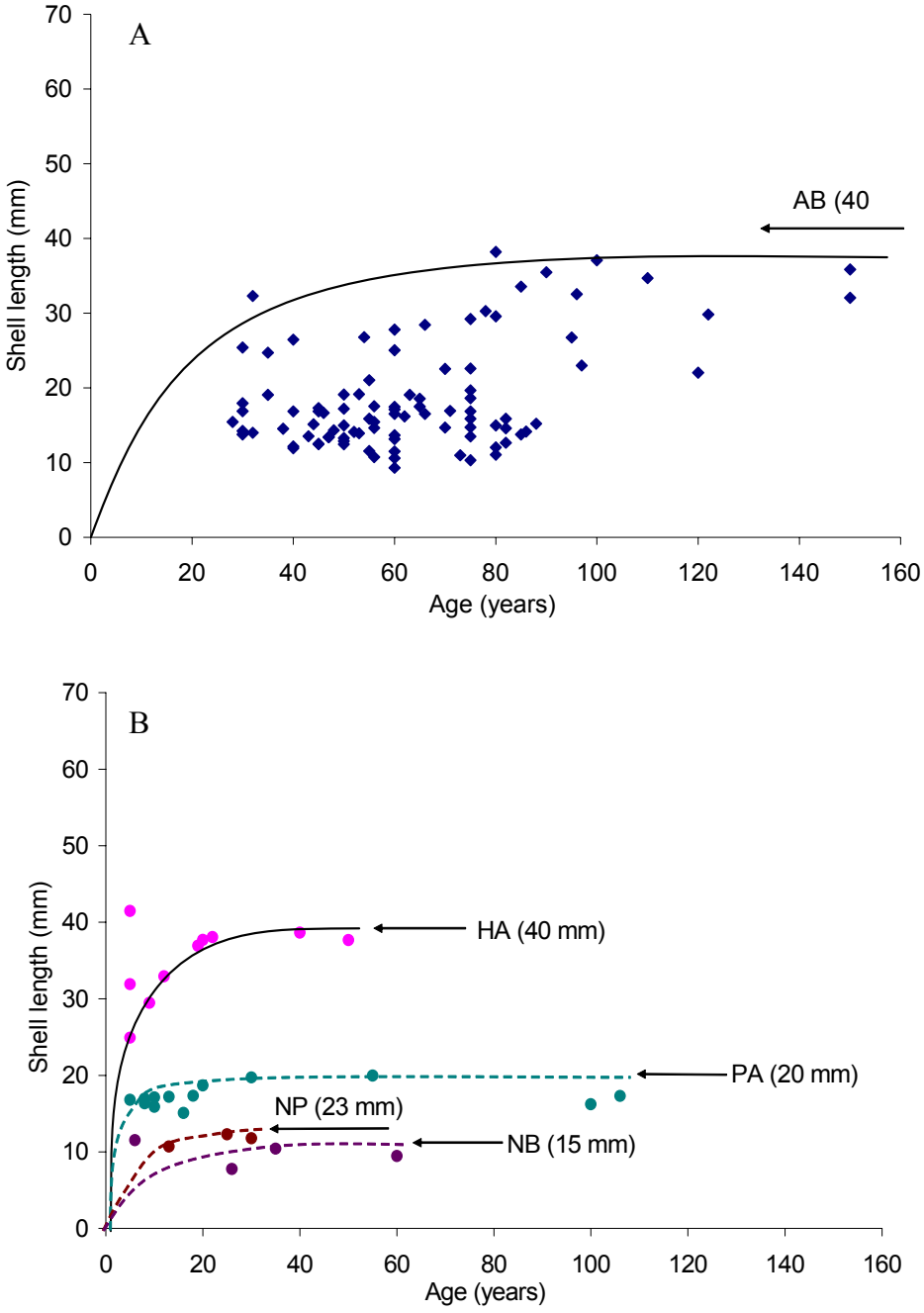

Figure 22: Length-at-age distribution for species of live-collected Arctic bivalves. A) *Astarte borealis* and B) *Nucula bellotti (*NB), *Nuculana pernula* (NP), *Portlandia arctica* (PA), and *Hiatella arctica* (HA). The arrows show the average maximum length for each species observed from other studies in the Arctic (Table 7). The solid lines show the VBGF curve fit to the length-at-age data for individual specimens of *Astarte borealis* and *Hiatella arctica* as illustrated in Figures 28 and 29.

3.5 Isotope Data

Sixteen bivalve shell cross-sections were milled and analyzed for $\delta^{13}C$ and $\delta^{18}O$ isotopic composition, including 5 specimens of *Hiatella arctica* collected from two depths at Bellot Island (14 and 22 meters), and 11 specimens of *Astarte borealis* collected from Bellot Island, Scoresby Bay, and Alexandra Fjord. These specimens were all collected from the western side of the channel, which exhibited greater spatial variability in temperature and salinity than the eastern side. If such variations in salinity hold throughout the year, the isotopic signatures in shells from these regions should reflect more variability than the specimens from the eastern side of the channel, which was sampled at Littelton Island (Station 1) and Offley Island (Station 3).

The shells that were drilled for complete isotopic profiles represent one or two of the oldest specimens collected at each depth for each site. Full-shell isotopic records were collected from *Astarte borealis* and *Hiatella arctica* because they were the oldest and most abundant species collected at each site (Fig. 20), thereby making it possible to obtain longer term isotopic records (up to 150 years). These longer term isotopic records provide some insight as to whether the anomalously light isotope values in the youngest shell sections were a modern occurrence, or if the signal can be traced back to the point where a change in freshwater influence may have started. The $\delta^{13}C$ and $\delta^{18}O$ profiles in *Astarte* shells generally show a shift towards lighter isotopic signatures during the most recent year of growth (Figs. 23-25).

Figure 23. A-I: Results of $\delta^{13}C$ (blue symbols) and $\delta^{18}O$ (pink symbols) analysis on *Hiatella arctica* and *Astarte borealis* shells from Bellot Island as a function of age. Zero age denotes the date of collection (2003) and arrow on x-axis indicates the age of each individual specimen.

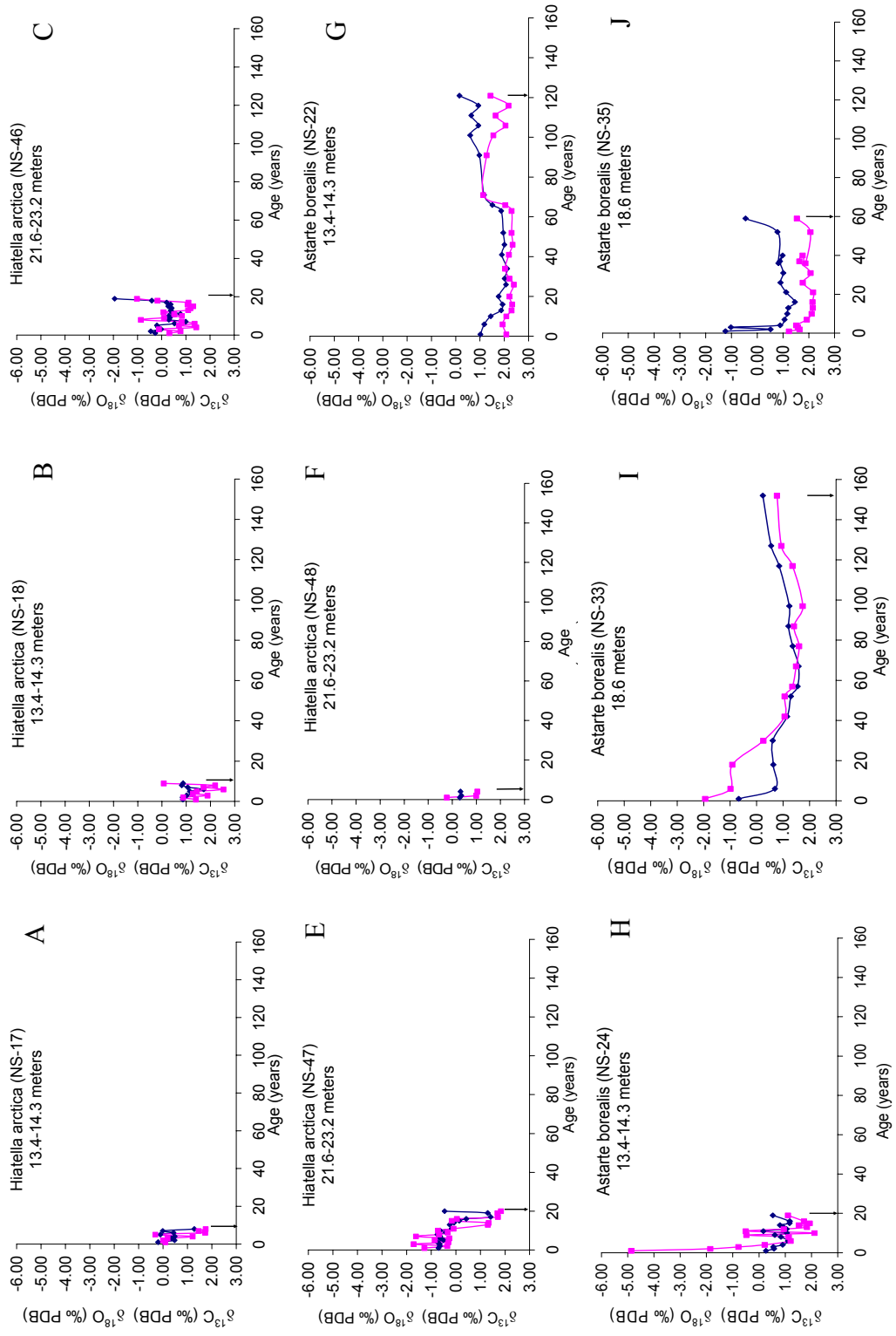
A
Hiatella arctica (NS-17)
13.4-14.3 meters
B
Hiatella arctica (NS-18)
13.4-14.3 meters
C
Hiatella arctica (NS-46)
21.6-23.2 meters
E
Hiatella arctica (NS-47)
21.6-23.2 meters
F
Hiatella arctica (NS-48)
21.6-23.2 meters
G
Astarte borealis (NS-22)
13.4-14.3 meters
H
Astarte borealis (NS-24)
13.4-14.3 meters
I
Astarte borealis (NS-33)
18.6 meters
J
Astarte borealis (NS-35)
18.6 meters
δ13C (‰ PDB) δ18O (‰ PDB)
Age (years)

Figure 23

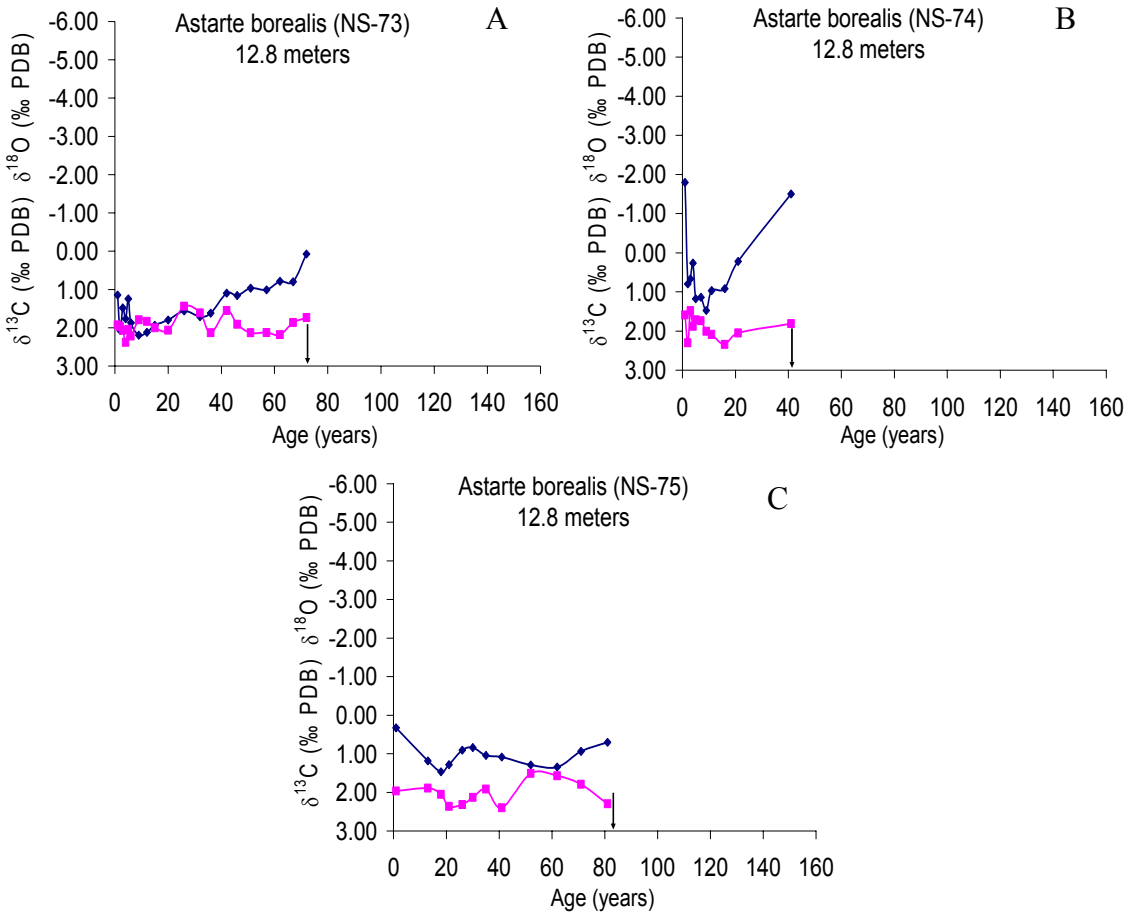

Figure 24, A-C: Results of $\delta^{13}C$ (blue symbols) and $\delta^{18}O$ (pink symbols) analysis on *Hiatella arctica* and *Astarte borealis* shells from Scoresby Bay. Zero age denotes the date of collection (2003) and arrow on x-axis indicates the age of each individual specimen.

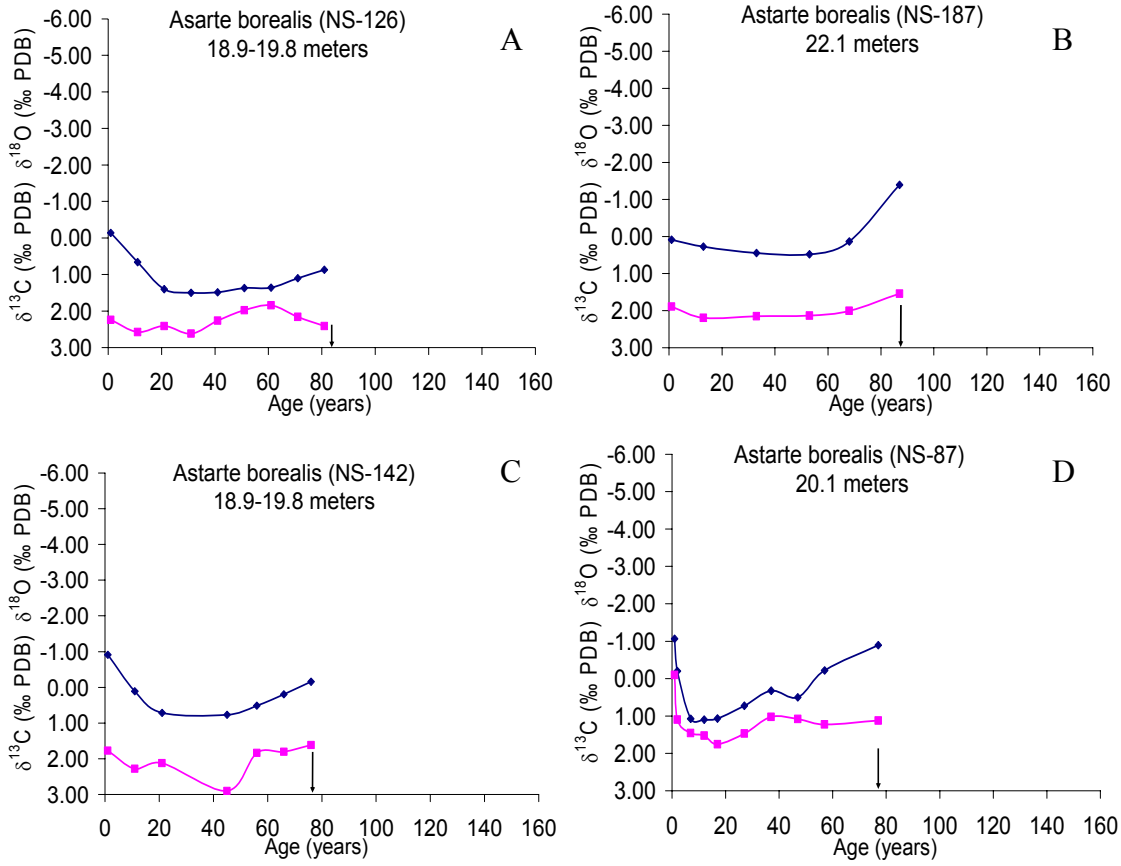

Figure 25, A-D: Results of $\delta^{13}C$ (blue symbols) and $\delta^{18}O$ (pink symbols) analysis on *Hiatella arctica* and *Astarte borealis* shells from Alexandra Fjord. Zero age denotes the data of collection (2003) and arrow on x-axis indicates the age of each individual specimen.

3.6 Carbon Isotopic Signatures

The $\delta^{13}C$ signatures in our shells vary by 4.5‰ (2.50‰ to -2‰). These results are comparable to the range of carbon isotopic signatures previously observed in specimens of *Astarte borealis* and *Hiatella arctica* from the Chuckchi Sea (-3‰ to 2‰; Khim et al., 2001; 2003), the Laptev Sea (-1.5‰ to 1‰; Mueller-Lupp et al., 2003), and the Kara Sea (-4‰ to 1‰; Simstich et al., 2005). The maximum and minimum carbon isotopic values represented in our shells have been observed in individual specimens from these other study regions, which suggests that the dominant source of carbon is marine derived inorganic calcium carbonate (≈ +1.5‰; Mook et al., 1974). Furthermore, it appears that changes in $\delta^{13}C$ are independent of changes in $\delta^{18}O$ profiles (Fig. 26). This figure also illustrates that the lightest $\delta^{18}O$ values occur most frequently in shells collected from Bellot Island (Station 2). The isotope data for these specimens are listed in Appendix III.

We do not have an explanation for why the $\delta^{13}C$ values vary significantly (nearly 4‰) in some cases within an individual shell, especially since we do not have ^{13}C measurements from water samples in this region. However, negative trends in carbon isotopic signatures from bivalves in other Arctic regions have been observed in response to input of reduced-salinity estuarine or riverine waters (Mueller-Lupp et al., 2003; 2004; Khim et al., 2003), which can range in isotopic composition from -5 or -6‰ (Macdonald et al., 2005; Macdonald, 2000) to nearly -26‰ (Macdonald, 2000). Trends toward lighter (more negative) $\delta^{13}C$ values in the later years for most of our bivalves suggests control by

ontogenetic factors, due to relationships between environmental variables, different growth phases, and the onset of sexual maturity.

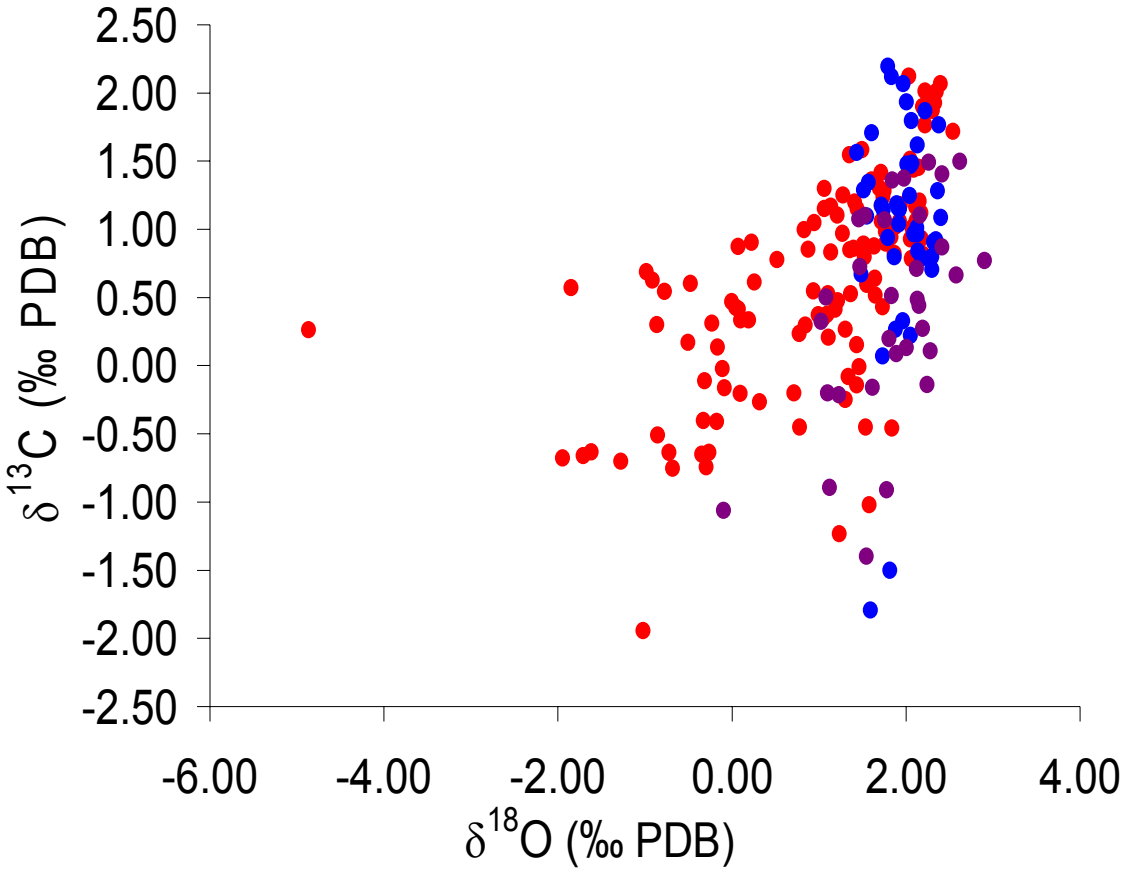

Figure 26: Relationship between $\delta^{13}C$ and $\delta^{18}O$ for *Hiatella arctica* and *Astarte borealis* from all stations in Nares Strait. Red, blue, and purple dots represent individuals collected from Bellot Island (Station 2), Scoresby Bay (Station 4), and Alexandra Fjord (Station 5) respectively.

The physiological change related to the transformation from a fast-growing juvenile stage to a slower-growing adult stage in which metabolic energy is primarily shunted into gametogenesis is manifested in very light shell $\delta^{13}C$ values (Jones et al., 1986). The mechanism proposed to be involved in this process is the inclusion of more

metabolically-derived CO_2 into the bicarbonate pool used in calcification (Krantz et al., 1987; Rodhouse, 1998). Furthermore, the $\delta^{13}C$ of the diet and the input of terrestrial material and light organic carbon material (-20‰ and -24‰ respectively) may be controlling factors on the carbon composition of the shell as well (Mook et al., 1974; Khim et al., 2001; 2003; Mueller-Lupp et al., 2003).

4. DISCUSSION

4.1 Arctic Bivalve Distribution and Abundance

The bivalve specimens collected in our study were most abundant in the 10 to 25 m depth interval (Fig. 21), which is within the intertidal to 50 m depth distribution range of similar species noted in other studies in the Canadian Archipelago and high Arctic, including Baffin Bay and Greenland (Tables 1 and 2). Specimens of *Macoma calcarea, Mya truncata, Serripes groenlandicus, Portlandia arctica, Nucula bellotti,* and *Nuculana pernula* were typically low and variable in abundance at our sampling sites (Fig. 20). *Astarte borealis* and *Hiatella arctica* were the most abundant species at all the sampling sites (Fig. 20). They are adapted to a wide range of environments and are generally found from shallow waters near glacier margins up to 50 m water depth (e.g. Dale et al., 1989; Syvitski et al., 1989), but in some cases they are present in fjords at depths greater than 50 m (e.g. Dale et al., 1989; Aitken and Fournier, 1993). At other high latitude sites, including Disco Bay Greenland and Baffin Island, *H. arctica* are concentrated at depths shallower than 50 m (Table 2). Similarly, *Astarte borealis* has been found at 0-50 meters in regions including the Chuckchi Sea (Khim et al., 2001; 2003), the Laptev Sea (Mueller-Lupp et al., 2003; 2004; Mueller-Lupp and Bauch, 2005), the Kara Sea (Simstich et al., 2005), Expedition Fjord and Western Axel Heiberg Island (Aitken and Gilbert, 1995; Gordillo and Aitken, 2000).

Previous studies in the Canadian Archipelago show these species to occupy a range of substrates, from fine to coarse-grained materials, including clay, and poorly sorted mixtures of sand, mud, and gravel (Table 2). Depth and depth variable substrate

have been shown to be critical determinants of benthic community composition and abundance (e.g. Thomson et al., 1986; Petersen, 1978). Most of the bivalve collection sites in our study were composed of fine-grained sand and soft muddy sediments that were organic rich (see Methods section on bivalve collection).

4.2 Arctic Bivalve Growth and Production

Except for *Hiatella arctica* and *Portlandia arctica*, lengths attained by the specimens in our study range from 52% to 88% of the maximum observed sizes throughout the Canadian Arctic and Archipelago (Table 7). Because the specimens of *Mya truncata*, *Macoma calcarea*, and *Serripes groenlandicus* that were collected were few in number, varied considerably in length, and were relatively young, conclusive determinations of the maximum attainable size were not made. Being so few in number, these species were not included in our considerations of the relationship between length and age.

The length-at-age data for *Hiatella arctica* and *Astarte borealis* were fit to a von Bertalanffy growth function (VBGF), one of the most commonly used descriptive models of size-at-age data for a variety of animals (von Bertalanffy, 1938; Cloern and Nichols, 1978; Essington et al., 2001; Urban, 2002). This model assumes than an organism grows towards some theoretical maximum length or weight, and incorporates metabolic considerations such as anabolism and catabolism (Urban, 2002) to account for the way in which the growth rate of organisms slows down with increasing age and length (De Graaf and Prein, 2005). As body size increases, the amount of energy produced by food consumption that goes into valve growth decreases relative to the amount of energy lost

as heat to respiration and sexual development. This mechanism is one likely explanation for the observed asymptotic growth curve in most bivalves (Rodhouse, 1998). The VBGF is defined as follows:

$$L_t = L_\infty \times [1 - e^{-K(t-to)}], \quad (1)$$

where L_t is the shell length at time t, L_∞ is the maximum asymptotic shell length, and K is the annual growth coefficient. Other functions can be substituted in for the growth coefficient (K) term in the VBGF model to account for seasonal fluctuations in food supply and temperature (Cloern and Nichols, 1978; Rodhouse, 1998; Porch et al., 2002), however, these models do not improve the fit the length-at-age data collected for the bivalves in our study.

The length-at-age data for the live collected *Hiatella arctica* generally show a behavior consistent with a VBGF growth (L_∞ = 37.2 mm, K = 0.14 yr^{-1}, and t_o = -1.4) but exhibit some variation, which we attribute to changes in the maximum length and shell shape of adult individuals (Fig. 27). The maximum shell length (L_∞) fit is smaller than the maximum length of about 45 mm observed in other Arctic regions (Table 7). This value used in calculations of production could result in as much as a 10% underestimation of production of *Hiatella* for both our study area and the Young Sound region, Northeast Greenland (Sejr et al., 2002). The estimated growth coefficient (K = 0.14 yr^{-1}) is within the range of values reported for 6 Antarctic bivalves (0.085 to 0.345 yr^{-1}; Brey and Clarke, 1993) and comparable to the growth of the Iceland scallop *Chlamys islandica* from West Greenland (0.12 yr^{-1}; Pedersen, 1994).

Table 7: Length ranges and typical maximum lengths for adult individuals of the bivalve species collected in this study, and from previous studies in the Arctic. Lengths from our study that are listed in italics represent species for which there were too few data points to be certain that the maximum length was represented in our sample set of collected bivalves. Numbers in parentheses under each species name indicates the references from which information on the length distribution for each species in other Arctic regions was compiled (Table 1).

Table 7

Species	Size range in other Arctic regions (mm)	Size range in our study (mm)	Typical maximum size in other Arctic regions (mm)	Typical maximum size in our study (mm)
Astarte borealis (8, 16, 28, 30)	10-40	8-35	40	35
Hiatella arctica (3, 8, 32, 33, 10)	15-45	10-41	40	38
Macoma calcarea (3, 8, 16, 26, 28)	10-45	10-30	30	*25*
Mya truncata (3, 8, 16, 26, 28)	10-70	20-55	60	*55*
Serripes groenlandicus (3, 8, 16, 26, 28)	10-100	18-60	90	*60*
Portlandia arctica (8)	10-25	10-20	20	20
Nucula bellotti (8)	6-17	8-10	15	10
Nuculana pernula (8)	10-30	8-10	25	12

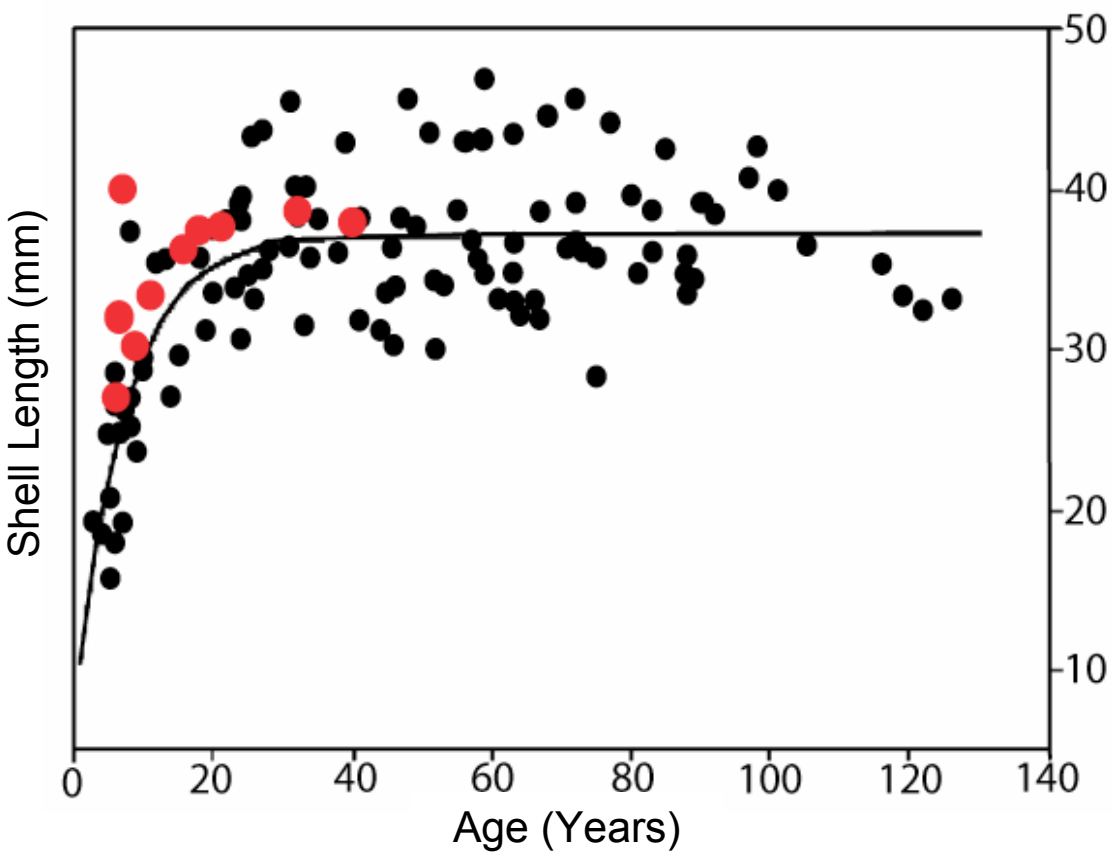

Figure 27: Von Bertalanfly growth curve fitted to length at age data for specimens of *Hiatella arctica.* Red circles represent length-at-age measurements for *H. arctica* from this study, and black circles represent measurements on *H. arctica* from Young Sound, Northeast Greenland (Sejr et al., 2002). Age was estimated from internal growth bands in the shell. L_∞ = 37.2 mm, K = 0.14 yr^{-1}, t_o = -1.4 yr.

The length-at-age data for *Nucula bellotti, Nuculana pernula*, and *Portlandia arctica* show that these species are smaller than their maximum observed sizes in the Arctic (Fig. 22, Panel B), but they are still within the range of sizes that has been observed (Table 7), and show an expected exponential growth pattern.

In contrast with the other species, there is a notable deviation from the modeled growth curve in most of the specimens of *Astarte borealis* (Fig. 22, Panel A), such that they are significantly smaller than their ages would suggest. To examine whether this

deviation from modeled growth was a species-specific phenomenon, the length at each year of age estimated from growth bands on individual specimens of *Hiatella arctica* (NS-49) and *Astarte borealis* (NS-95) were fit to the VBGF (Figs. 28 and 29). Each of these specimens followed the predicted pattern reasonably closely, although they appeared to grow somewhat slower than predicted in the first 15 years of age. These results suggest that individuals of both *Hiatella arctica* and *Astarte borealis* appear to follow expected growth patterns. Observed deviations from expected exponential growth behavior in the studied specimens of *Astarte borealis* may reflect the effect of environmental variables.

The predominance of relatively young and small bivalves at our sampling sites may be a result of ice scour at the seafloor. Other potential factors hindering growth to the expected maximum sizes in *Astarte borealis* could include temperature and nutrient availability. A combination of low temperatures and short period of food supply have indeed been invoked as parameters responsible for the low growth observed in polar organisms (Petersen, 1978; Lubinsky, 1980; Thomson et al., 1986; Brey and Clarke, 1993; Arntz et al., 1994; Aitken and Gilbert, 1995; Gordillo and Aitken, 2000; Ambrose et al., 2006). The optimal growth temperatures for the bivalves examined in our study have been determined to range from -2ºC to 6ºC (Gordillo and Aitken, 2000), which are well within the range observed at our sampling locations (-2ºC to 4ºC; Table 4). Thus temperature-limitation is probably not the dominant factor hindering the growth of *Astarte borealis* individuals.

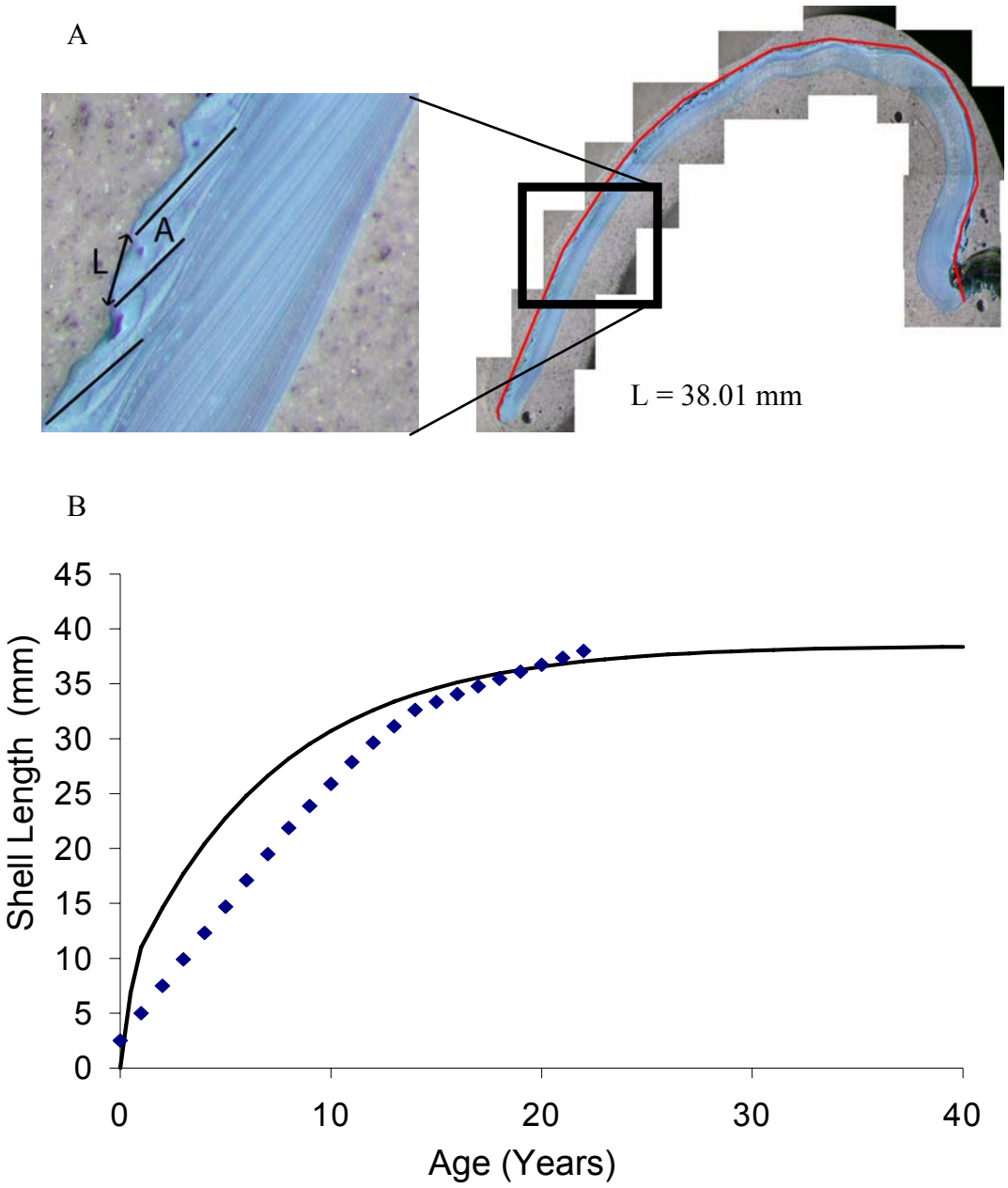

Figure 28: A) Cross-section of the shell of an individual specimen of *Hiatella arctica* (NS-49) showing the total length (L) measured from the umbo to the tip of the ventral margin (red line). The inset shows a magnification of the boxed area that indicates the location of annual growth lines (diagonal lines), a layer of shell growth equivalent to one year of age (A), and the length of one shell layer of growth (L). B) Bertalanffy growth function fit to length-at-age data from the individual specimen of *Hiatella*, where $L\infty$ = 38.5 mm, K = -0.14 yr^{-1}, and t_o = -1.4 yr.

A

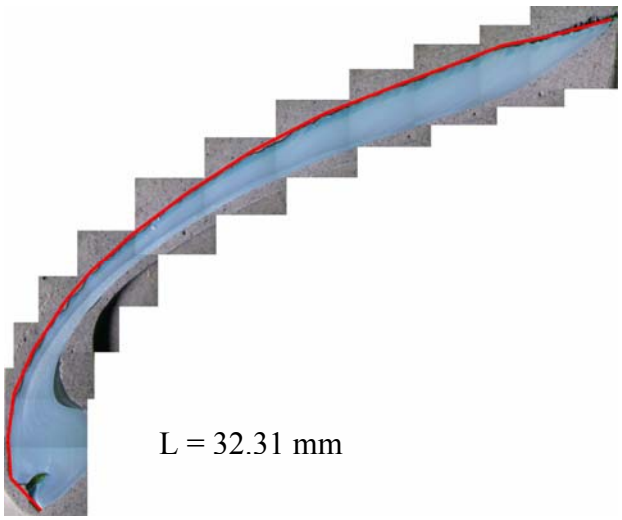

B

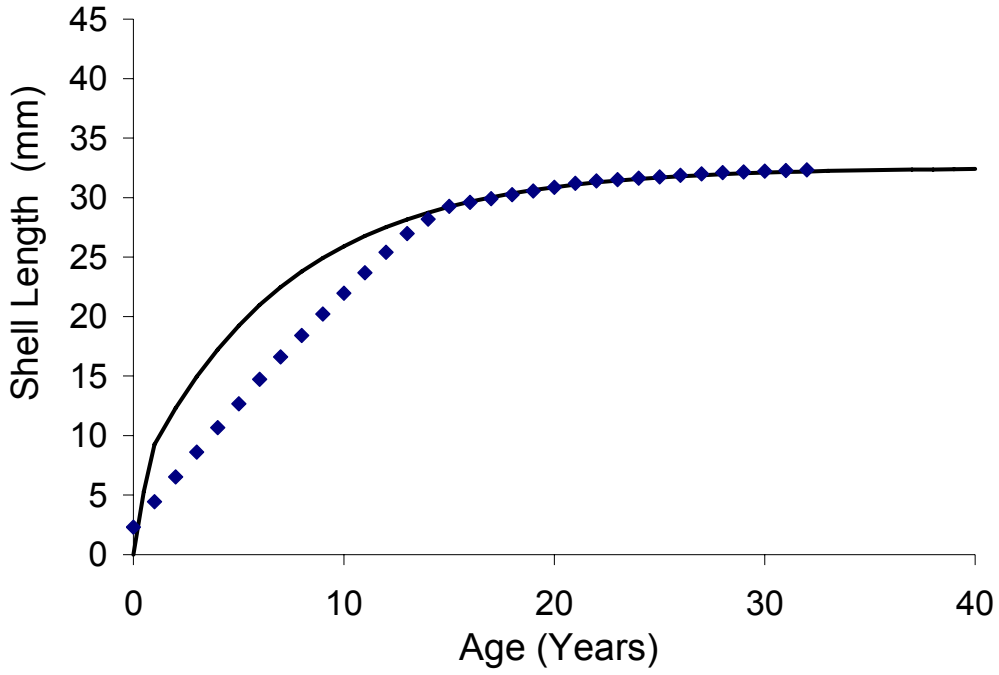

Figure 29: Cross-section of an individual specimen of *Astarte borealis* (NS-95) showing the total length (L) measured from the umbo to the tip of the ventral margin. B) Bertalanffy growth function fit to length-at-age data from the individual specimen of *Astarte borealis*, where $L\infty = 32.5$ mm, $K = -0.14$ yr^{-1}, and $t_o = -1.4$ yr.

Studies of the mussel *Mytilus edulis* have shown that primary production and food supply to the benthos is the dominant variable controlling their growth (Ambrose et al., 2006). We do not have data to evaluate whether these organisms we collected were limited by the quantity or quality of food reaching their depth of growth in the Nares Strait. However, it is puzzling that only *Astarte borealis* seems to show significant deviation from the expected exponential growth, suggesting perhaps that this species is more vulnerable to environmental conditions.

4.3 Bivalve Reliability as Hydrographic Indicators

If our bivalve collection sites are in fact not impacted by limited local influences of freshwater, then the isotopic composition ($\delta^{18}O$) of the shell should reflect the ambient $\delta^{18}O_{water}$ and possibly temperature. The variation of the $\delta^{18}O_{water}$ as a function of salinity is shown in Fig. 30. The data appear to show a linear fit, following the relationship:

$$\delta^{18}O_{water} = 0.69 \cdot \text{Salinity} - 24.17‰ \quad (2)$$

The high correlation is the result of a two-endmember mixing pattern, where saline Atlantic water of neutral (0‰) isotopic composition mixes with highly negative $\delta^{18}O$ values associated with fresher Arctic riverine inputs. Taking into account error in both the salinity and $\delta^{18}O_{water}$ measurements, this relationship implies a freshwater $\delta^{18}O$ endmember of -24.17‰ (+/- 1.10 at the 95% confidence interval; n =170; $R^2 = 0.95$), which was depleted in comparison to the measured value for a river discharging near the Scoresby Bay collection site during this study ($\delta^{18}O$ = -23.40‰), but enriched with respect to the measurements for river input and ice melt (~ $\delta^{18}O$ =

-25.85‰) near Offley Island (Table 8; MacDonald and Falkner, unpublished data). More significantly, the calculated $\delta^{18}O$ value for the freshwater endmember in this study is depleted in comparison to the annual range of variability in values previously documented for six major rivers in the Arctic (Table 8), which can range from -14.8 to -16.3‰ in the Ob River (e.g. Cooper et al., 2005; Bauch et al., 2005), to -18.9 or -22.6‰ in the Lena River (Cooper et al., 2005).

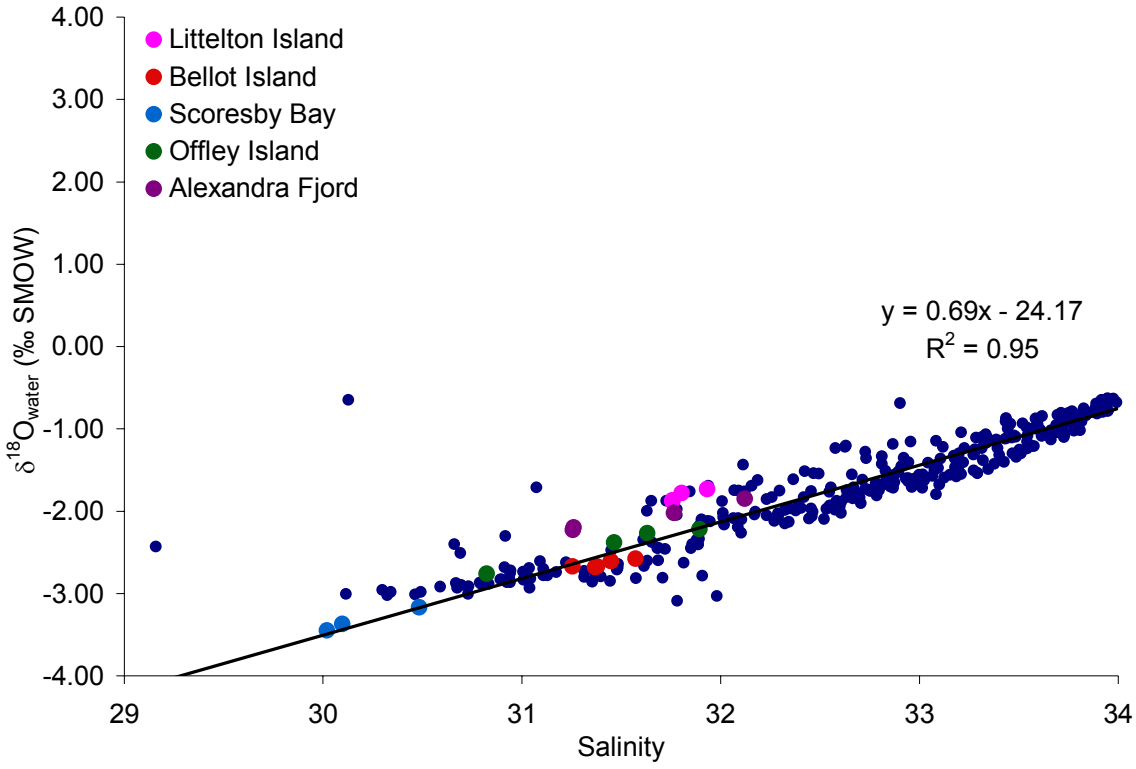

Figure 30: Relationship between salinity and $\delta^{18}O_{water}$ for the Nares Strait region. The equation describes the extrapolation of the salinity-$\delta^{18}O_{water}$ relationship for Nares Strait to the implied freshwater (S=0) endmember $\delta^{18}O_{water}$ value (-24.17‰ at the 95% confidence interval).

Table 8: Measured $\delta^{18}O_{water}$ values for freshwater sources to the Arctic, including the ranges of variability for six major rivers, mean values for ice and rivers near bivalve collection sites from this study, and mean salinity Arctic Ocean water.

River	River $\delta^{18}O$	Data Source(s)
River near Offley Island	-25.15	This study (MacDonald and Falkner, unpublished data)
River near Scoresby Bay	-23.4	This study (MacDonald and Falkner, unpublished data)
Ice melt near Offley Island	-25.85	This study (MacDonald and Falkner, unpublished data)
Yukon River	-20.0 to -20.8	Cooper et al., 2005
Lena River	-18.9 to -22.6	Letolle et al., 1993; Mueller-Lupp and Bauch, 2005; Bauch et al., 2005 Cooper et al., 2005
Mackenzie River	-18.8 to -20.3	MacDonald et al., 1995; MacDonald, 2000; Bauch et al., 2005; Cooper et al., 2005
Kolyma River	-21.0 to -22.4	Bauch et al., 2005 Welp et al., 2005
Yenisey River	-17.1 to -21.3	Bauch et al., 1995; Bauch et al., 2005; Ekwurzel et al., 2001; Mueller-Lupp et al., 2004 Cooper et al., 2005
Ob River	-14.8 to -16.3	Bauch et al., 1995; Bauch et al., 2005; Ekwurzel et al., 2001; Mueller-Lupp et al., 2004 Cooper et al., 2005
Mean salinity Arctic water (34.8)	-2.46	Aagaard and Carmack, 1989

It is evident from Fig. 30 that the sites from which bivalves were collected fall in line with the salinity-$\delta^{18}O$ relationship for the upper waters of the Nares Strait region within the error estimates for the freshwater endmember (+/- 1.10). Therefore, the $\delta^{18}O$ isotopic compositions of the bivalve shells should reflect the $\delta^{18}O_{water}$, which in turn can

be used as a proxy for salinity variability in Nares Strait because of the high correlation between these two parameters.

A well-known factor that complicates the use of $\delta^{18}O$ in bivalve shells as a salinity proxy is that oxygen isotopes fractionate during carbonate formation, and this fractionation is a function of temperature. Previous theoretical investigations as well as laboratory and field studies have derived empirical relationships that relate the oxygen isotopic composition of the ambient water ($\delta^{18}O_{water}$) and temperature (T) as carbonate is accreted by molluscs, foraminiferans (Grossman and Ku, 1986), gastropods (Rhamipour-Bonab et al., 1997), coralline aragonitic sponges (Bohm et al., 2000). Similar studies have been conducted using synthetic aragonite (Tarutani et al., 1969), calcite (Kim and O'Neil, 1997), and other alkaline-earth carbonates (O'Neil et al., 1969). The relationships derived by all of these studies appear linear over a wide range of temperatures from 0 to 25ºC. Of these, the two most commonly used relationships are those of Grossman and Ku (1986) (Eq. 3) and Bohm (2000) (Eq. 4):

$$\delta^{18}O_{exp,\,GK} = 4.65 - 0.21T + \delta^{18}O_{water} \quad (3)$$

$$\delta^{18}O_{exp,\,B} = 4.52 - 0.23T + \delta^{18}O_{water} \quad (4)$$

We employed the empirical relationship of Bohm (2000) (Eq. 4) to constrain the maximum variability of the $\delta^{18}O$ in our shells over the maximum temperature range that could be expected for Nares Strait. The temperature range in our study area is ~8 degrees (-2 to 6ºC) based on time series data collected continuously over a three year time period from 2003 to 2006 (Falkner et al., 2006). To bracket the variations in the isotopic composition of the water, we used the average (-1.75‰), lowest (-4.00‰), and highest (0.50‰) $\delta^{18}O_{water}$ values measured in upper Nares Strait waters during August 2003.

This exercise allowed us to determine the window of expected shell isotopic values over the full range of potential temperatures for the region assuming constant values for the $\delta^{18}O_{water}$ (Lines in Fig. 31, Panel A).

The expected $\delta^{18}O_{shell}$ were also calculated over the range of $\delta^{18}O_{water}$ values measured in Nares Strait during August 2003 assuming constant temperature (Fig. 31, Panel B). We used an average temperature of 1ºC for the region determined by CTD-Rosette casts, as well as a lowest temperature estimate of -2ºC, and high temperature estimates of 4ºC and 6ºC (Lines in Fig. 31, Panel B). Calculations were made using a modified version of the Bohm (2000) equation for temperature effects, substituting in the derived $\delta^{18}O_{water}$ using the relationship between salinity and $\delta^{18}O_{water}$ for Nares Strait (Eq. 2), such that:

$$\delta^{18}O_{exp} = (4.52 - 0.23T) + (0.69S - 24.17) \quad (5)$$

We are assuming the $\delta^{18}O_{water}$ is reflective of salinity variability at the collection sites, and that this variability can be adequately parameterized by Eq. (2). Over the range of salinities observed in Nares Strait, bivalves are exposed to a maximum variation in salinity of 6 units, from 29 to 35 (Falkner et al., 2006). Within this salinity range and a constant temperature of -2ºC (the lowest measured in the Strait), bivalves can experience a maximum shift in isotopic values of 4.17‰, which is more than twice the change expected from a 6 degree change in temperature from -2ºC to 4ºC (1.26‰; Eq. 4).

Figure 31: Measured $\delta^{18}O$ shell composition in the youngest sections of bivalve shells collected from all stations in Nares Strait as a function of temperature (A) and salinity (B) for this region using the empirical relationship of Bohm (2000). The lowest (-4.00‰), highest (0.50‰), and average (-1.75‰) $\delta^{18}O_{water}$ values measured in upper Nares Strait waters in August 2003 were used to calculate the effects of the potential temperature range on the $\delta^{18}O$ composition in bivalve shells. In panel B, the measured $\delta^{18}O$ shell composition in the youngest sections of bivalve shells collected from all stations in Nares Strait are plotted as a function of salinity. Salinity changes are inferred from the salinity-$\delta^{18}O_{water}$ relationship described in Eq. (2), using constant temperature values. The lowest (2ºC), two highest (4ºC and 6ºC), and average (1ºC) temperatures were used to determine the effects of different salinity waters on the $\delta^{18}O$ of the bivalve shells. Red circles represent samples from Bellot Island, purple circles designate Alexandra Fjord, green circles represent Offley Island, and blue circles represent Scoresby Bay. Numbers denote stations and letters represent the bivalve species (Appendix III).

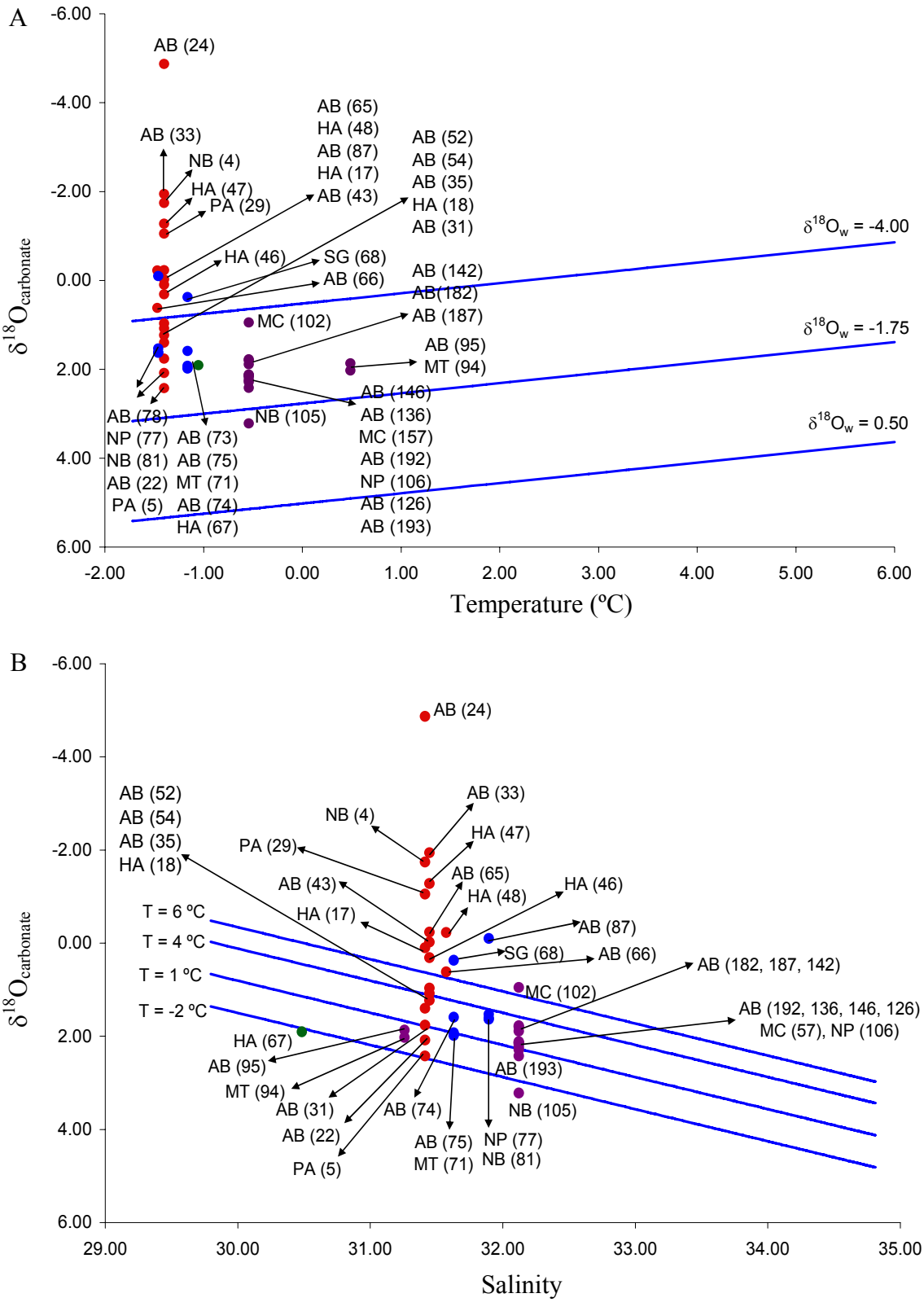
A
δ18Ocarbonate
Temperature (ºC)
δ18Ow = -4.00
δ18Ow = -1.75
δ18Ow = 0.50
AB (24)
AB (33)
NB (4)
HA (47)
PA (29)
AB (65)
HA (48)
AB (87)
HA (17)
AB (43)
AB (52)
AB (54)
AB (35)
HA (18)
AB (31)
HA (46)
SG (68)
AB (66)
AB (142)
AB(182)
AB (187)
MC (102)
AB (95)
MT (94)
AB (146)
AB (136)
MC (157)
AB (192)
NP (106)
AB (126)
AB (193)
AB (78)
NP (77)
NB (81)
AB (22)
PA (5)
AB (73)
AB (75)
MT (71)
AB (74)
HA (67)
NB (105)
B
δ18Ocarbonate
Salinity
T = 6 ºC
T = 4 ºC
T = 1 ºC
T = -2 ºC
AB (24)
AB (52)
AB (54)
AB (35)
HA (18)
AB (33)
NB (4)
HA (47)
PA (29)
AB (43)
AB (65)
HA (48)
HA (17)
HA (46)
AB (87)
SG (68)
AB (66)
AB (182, 187, 142)
MC (102)
AB (192, 136, 146, 126)
MC (57), NP (106)
HA (67)
AB (95)
MT (94)
AB (31)
AB (22)
PA (5)
AB (74)
AB (75)
MT (71)
NP (77)
NB (81)
AB (193)
NB (105)

Figure 31

The youngest portions of the shells were drilled at the ventral margin to isolate the isotopic composition of the carbonate accreted during the latest year of bivalve growth (2003). The measured isotopic compositions in the youngest sections of 42 shells collected from all stations were compared to expected $\delta^{18}O$ shell values for this region. The expected $\delta^{18}O$ shell values due to temperature variations were derived using empirical relationships that assume constant $\delta^{18}O_{water}$ (Fig. 31, Panel A). Similarly, the effects of changes in the $\delta^{18}O_{water}$ due to admixing of waters with different salinities was evaluated assuming constant temperatures that bracket values observed in this region over a 3 year time period (Fig. 31, Panel B).

Our results show that in the most recent years, many of the shells collected from Bellot Island (Station 2), and some specimens from Scoresby Bay (Station 4) show isotopic values that are significantly lighter than expected based on variability in temperature and salinity. These deviations are also apparent in the excursions to very light values recorded in the youngest sections of the shells relative to past years (Figs. 23-25). The deviations from expected values are apparent in all species analyzed, and are independent of the depth of collection and specimen age (Appendix III).

The observed $\delta^{18}O$ in the shell samples that reach values as light as -2‰ and -6‰ would require that bivalves accrete the carbonate at temperatures ranging from 6 to 23ºC (Eq. 4), assuming a $\delta^{18}O_{water}$ of -4.00‰. These temperatures are significantly higher than those observed in this region (Falkner et al., 2006). Therefore, temperature changes are unlikely to play a dominant role in influencing the $\delta^{18}O$ composition of the shells. Temperatures near 6ºC can occur in this region in the summer due to solar heating of the upper mixed layer (Falkner et al., 2006). Heating of the surface layer can lead to thermal

stratification in the upper 50 m of the water column, where the temperature could vary by as much as 8ºC. For example, surface waters in Baffin Bay may be as high as 6ºC in the summer, but underlying the surface from 50 to 200 m is a cold (-1.8 < TºC < 0) layer that contains a temperature minimum and strong halocline (Falkner et al., 2006). If the maximum temperature change in the upper 50 m of the water column is in fact 8ºC (6ºC to -1.8ºC), it is possible that $\delta^{18}O$ values in the shells could be as light as -7‰ (Eq. 3). However, it is intriguing that these larger fluctuations occur predominantly in the youngest sections of the shells.

Alternatively, the large magnitude of variations in the youngest shell sections could be attributed to $\delta^{18}O_{water}$ variations in Arctic source waters. The measured $\delta^{18}O$ of -2 to -4‰ would reflect precipitation of carbonate in equilibrium with water having a $\delta^{18}O_{water}$ composition of -6 to -9‰ at an average temperature of 1ºC. If our observed relationship between $\delta^{18}O_{water}$ and salinity indeed holds throughout the year, these $\delta^{18}O_{water}$ values would imply a dilution by enhanced river runoff to salinities ranging from 23 to 26 (Eq. 5). Evidence of the effects of variable $\delta^{18}O_{water}$ on the $\delta^{18}O_{shell}$ may be dampened with increasing distance from freshwater sources entering Nares Strait, since upper Arctic waters are subject to considerable mixing as they transit the passages of the Canadian Archipelago, and particularly from north to south in Nares Strait (Melling, 1984; Falkner et al., 2006). Thus, stations near the northern end of Nares Strait (e.g.- Bellot Island) can be expected to show more variability in shell isotopic compositions with respect to the $\delta^{18}O_{water}$ because of physical proximity to undiluted waters from the Transpolar Drift and Beaufort Gyre (Falkner et al., 2006). This variability may not be as pronounced near the outlet of Nares Strait at the southern end (e.g. Littelton Island and

Alexandra Fjord), because waters here have mixed considerably with Baffin Bay waters as they transited the Strait.

This pattern is indeed reflected in the measured isotopic compositions for the most recent year of shell accretion (Fig. 31, Panel B). Deviations to anomalously light $\delta^{18}O$ values in the shells are most pronounced in specimens collected from Bellot Island (Station 2) at the northern end of Nares Strait, and the magnitude of the deviation from expected ranges decrease from north to south. At locations further north in the Strait, source waters with low salinity and highly negative $\delta^{18}O_{water}$ values are introduced. As these waters transit south through Nares Strait, they are mixed with saltier waters of Atlantic origin introduced from Baffin Bay that have more neutral $\delta^{18}O_{water}$ compositions. This mixing process dampens the influence of the highly negative $\delta^{18}O$ source waters introduced in the north, and the isotopic composition of the bivalve shells towards the southern end of Nares Strait reflect the more neutral $\delta^{18}O$ of the water due to enhanced mixing.

We also examined the records of shells corresponding to 10, 20, 30, and 40 years in specimens of *Astarte borealis* and *Hiatella arctica* collected from Bellot Island (Station 2), Offley Island (Station 3), and Alexandra Fjord (Station 5), which represented stations at the inlet, mid-point, and outlet of Nares Strait respectively (Fig. 32). These stations were selected because they experience very different temperature and salinity ($\delta^{18}O_{water}$) characteristics (Figs. 12-15) as a result of circulation patterns in Nares Strait and differing proximity to freshwater sources. Specifically, stations to the north and on the western side of Nares Strait are closer to freshwater sources. Consequently, the

measured $\delta^{18}O$ values in the shells showed varying magnitudes of deviation to lighter $\delta^{18}O$ compositions than expected based on the regional hydrography.

Measured isotopic records in *Astarte borealis* and *Hiatella arctica* corresponding to the 10 and 20 year shell sections indicate that the specimens from Bellot Island (Station 2) were then recording $\delta^{18}O$ values significantly lighter than those expected (Fig. 32, Panels A and B), even if we assume a high temperature of 6ºC. This pattern appears to be independent of species, depth of collection, and age of the specimen. The shell sections accreted 30 to 40 years ago show isotopic values that fall within the expected range over the salinities and temperatures measured in Nares Strait. This is true for all specimens except for a 100 year old *Astarte borealis* (Fig. 32, Panels C and D). The isotopic signature in another 105 year old specimen from Scoresby Bay (Station 4) was close to the expected values at the maximum temperature in Nares Strait.

These data are compiled in Figure 33, which shows that the largest deviations from expected oxygen isotopic values at the average and maximum temperatures recorded in the Strait (1ºC and 6ºC) occur most frequently in the youngest shell sections (age 0 time slice), and decrease progressively in frequency and magnitude to the 30 and 40 year time slices. Although the range of variability for all the age sections is larger with respect to calculations made assuming a temperature of 1ºC rather than the maximum possible temperature of 6ºC, these data clearly indicate that the measured $\delta^{18}O$ values in the bivalve shells have been getting significantly lighter in the recent past compared to 30, 40, and even 20 years ago.

Figure 32: Measured $\delta^{18}O$ shell composition of A) 10 year shell sections, B) 20 year shell sections, C) 30 year shell sections, and D) 40 year shell sections from bivalve shells collected from all stations in Nares Strait. Measured values were compared to expected shell isotopic compositions over the range of potential salinities ($\delta^{18}O_{water}$) for this region using a combination of the equation of Bohm (2000), the relationship between salinity and $\delta^{18}O_{water}$, and using constant temperature values. The average (1ºC), lowest (-2ºC), highest (4ºC), and extreme high (6ºC) temperatures were used to calculate the effects of water sources (with different salinities and $\delta^{18}O_{water}$) on the $\delta^{18}O$ composition in bivalve shells over the entire range of potential temperatures in Nares Strait, and are represented by the blue lines. The numbers represent the specimen identification number used for drilling, and the letters represent the bivalve species (Appendices III and IV).

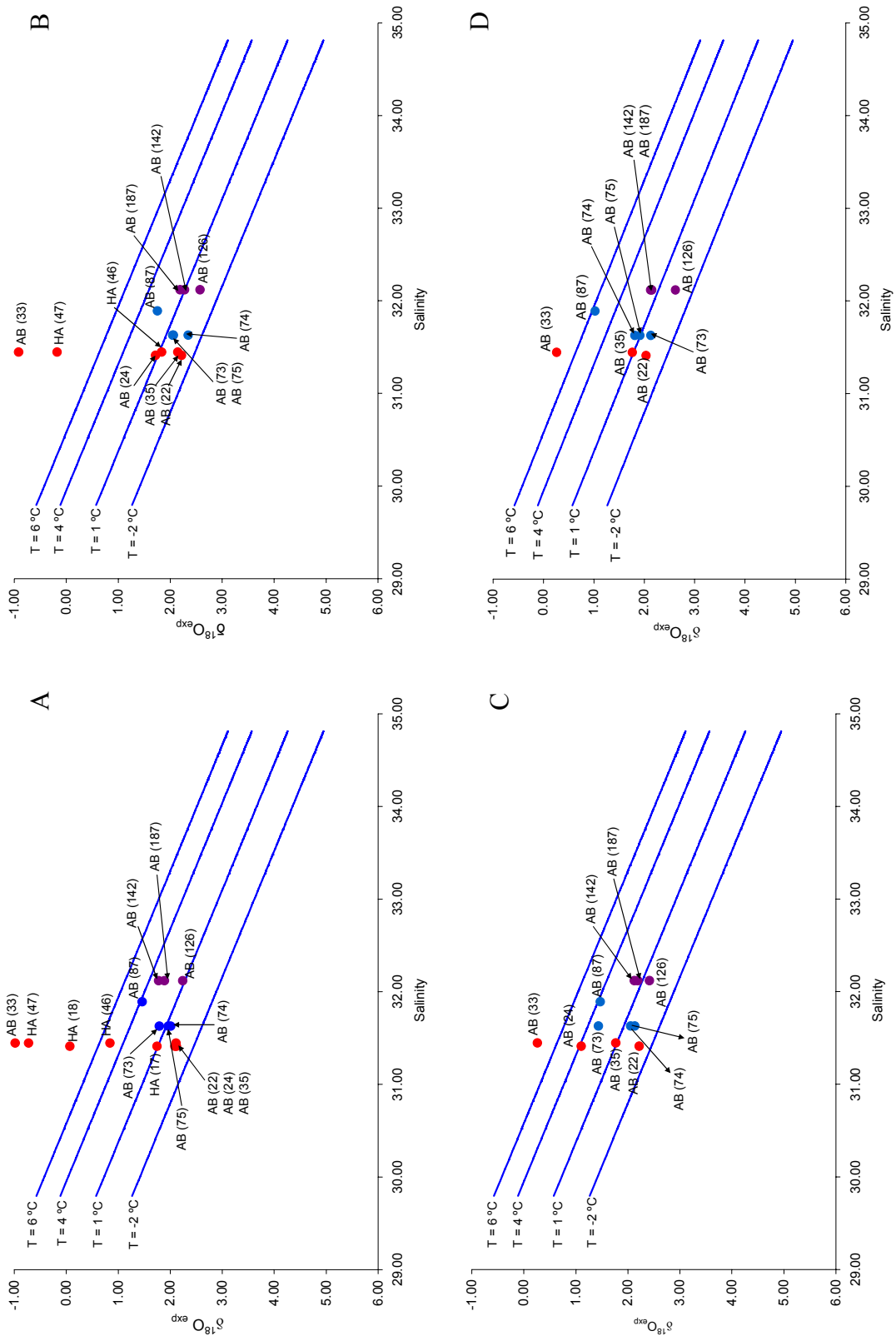
A
B
C
D
T = 6 °C
T = 4 °C
T = 1 °C
T = -2 °C
Salinity
AB (33)
HA (47)
HA (18)
HA (46)
AB (87)
AB (142)
AB (187)
AB (126)
AB (74)
AB (73)
HA (17)
AB (75)
AB (22)
AB (24)
AB (35)

Figure 32

The measured isotopic signatures in the 10 and 20 year shell sections for at least some specimens suggests that the Bellot Island site (Station 2) began experiencing some sort of increased freshwater input event as far back as 20 years ago (1983). This trend is more evident in the 10 year section, and is persistent in the youngest shell sections (Figs. 31 and 32), which indicates that these lighter than expected isotopic values are not only a recent occurrence. Our results are consistent with historical hydrographic data that have pointed to notable freshening in Baffin Bay both recently (Muenchow, 2006), and as early as 1977 (Falkner et al., 2006). The lack of such a signal in the 30 and 40 year sections indicates that the bivalves at all stations for the most part were not exposed to this freshwater input, however, too few specimens were analyzed at this age section to make definitive conclusions. The Scoresby Bay (Station 4) and Alexandra Fjord (Station 5) collection sites fall within the same range of expected isotopic values from 40 years back to the present, which suggests that the shells at these stations were not experiencing as significantly variable salinity and temperature conditions as the Bellot Island site (Fig. 33). These findings are consistent with the notion that since Bellot Island is at the inlet of Nares Strait it is closest to Arctic freshwater sources. Alternatively, the Scoresby Bay and Alexandra Fjord sites at the mid-point and southern end of Nares Strait respectively experience less isotopic variability due to increased mixing with saltier waters having more neutral $\delta^{18}O_{water}$ compositions as they transit south.

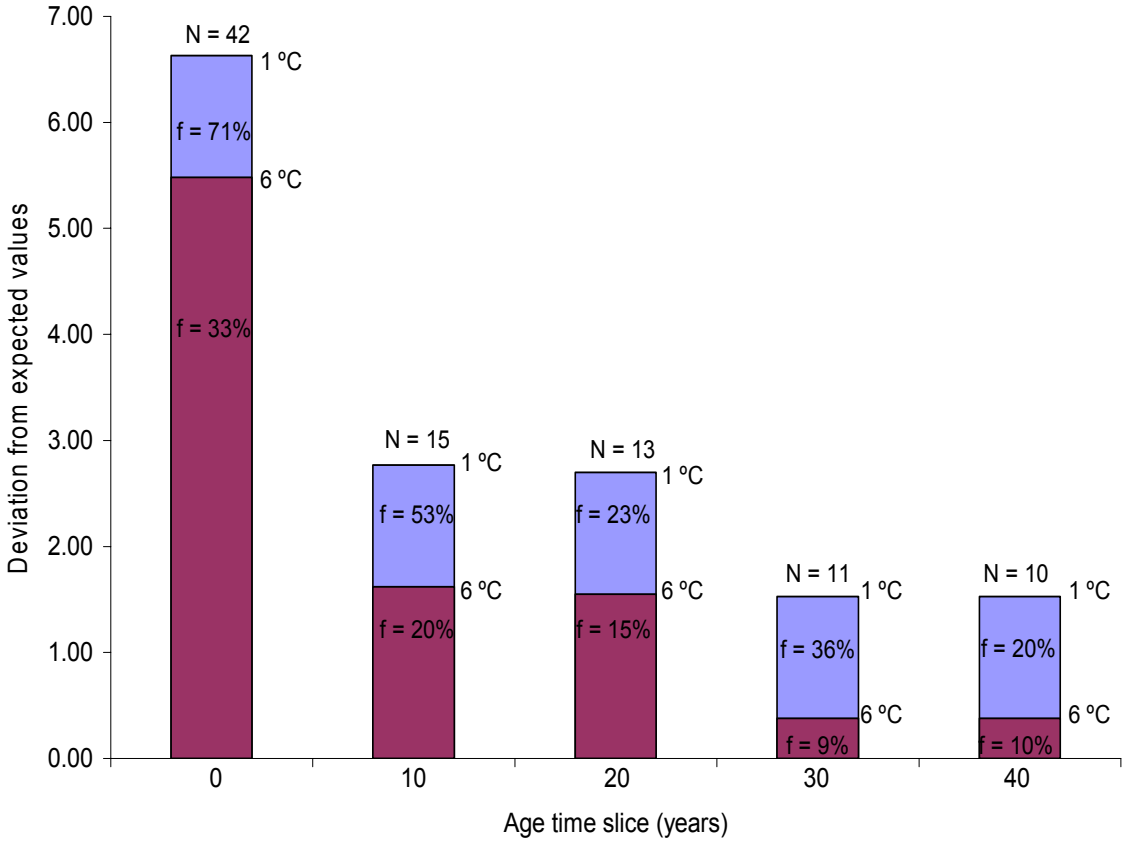

Figure 33: Frequency distribution and ranges of deviation from expected ^{18}O shell values to lighter measured values in shell sections corresponding to the most recent year of growth (Age 0), 10, 20, 30 and 40 years. Blue boxes represent the maximum range of deviation from expected values assuming an average temperature of 1ºC, and purple boxes represent the range of deviation at 6ºC. N is the total number of shells that were drilled for the corresponding time slice, and f is the percentage of the drilled shells that were lighter in isotopic composition than expected.

5. CONCLUSIONS

The species diversity and number of individuals of bivalve specimens collected in our study varied with location in Nares Strait. The most numerous, older, and larger specimens were *Astarte borealis* and *Hiatella arctica*. *Nucula bellotti, Macoma calcarea, Mya truncata, Serripes groenlandicus, Portlandia arctica,* and *Nuculana pernula* were generally low in number, younger, and smaller. These results are consistent with those for the same species from other studies at high latitudes, including the high Arctic and Canadian Archipelago, the Baffin Islands, and Greenland (Vibe, 1939; 1950; Thorson, 1957; Ockelman, 1958; Ellis, 1960; Lubinsky, 1980; Thomson et al., 1986; Dale et al., 1989; Syvitski et al., 1989; Aitken and Gilbert, 1996; Gordillo and Aitken, 2000; Sejr et al., 2000, 2002; Khim et al., 2001, 2003; Mueller-Lupp et al., 2003, 2004; Mueller-Lupp and Bauch, 2005; Simstich et al., 2005).

Individual specimens of *Hiatella arctica* and *Astarte borealis* follow an asymptotic growth curve with a growth rate (K) of $0.14yr^{-1}$, and maximum sizes that are consistent with a Von Bertalanffy Growth Function (VBGF) that involves decreased metabolic expenditure on shell production as bivalves age. The sizes of the *Hiatella arctica* specimens collected in our study are consistent with the VBGF and with individuals of *H. arctica* in Young Sound, Northeast Greenland (Sejr et al., 2000, 2002). The maximum length (L_∞) attained by our specimens is slightly smaller than observed in other Arctic regions (e.g.-Sejr et al., 2000, 2002), suggesting that low temperatures and limited nutrient availability is most likely hindering growth at the high latitude of our study. Specifically, low light levels may be limiting primary productivity in this seasonally ice covered region. However, the growth rate (K) is within the range of values

for six Antarctic bivalves and the Iceland scallop (Brey and Clarke, 1993; Pedersen, 1994).

The *Astarte borealis* specimens collected in our study were significantly smaller than previously seen in the Canadian Arctic and Archipelago (Petersen, 1978; Lubinsky, 1980; Dale et al., 1989; Syvitski et al., 1989; Aitken and Fournier, 1993; Aitken and Gilbert, 1996; Gordillo and Aitken, 2000) and their growth deviates notably from the modeled VBGF curve with a growth rate (K) of $0.14yr^{-1}$. This suggests that our *A. borealis* specimens likely experienced some environmental factors that limited their growth. The specimens of other bivalve species collected in our study were generally smaller than previously observed in the Arctic (Petersen, 1978; Lubinsky, 1980; Thomson et al., 1986), but still within the range of possible sizes, and appeared to follow an asymptotic growth pattern. However, not enough samples were collected to make conclusions about the growth patterns of these specimens.

Bivalve shells have proven to be useful recorders of the ambient hydrographic conditions in which these animals grow. However, a robust interpretation of these proxies relies on understanding the features of the modern system. Here we have analyzed the potential of bivalve shells to trace recent changes in the temperature and $\delta^{18}O_{water}$ of shallow (<30 m) waters of Nares Strait. Our data show that at the stations where bivalves were collected, the $\delta^{18}O_{water}$ is largely dominated by variations in salinity, consistent with the general relationship observed in the greater Nares Strait region. This high correlation allowed us to use the $\delta^{18}O_{water}$ as a proxy for salinity.

Measured isotopic records from shell sections in specimens of *Hiatella arctica* and *Astarte borealis* corresponding to time slices from the time of collection or age 0 (+/-

2), 10 years (+/- 5), 20 years (+/- 10) and 40 years (+/- 10) indicate that the largest range of deviations from predicted isotopic values occur most frequently in the latest 20 years, and decrease successively in frequency of occurrence and magnitude through the 30 and 40 year time slices. These results show variable freshening from north to south. Lighter than expected isotopic values are most prevalent at Station 2, and suggest that specimens at the northern end of Nares Strait began experiencing an increase in freshwater input as far back as 20 year ago (1983), while other stations at the midpoint and southern end did not experience as variable conditions. These results are consistent with historical hydrographic data that have indicated notable freshening in Baffin Bay both recently (Muenchow, 2006), and as early as 1997 (Falkner et al., 2006). Greater variability in the isotopic signatures at the northern stations in Nares Strait is reflective of the proximal influence of fresh Arctic source waters (Melling, 1984; Falkner et al., 2006). Along-Strait mixing results in diminished variability of the $\delta^{18}O_{water}$ and temperatures further south.

BIBLIOGRAPHY

Aagaard, K. and Carmack, E.C. (1989) The role of sea ice and other fresh water in the Arctic Circulation. *J. Geophys. Res.* **14**, 14,485-14,498

Aitken, A.E., and Fournier, J. (1993) Macrobenthos communities of Cambridge, McBeth, and Itirbilung fjords, Baffin Islands, Northwest Territories, Canada. *Arctic*. **46**, 60-71.

Aitken, A.E., and Gilbert, R. (1996) Marine Mollusca from Expedition Fjord, western Axel Heiberg Island, Northwest Territories, Canada. *Arctic*. **49**, 29-43.

Ambrose, W.G. Jr., Carroll, M.L., Greenacre, M., Thorrold, S.R., and McMahon, K.W. (2006) Variation in *Serripes groenlandicus* (Bivalvia) growth in a Norwegian high-Arctic fjord: evidence for local- and large-scale climatic forcing. *Global Change Biol.* **12**, 1595-1607.

Arntz, W.E., Brey, T., Gallardo, V.A. (1994) Antarctic zoobenthos. *Oceanogr. Mar. Biol. Annu. Rev.* **32**, 241-304.

Barry, R.G. and Serreze, M.C. (2000) Atmospheric components of the Arctic Ocean freshwater balance and their interannual variability, in *The Freshwater Budget of the Arctic Ocean* (ed E.L. Lewis), pp. 45-56.

Bauch, D., Schlosser, P., and Fairbanks, R.G. (1995) Freshwater balance and the sources of deep and bottom waters in the Arctic Ocean inferred from the distribution of $H_2{}^{18}O$. *Prog. Oceanogr.* **35**, 53-80.

Bauch, D., Erlenkeuser, H., and Andersen, N. (2005) Water mass processes on Arctic shelves as revealed from $\delta^{18}O$ of H_2O. *Global and Planetary Change*. **48**, 165-174.

Belkin, I.M., Levitus, S., Antonov, J., and Malmberg, S.A. (1998) "Great Salinity Anomalies" in the North Atlantic. *Prog. Oceanogr.* **41** (1), 1-68.

Benhnke, O., and Zelander, T. (1970) Preservation of intercellular substances by the cationic dye alcian blue in preparative procedures for electron microscopy. *J. Ultrastruct. Res.* **31**, p. 424.

Böhm, F., Joachimski, M.M., Dullo, W.-C., Eisenhauer, A., Lehnert, H., Reitner, J., and Wörheide, G. (2000) Oxygen isotope fractionation in marine aragonite of coralline sponges. *Geochim. Cosmochim. Acta.* **64**, 1695-1703.

Boyd, T.J., Steele, M., Muench, R.D., and Gunn, J.T. (2002) Partial recovery of the Arctic Ocean halocline. *Geophys. Res. Lett.* **29** (14), doi:10.1029/2001GL014047.

Brey, T., and Clark, A. (1993) Population dynamics of marine benthic invertebrates in Antarctic and subantarctic environments: are there unique adaptations? *Antarct. Sci.* **5**, 253-266.

Carmack. E.C., Macdonald, R.W., Perkin, R.G., McLaughlin, F.A., and Pearson, R.J. (1995) Evidence for warming of Atlantic water in the southern Canadian Basin of the Arctic Ocean: Results from the Larsen-93 expedition. *Geophys. Res. Lett.* **22** (9), 1061-1064.

Cloern, J.E., and Nichols, F.H. (1978) A von Bertalanffy growth model with a seasonally varying coefficient. *J. Fish. Res. Board Can.* **35**, 1479-1482.

Collin, A.E. (1962) Oceanographic observations in the Canadian Arctic and the adjacent Arctic Ocean. *Arctic*. **15**, 194-201.

Cooper, L.W., Benner, R., McClelland, J.W., Peterson, B.J., Holmes, R.M., Raymond, P.A., Hansell, D.A., Grebmeier, J.M., and Codispoti, L.A. (2005) Linkages among runoff, dissolved organic carbon, and the stable oxygen isotope composition of seawater and other water mass indicators in the Arctic Ocean. *J. Geophys. Res.* **110**, G02013, doi:10.1029/2005JG000031.

Coote, A. R., and Jones, E. P. (1982) Nutrient distributions and their relationships to water masses in Baffin Bay. *Canadian Journal of Fisheries and Aquatic Science*. **39**, 1210-1214.

Curtis, M.A. (1975) The marine benthos of arctic and subarctic continental shelves. *Polar Record*. **17**, 595-626.

Dale, J.E., Aitken, A.E., Gilbert, R., and Risk, M.J. (1989) Macrofauna of Canadian arctic fjords. *Marine Geology*. **85**, 331-385.

De Graaf, G., and Prein, M. (2005) Fitting growth with the von Bertalanffy growth function: a comparison of three approaches of multivariate analysis of fish growth in aquaculture experiments. *Aquaculture Research*. **36**, 100-109.

Delworth, T.L, and Dixon, K.W. (2000) Implications of recent trends in the Arctic/North Atlantic Oscillation for the North Atlantic thermohaline circulation. *J. Clim.* **13**, 3271-3277.

Dettman, D. L., Flessa, K. W., Roopnarine, P. D., Schöne, B. R., and Goodwin, D. H. (2004) The use of oxygen isotope variation in shells of estuarine mollusks as a quantitative record of seasonal and annual Colorado River discharge. *Goechimica et Cosmochimica Acta*, **68**, 1,253-1,263.

Dickson, R., Meincke, J., Malmberg, S.A., and Lee, A.J. (1988) The "Great Salinity Anomaly" in the northern North Atlantic 1968-1982. *Prog. Oceanogr.* **20**, 103-151.

Dickson, R., Lazier, J., Meincke, J., Rhines, P., and Swift, J. (1996) Long-term coordinated changes in the convective activity of the North Atlantic. *Prog. Oceanogr.* **38**, 241-295.

Dickson, R.R., Osborn, T.J., Hurrell, J.W., Meincke, J., Blindheim, J., Adlandsvik, B., Vinje, T., Alekseev, G., and Maslowski, W. (2000) The Arctic Ocean response to the North Atlantic Oscillation. *J. Clim.* **13,** 2671-2696.

Dickson, R., Yashayaev, I., Meincke, J., Turrel, B., Dye, S., and Holfort, J. (2002) Rapid freshening of the deep North Atlantic over the past four decades. *Nature*. **416**, 832-837.

Dunca, E., Schone, B.R., and Mutvei, H. (2005) Freshwater bivalves tell of past climates: But how clearly do shells from polluted rivers speak? *Palaeogeography, Palaeoclimatology, Palaeoecology*. **228** (1-2), 43-57.

Ekwurzel, B., Schlosser, P., Mortlock, R.A., and Fairbanks, R.G. (2001) River runoff, sea ice meltwater, and Pacific water distribution and mean residence times in the Arctic Ocean. *J. Geophys. Res.* **106** (5), 9,075-9,092.

Ellis, D.V. (1960) Marine infaunal benthos in Arctic North America. *Arctic Institute of North America Technical Paper*. No. **5**.

Epstein, S., Buchsbaum, R., Lowenstam, H., and Urey, U. (1953) Revised carbonate-water isotopic temperature scale. *Geol. Soc. Am. Bull.* **64**, 1,315-1,325.

Essington, T.E., Kitchell, J.F., and Walters, C.J. The von Bertalanffy growth function, bioenergetics, and the consumption rates of fish. *Can. J. Fish. Aquat. Sci.* **58**, 2129-2138.

Falkner, K.K., Carmack, E., Jones, P., McLaughlin, F., Melling, H., Muenchow, A., O'Brien, M., and Strain, P. (2006) Implications of nutrient variability in passages of the Canadian Archipelago and Baffin Bay for freshwater throughflow and local productivity. *Biogeosciences special issue on the Arctic Freshwater Cycle*. *Submitted **2006***.

Falkner, K.K., *et al.* (2003) Research Cruise Report: Mission HLY 031. *Variability and Forcing of Fluxes through Nares Strait and Jones Sound: A Freshwater Emphasis.* http://newark.cms.udel.edu/~cats/reports/HLY031CruiseReport102203.pdf

Fissel, D. B., et al. (1988) *Non-tidal flows in the Northwest Passage*. Institute of Ocean Sciences, Sidney, BC. 143 pp.

Gordillo, S., and Aitken, A.E. (2000) Paleoenvironmental interpretation of Late Quaternary marine molluscan assemblages, Canadian Arctic Archipelago. *Geographie physique et Quaternaire*. **54**, 301-315.

Gotliv, B.-A., Addadi, L., and Weiner, S. (2003) Mollusk shell acidic proteins: in search of individual functions. *Chemciochem*. **4**, 522-529.

Graber, E.R., and Aharon, P. (1991) An improved microextraction technique for measuring dissolved inorganic carbon (DIC), $\delta^{13}C_{DIC}$, and $\delta^{18}O_{H2O}$ from milliliter-size water samples. *Chem. Geol. (Isotope Geoscience Section)*. **94**, 137-144.

Grossman, E.L., and Ku, T.L. (1986) Oxygen and carbon isotope fractionation in biogenic aragonite: temperature effects. *Chem. Geol. (Isotope Geosciences Section)*. **59**, 59-74.

Hakkinen, S., and Proshutinsky, A. (2004) Freshwater content variability in the Arctic Ocean. *J. Geophys. Res.* **109** (C03051), doi:10.1029/2003JC009140.

Karcher, M.J., and Oberhuber, J.M. (2002) Pathways and modification of the upper and intermediate waters of the Arctic Ocean. *J. Geophys. Res.* **107** (C6), doi:10.1029/2000JC000530.

Khim, B.K., Krantz, D.E., and Brigham-Grette, J. (2001) Stable isotope profiles of last interglacial (Pelukian Transgression) molluscks and paleoclimate implications in the Bering Strait Region. *Quat. Sci. Rev.* **20**, 461-481.

Khim, B.K., Krantz, D.E., Cooper, L.W., and Grebmeier J.M. (2003) Seasonal discharge of estuarine freshwater to the western Chuckchi Sea shelf identified in stable isotope profiles of mollusk shells. *J. Geophys. Res.* **108** (9), 3300, doi:10.1029/2003JC001816.

Kim, S.T., and O'Neil, J.R. (1997) Equilibrium and nonequilibrium oxygen isotope effects in synthetic carbonates. *Geochim. Cosmochim. Acta*. **61**, 3461-3475.

Kleim, N., and Greenberg, D.A. (2003) Diagnostic simulations of the summer circulation in the Canadian Archipelago. *Atmosphere-Ocean*. **41**, 273-289.

Krantz, D.E., Williams, D.F., and Jones, D.S. (1987) Ecological and paleoenvironmental information using stable isotope profiles from living and fossil molluscs. *Palaeogeography, Palaeoclimatology, Palaeoecology*. **58**, 249-266.

Kroopnick, P. (1974) The dissolved O_2-CO_2-^{13}C system in the eastern equatorial Pacific. *Deep-Sea Research*. **21**, 211-227.

Lachenbruch, A.H., Marshall, B.V. (1986) Changing climate: Geothermal evidence from the permafrost in the Alaskan Arctic. *Science*. **234,** 689-696.

Létolle R., Martin, J.M., Thomas, A.J., Gordeev, V.V., Gusarova, S., and Sidorov, I.S. (1993) 18O abundance and dissolved silicate in the Lena delta and Laptev Sea (Russia). *Mar. Chem.* **43**, 47-64.

Lubinsky, I. (1980) Marine bivalve mollusks of the Canadian Central and Eastern Arctic: Faunal composition and zoogeography. *Canadian Bulletin of Fisheries and Aquatic Sciences*. Bulletin **207**, 111 pp.

Lutz, R.A, and Rhoads, D.C. (1980) Growth patterns within the molluscan shell: an overview, in *Skeletal growth of aquatic organisms* (eds D.C. Rhoads and R.A. Lutz), pp. 203-248. Plenum Press, New York.

Macdonald, R.W., Paton, D.W., and Carmack, E.C. (1995) The freshwater budget and under-ice spreading of Mackenzie River water in the Canadian Beaufort Sea based on salinity and $^{18}O/^{16}O$ measurements in water and ice. *J. Geophys. Res.* **100** (1), 895-919.

Macdonald, R.W. (2000) Arctic estuaries and ice: A positive-negative estuarine couple, in *The Freshwater Budget of the Arctic Ocean* (ed E.L. Lewis), pp. 383-407. Kluwer, Boston.

Marxen, J.C., Hammer, M., Gehrke, M., and Becker, W. (1998) Carbohydrates of the shell matrix and the shell-forming tissue of the snail. *Biomphalaria glabrata* (Say), *Biol. Bull.* **194**, 231-240.

Maslanik, J.A., Serreze, M.C., and Barry, R.G. (1996) Recent decreases in Arctic ice cover and linkages to atmospheric circulation anomalies. *Geophys. Res. Lett.* **23** (13), 1677-1680.

McLaughlin, F.A., Carmack, E.C., Macdonald, R.W., and Bishop, J.K.B. (1996) Physical and geochemical properties across the Atlantic/Pacific water mass front in the southern Canadian Basin. *J. Geophys. Res.* **101**, 1183-1197.

Melling, H., Lake, R.A., Topham, D.R., and Fissel, D.B. (1984) Oceanic thermal structure in the western Canadian Arctic. *Conctinental Shelf Res.* **3**, 233-258.

Melling, H. (2000) Exchanges of freshwater through the shallow straits of the North American Arctic, in *The Freshwater Budget of the Arctic Ocean* (ed E.L. Lewis), pp. 479-502. Kluwer, Boston.

Mook, W.G., Bommerson, J.C., and Staverman, W.H. (1974) Carbon isotope fractionation between dissolved bicarbonate and gaseous carbon dioxide. *Earth Planet. Sci. Lett.* **22**, 169-176.

Morison, J., Steele, M., and Anderson, R. (1998) Hydrography of the upper Arctic Ocean measured from the nuclear submarine USS *Pargo*. *Deep Sea Res. Part I.* **45**, 15-38.

Mueller-Lupp, T., Erlenkeuser, H., and Bauch, H.A. (2003) Seasonal and interannual variability of Siberian river discharge in the Laptev Sea inferrd from stable isotopes in modern bivalves. *Boreas*. **32**, 292-303.

Mueller-Lupp, T., Bauch, H.A., and Erlenkeuser, H. (2004) Holocen hydrographical changes of the eastern Laptev Sea (Siberian Arctic) recorded in $\delta^{18}O$ profiles of bivalve shells. *Boreas*. **61**, 32-41.

Mueller-Lupp, T., and Bauch, H. (2005) Linkage of Arctic atmospheric circulation and Siberian shelf hydrography: A proxy validation using δ18O records of bivalve shells. *Glob. and Planet. Change*. **48**, 175-186.

Muench, R.D. (1971) *The physical oceanography of the northern Baffin Bay region*, Arctic Inst. of N. America, Montreal.

Ockelmann, W.K. (1958) The zoology of East Greenland. Marine Lamellibranchiata. *Meddelelser om Grønland.* **122** (4), 256 pp.

O'Neil, J.R., Clayton, R.N., and Mayeda, T.K. (1969) Oxygen isotope fractionation in divalent metal carbonates. *J. Chem. Phys.* **51**, 5547-5558.

Ortiz, J.D., Mix, A.C., Wheeler, P.A., and Key, R.M. (2000) Anthropogenic CO2 invasion into the northeast Pacific based on concurrent d13CDIC and nutrient profiles from the California Current. *Global Biogeochem. Cycles*. **14**, 917-929.

Osterkamp, T.E., Romanovsky, V.E. (1999) Evidence for warming and thawing of discontinuous permafrost in Alaska. *Permafrost Periglac.* **10**, 17-37.

Ottera, O. H., et al. (2003) The sensitivity of the present-day Atlantic meridional overturning circulation to freshwater forcing. *Geophysical Research Letters*. **30**, 1898, doi:1810.1029/2003GL017578.

Pavlov, A.V. (1994) Current changes of climate and permafrost in the Arctic and sub-arctic of Russia. *Permafrost Periglac*. **5**, 101-110.

Peck, L.S., and Bullough, W. (1993) Growth and population structure in the infaunal bivalve *Yoldia eightsi* in relation to icberg activity at Signy Island, Antarctia. *Mar. Biol.* **117**, 235-241.

Pedersen, S.A. (1994) Population parameters of the Iceland scallop *Chlamys islandica* (Muller) from West Greenland. *J. Northwest Atl. Fish. Sci.* **16**, 75-87.

Petersen, G.H. (1978) Life cycles and population dynamics of marine benthic bivalves from the Disco Bugt area of West Greenland. *Ophelia*. **17**, 95-120.

Peterson, B.J., Holmes, R.M., McClelland, J.W., Vorosmarty, C.J., Lammers, R.B., Shiklomanov, A.I., Shiklomanov, I.A., and Rahmstorf, S. (2002) Increasing river discharge to the Arctic Ocean. *Science*. **298**, 2171-2173.

Porch, C.E., Wilson, C.A., and Nieland, D.L. (2002) A new growth model for red drum (*Sciaenops ocellatus*) that accommodates seasonal and ontogenic changes in growth rates. *Fish. Bull.* **100**, 149-152.

Proshutinsky, A.Y., and Johnson, M.A. (1997) Two circulation regimes of the wind driven Arctic Ocean. *J. Geophys. Res.* **102**, 12,493-12,514.

Quadfasel, D., Sy, A., Wells, D., and Tunik, A. (1991) Warming in the Arctic. *Nature*. **350,** 385.

Rahmstorf, S., and Ganopolski, A. (1999) Long-term global warming scenarios computed with an efficient coupled climate model. *Clim. Change.* **43**, 353-367.

Renssen, H., Goosse, H., Fichefet, T., Campin, J.M. (2001) The 8.2 kyr BP event simulated by a global atmosphere-sea-ice-ocean model. *Geophys. Res. Lett.* **28**, 1,567-1,570.

Rahimpour-Bonab H., Bone, Y., and Moussavi-Harami, R. (1997) Stable isotope aspects of modern molluscs, brachiopods, and marine cements from cool-water carbonates, Lapecede Shelf, South Australia. *Geochim. Cosmochim. Acta*. **61**, 207-218.

Rigor, I. G., J.M. Wallace, and Colony, R.L. (2002) On the Response of Sea Ice to the Arctic Oscillation. *J. Climate*. **15** (18), 2,546–2,663.

Rodhouse, P.G. (1998) Physiological Progenesis in Cephalopod Molluscs. *Biol. Bull.* **195**, 17-20.

Rothrock, D.A., Yu, Y., and Maykut, G.A. (1999) Thinning of the Arctic sea ice cover. *Geophys. Res. Lett.* **26,** 3469-3472.

Rudels, B. (1986) The outflow of polar water through the Arctic Archipelago and the oceanographic conditions in Baffin Bay. *Polar Res.* **4**, 161-181.

Saenko, O. A., et al. (2003) North Atlantic response to the above-normal export of sea ice from the Arctic. *J. Geophys. Res.*, **108**, 3227, doi:3210.1029/2001JC001166.

Salata, G. G., Roelke, L.A., and Cifuentes, L.A. (2000) A rapid and precise method for measuring stable carbon isotope ratios of dissolved inorganic carbon. *Mar. Chem.* **69**, 153-161.

Schmid, M.K., and Peipenberg, D. (1993) The benthos zonation of the Disko Fjord, West Greenland. *Meddelelser om Grønland, Bioscience*. **37**, 3-21.

Schofield, B.H., Williams, B.R., and Doty, S.B. (1975) Alcian blue staining of cartilage for electron microscopy. Application of the critical electrolyte concentration principle. *Histochem. J.* **7**, 139-149.

Schöne, BR, Freyre Castro, AD, Fiebig, J, Houk, SD, Oschmann, W & Kröncke, I. (2004) Sea surface water temperatures over the period 1884-1983 reconstructed from oxygen isotope ratios of a bivalve mollusk shell (*Arctica islandica*, southern North Sea). *Palaeogeography, Palaeoclimatology, Palaeoecology.* **212**, 215-232.

Schone, B.R., Fiebig, J., Pfeiffer, M., Gleβ, R., Hickson, J., Johnson, A.L.A., Dreyer, W., and Oschmann, W. (2005) Climate records from a bivalved Methuselah (*Arctica islandica*, Mollusca; Iceland). *Palaeogeography, Palaeoclimatology, Palaeoecology*. **228**, 130-148.

Schöne, BR, Dunca, E, Fiebig, J & Pfeiffer, M, (2005) Mutvei's solution: an ideal agent for resolving microgrowth structures of biogenic carbonates. *Palaeogeography, Palaeoclimatology, Palaeoecology.* **228**, 149-166.

Sejr, M.K., Jensen, K.T., and Rysgaard, S. (2000) Macrozzoobenthic community structure in a high-Arctic East Greenland fjord. *Polar Biol.* **23**, 792-801.

Sejr, M.K., Jensen, K.T., and Rysgaard, S. (2002) Annual growth line formation in the bivalve *Hiatella arctic* validated by a mark-recapture study in NE Greenland. *Polar Biol.* **25**, 794-796

Sejr, M.K., Sand, M.K., Jensen K.T., Petersen J.K., Christensen, P.B., and Rysgaard, S. (2002) Growth and production of *Hiatella arctica* (Bivalvia) in a high-Arctic fjord (Young Sound, Northeast Greenland). *Mar. Ecol. Prog. Ser.* **244**, 163-169.

Serreze, M.C., Walsh, J.E., Chapin, F.S.I., Osterkamp, T., Dyurgerov, M., Romanovsky, V., Oechel, W.C., Morison, J., Zhang, T., and Barry, R.G. (2000) Observational evidence of recent change in the northern high-latitude environment. *Climatic Change*. **46**, 159-207.

Serreze, M. C., Maslanik, J.A., Scambos, T.A., Fetterer, F., Stroeve, J., Knowles, K., Fowler, C., Drobot, S., Barry, R.G., and Haran, T.M. (2003) A record minimum arctic sea ice extent and area in 2002. *Geophys. Res. Lett.* **30** (3), 1110, doi:10.1029/2002GL016406.

Simstich, J., Harms, I., Karcher, M.J., Erlenkeuser, H., Stanovoy, V., Kodina, L., Bauch, D., and Spielhagen, R.F. (2005) Recent freshening in the Kara Sea (Siberia) recorded by stable isotopes in Arctic bivalve shells. *J. Geophys. Res.* **110**, C08006, doi:10.1029/2004JC002722.

Smith, D.M. (1998) Recent increase in the length of the melt season of perennial Arctic sea ice. *Geophys. Res. Lett.* ***25*** (5), 655-658.

Steele, M.D., Thomas, D., and Rothrock, D. (1996) A simple model study of the Arctic Ocean freshwater balance, 1979-1985. *J. Geophys. Res.* **20**, 20,833-20,848.

Steele, M., and Boyd, T. (1998) Retreat of the cold halocline layer in the Arctic Ocean. *J. Geophys. Res.* **103**, 10,419-10,435.

Steele, M., Morison, J., Ermold, W., Rigor, I., Ortmeyer, M., and Shimada, K. (2004) Circulation of summer Pacific halocline water in the Arctic Ocean. *J. Geophys. Res.* **109** (C2), C0202, doi:10.1029/2003JC002009.

Stewart, P.L., Pocklington, P., and Cunjak, R.A. (1985) Distribution, abundance and diversity of benthic macroinvertebrates on the Canadian continental shelf and slope of southern Davis Strait and Ungava Bay. *Arctic*. **38**, 281-291.

Syvitski, J.P.M, Farrow, G.E., Atkinson, R.J.A., Moore, P.G., and Andrews, J.T. (1989) Baffin Island macrobenthos: Bottom communities and environmental significance. *Arctic*. **42**, 232-247.

Tang, C. C. L., et al. (2004) The circulation, water masses and sea-ice of Baffin Bay. *Prog. Oceanogr.* **63**, 183-22.

Tarutani T., Clayton, R.N., and Mayeda, T.K. (1969) The effect of polymorphism and magnesium substitution on oxygen isotope fractionation between calcium carbonate and water. *Geochim. Cosmochim. Acta.* **33**, 987-996.

Thomson, D.H. (1982) Marine benthos in the eastern Canadian Arctic: Multivariate analyses of standing crop and community structure. *Arctic*. **35**, 61-74.

Thomson, D.H., Martin, C.M., Cross, W.E. (1986) Identification and characterization of Arctic nearshore benthic habitats. *Can. Tech. Rep. Fish. Aqua. Sci.* No. **1434**.

Thorson, G. (1957) Bottom communities. *Geological Society of America Memoir*. **67**, 461-534.

Urban, H.J. (2002) Modeling growth of different developmental stages in bivalves. *Mar. Ecol. Prog. Ser.* **238**, 109-114.

Vibe, C. (1939) Preliminary investigations on shallow water animal communities in the Upernavik- and Thule-Districts (Northwest Greenland). *Meddelelser om Grønland*. **124** (2), 42 pp.

Vibe, C. (1950) The marine mammals and the marine fauna in the Thule district (Northwest Greenland) with observations on ice conditions in 1939-41. *Meddelelser om Grønland*. **150** (6). 115 pp.

von Bertalanffy, L. (1938) A quantitative theory of organic growth (Inquiries on growth laws II). *Human Biology*. **10** (2), 181-213.

Wada, K. (1961) Crystal growth of molluscan shells. *Bull. Natl. Pearl. Res. Lab.* **7**, 703-828.

Wada, K. (1980) Initiation of mineralization in bivalve molluscs, in *The Mechanisms of Biomineralization in Animals and Plants* (eds M. Omori and N. Watabe), pp 79-92.

Walter, K.M., Zimov, S.A., Chanton, J.P., Verbyla, D., and Chappin, F.S. III. (2006) Methane bubbling from Siberian thaw lakes as a positive feedback to climate warming. *Nature*. **443**, 71-75.

Weaver, A.J., Aura, S.M., and Myers, P.G. (1994) Interdecadal variability in an idealized model of the North Atlantic. *J. Geophys. Res.* **99** (C9), 12423-12441.

Welch, H.E., Bergmann, M.A., Siferd, T.S., Martin, K.A., Curtis, M.F., Crawford, R.E., Conover, R.J., and Hop, H. (1992) Energy flow through the marine ecosystem of Lancaster Sound region, Arctic Canada. *Arctic*. **4**, 343-357.

Welp, L.R., Randerson, J.T., Finlay, J.C., Davydov, S.P, Zimova, G.M., Davydova, A.I., and Zimov, S.A. (2005) A high-resolution time series of oxygen isotopes from the Kolyma River: Implications for the seasonal dynamics of discharge and basin-scale water use. *Geophy. Res. Lett.* **32**, L14401, doi:10.1029/2005GL022857.

Wohlleben, T.M.H. and Weaver, A.J. (1995) Interdecadal climate variability in an idealized model of the North Atlantic. *Climate Dynamics*. **11,** 459-467.

Zweng, M.M., and Muenchow, A. (2006) Warming and freshening of Baffin Bay, 1916-2003. *J. Geophys. Res.* **111**, C07016, doi:10.129/2005JC003093.

APPENDICES

Appendix I: Summary of species collected and age for live collected Arctic bivalves organized by station and depth of collection. Site numbers refer to the locations in Figure 2.

Site #	Station Depth (m)	Clam ID No.	Species	Age (years)	Error (+/-)
1	13.3	NS002	Serripes groenlandicus	8	2
2	13.3-14.2	NS003	Serripes groenlandicus	3	2
2	13.3-14.2	NS004	Nucula belloti	6	2
2	13.3-14.2	NS005	Portlandia arctica	30	2
2	13.3-14.2	NS006	Portlandia arctica	20	2
2	13.3-14.2	NS007	Portlandia arctica	100	2
2	13.3-14.2	NS008	Portlandia arctica	18	2
2	13.3-14.2	NS009	Portlandia arctica	8	2
2	13.3-14.2	NS010	Portlandia arctica	13	2
2	13.3-14.2	NS011	Portlandia arctica	106	5
2	13.3-14.2	NS012	Portlandia arctica	5	2
2	13.3-14.2	NS013	Portlandia arctica	16	2
2	13.3-14.2	NS014	Portlandia arctica	8	2
2	13.3-14.2	NS015	Portlandia arctica	10	2
2	13.3-14.2	NS017	Hiatella arctica	5	2
2	13.3-14.2	NS018	Hiatella arctica	9	2
2	13.3-14.2	NS020	Hiatella arctica	5	2
2	13.3-14.2	NS021	Mya truncata	20	2
2	13.3-14.2	NS022	Astarte borealis	125	2
2	13.3-14.2	NS024	Astarte borealis	20	2
2	13.3-14.2	NS026	Astarte borealis	77	2
2	13.3-14.2	NS027	Astarte borealis	100	2
2	13.3-14.2	NS028	Astarte borealis	50	5
2	15.8	NS029	Portlandia arctica	55	2
2	15.8	NS030	Portlandia arctica	10	2
2	15.8	NS031	Astarte borealis	95	2
2	15.8	NS032	Astarte borealis	78	2
2	18.5	NS033	Astarte borealis	150	10
2	18.5	NS034	Astarte borealis	63	2
2	18.5	NS035	Astarte borealis	65	2
2	18.5	NS036	Astarte borealis	45	2
2	18.5	NS037	Astarte borealis	50	2
2	18.5	NS038	Astarte borealis	56	2
2	18.5	NS039	Astarte borealis	60	2
2	18.5	NS040	Astarte borealis	90	2
2	18.5	NS041	Astarte borealis	50	5
2	18.5	NS042	Astarte borealis	NO AGE	NO AGE

Continued on next page.

Appendix I, continued.

Site #	Station Depth (m)	Clam ID No.	Species	Age (years)	Error (+/-)
2	18.5	NS043	Astarte borealis	45	5
2	21.5-23.0	NS046	Hiatella arctica	19	2
2	21.5-23.0	NS047	Hiatella arctica	22	2
2	21.5-23.0	NS048	Hiatella arctica	5	2
2	21.5-23.0	NS049	Hiatella arctica	40	2
2	21.5-23.0	NS050	Hiatella arctica	50	2
2	21.5-23.0	NS051	Hiatella arctica	12	2
2	21.5-23.0	NS052	Astarte borealis	90	2
2	21.5-23.0	NS053	Astarte borealis	110	2
2	21.5-23.0	NS054	Astarte borealis	54	2
2	21.5-23.0	NS055	Astarte borealis	30	2
2	21.5-23.0	NS056	Astarte borealis	30	2
2	27.3	NS065	Astarte borealis	35	2
2	27.3	NS066	Astarte borealis	60	2
3	19.1	NS067	Hiatella arctica	20	2
4	9.7	NS068	Serripes groenlandicus	8	2
4	12.7	NS069	Serripes groenlandicus	10	2
4	12.7	NS071	Mya truncata	20	2
4	12.7	NS072	Mya truncata	14	2
4	12.7	NS073	Astarte borealis	75	3
4	12.7	NS074	Astarte borealis	40	3
4	12.7	NS075	Astarte borealis	80	5
4	12.7	NS076	Astarte borealis	60	2
4	16.7	NS077	Nuculana pernula	25	2
4	16.7	NS078	Astarte borealis	40	3
4	16.7	NS079	Astarte borealis	35	5
4	16.7	NS080	Astarte borealis	40	5
4	16.7	NS081	Nucula belloti	26	5
4	20.0	NS087	Astarte borealis	80	5
5	6.7	NS093	Serripes groenlandicus	3	2
5	6.7	NS094	Mya truncata	14	2
5	6.7	NS095	Astarte borealis	32	2
5	6.7	NS096	Nucula belloti	35	2
5	18.8-19.7	NS102	Macoma calcarea	23	2
5	18.8-19.7	NS103	Macoma calcarea	20	2
5	18.8-19.7	NS104	Macoma calcarea	3	1
5	18.8-19.7	NS105	Nucula belloti	60	5
5	18.8-19.7	NS106	Nuculana pernula	13	BROKEN SHELL

Continued on next page.

Appendix I, continued.

Site #	Station Depth (m)	Clam ID No.	Species	Age (years)	Error (+/-)
5	18.8-19.7	NS107	Astarte borealis	96	5
5	18.8-19.7	NS108	Astarte borealis	80	5
5	18.8-19.7	NS109	Astarte borealis	122	5
5	18.8-19.7	NS110	Astarte borealis	75	5
5	18.8-19.7	NS111	Astarte borealis	150	5
5	18.8-19.7	NS112	Astarte borealis	60	2
5	18.8-19.7	NS113	Astarte borealis	75	2
5	18.8-19.7	NS114	Astarte borealis	65	5
5	18.8-19.7	NS115	Astarte borealis	75	5
5	18.8-19.7	NS116	Astarte borealis	120	5
5	18.8-19.7	NS117	Astarte borealis	96	2
5	18.8-19.7	NS118	Astarte borealis	110	5
5	18.8-19.7	NS119	Astarte borealis	30	5
5	18.8-19.7	NS120	Astarte borealis	40	2
5	18.8-19.7	NS121	Astarte borealis	71	2
5	18.8-19.7	NS122	Astarte borealis	62	2
5	18.8-19.7	NS123	Astarte borealis	52	5
5	18.8-19.7	NS124	Astarte borealis	75	2
5	18.8-19.7	NS125	Astarte borealis	75	5
5	18.8-19.7	NS126	Astarte borealis	80	5
5	18.8-19.7	NS127	Astarte borealis	75	2
5	18.8-19.7	NS128	Astarte borealis	44	5
5	18.8-19.7	NS129	Astarte borealis	56	5
5	18.8-19.7	NS130	Astarte borealis	48	2
5	18.8-19.7	NS131	Astarte borealis	53	2
5	18.8-19.7	NS132	Astarte borealis	32	2
5	18.8-19.7	NS133	Astarte borealis	28	5
5	18.8-19.7	NS134	Astarte borealis	96	5
5	18.8-19.7	NS135	Astarte borealis	60	2
5	18.8-19.7	NS136	Astarte borealis	30	2
5	18.8-19.7	NS137	Astarte borealis	60	2
5	18.8-19.7	NS138	Astarte borealis	60	2
5	18.8-19.7	NS139	Astarte borealis	85	2
5	18.8-19.7	NS140	Astarte borealis	56	5
5	18.8-19.7	NS141	Astarte borealis	60	2
5	18.8-19.7	NS142	Astarte borealis	80	5
5	18.8-19.7	NS143	Astarte borealis	47	2
5	18.8-19.7	NS144	Astarte borealis	82	5
5	18.8-19.7	NS145	Astarte borealis	100	5

Continued on next page.

Appendix I, continued.

Site #	Station Depth (m)	Clam ID No.	Species	Age (years)	Error (+/-)
5	18.8-19.7	NS146	Astarte borealis	150	5
5	22.0	NS156	Nuculana pernula	30	2
5	22.0	NS157	Macoma calcarea	10	2
5	22.0	NS158	Macoma calcarea	4	1
5	22.0	NS159	Macoma calcarea	20	3
5	22.0	NS160	Astarte borealis	85	5
5	22.0	NS161	Astarte borealis	78	5
5	22.0	NS162	Astarte borealis	66	2
5	22.0	NS163	Astarte borealis	60	2
5	22.0	NS164	Astarte borealis	97	2
5	22.0	NS165	Astarte borealis	70	5
5	22.0	NS166	Astarte borealis	55	2
5	22.0	NS167	Astarte borealis	75	2
5	22.0	NS168	Astarte borealis	66	2
5	22.0	NS169	Astarte borealis	NO AGE	NO AGE
5	22.0	NS170	Astarte borealis	45	2
5	22.0	NS171	Astarte borealis	60	2
5	22.0	NS172	Astarte borealis	75	5
5	22.0	NS173	Astarte borealis	96	2
5	22.0	NS174	Astarte borealis	82	2
5	22.0	NS175	Astarte borealis	80	2
5	22.0	NS176	Astarte borealis	56	2
5	22.0	NS177	Astarte borealis	55	2
5	22.0	NS178	Astarte borealis	98	2
5	22.0	NS179	Astarte borealis	46	5
5	22.0	NS180	Astarte borealis	86	5
5	22.0	NS181	Astarte borealis	82	5
5	22.0	NS182	Astarte borealis	30	5
5	22.0	NS183	Astarte borealis	70	2
5	22.0	NS184	Astarte borealis	38	2
5	22.0	NS185	Astarte borealis	47	5
5	22.0	NS186	Astarte borealis	50	5
5	22.0	NS187	Astarte borealis	90	5
5	22.0	NS188	Astarte borealis	50	2
5	22.0	NS189	Astarte borealis	40	2
5	22.0	NS190	Astarte borealis	43	2
5	22.0	NS191	Astarte borealis	73	5
5	22.0	NS192	Astarte borealis	50	5
5	22.0	NS193	Astarte borealis	80	2

Continued on next page.

Appendix I, continued.

Site #	Station Depth (m)	Clam ID No.	Species	Age (years)	Error (+/-)
5	22.0	NS194	Astarte borealis	45	2
5	22.0	NS195	Astarte borealis	55	5
5	22.0	NS196	Astarte borealis	60	2
5	22.0	NS197	Astarte borealis	75	2
5	22.0	NS198	Astarte borealis	46	5

Appendix II: Summary of live-collected Arctic bivalve sizes and weights. Data are organized by clam ID number. The species corresponding to the ID number and the stations and depths of their collection are listed in Appendix I. Wet weight is the weight of the body and shell, body WWT is the wet weight of the body only after removal from the shell, shell WWT is the wet weight of the shell only after removal of the body, and shell DWT is the weight of the shell only after drying when this number is available. Site locations are illustrated in Figure 2.

Clam ID No.	Length(mm)	Width(mm)	Wet Weight (g)	Body WWT (g)	Shell WWT (g)	Shell DWT (g)
NS002	59.01	50.31	41.27	-9.04	13.36	
NS003	23.22	19.74	2.12	-17.62	0.65	
NS004	11.53	9.98	0.29	0.14	0.11	0.10
NS005	19.73	11.56	1.14	0.65	0.43	0.40
NS006	18.69	10.47	0.86	0.37	0.36	0.33
NS007	16.23	9.44	0.55	0.28	0.21	0.19
NS008	17.34	10.65	0.66	0.37	0.27	0.26
NS009	16.97	9.99	0.56	0.29	0.22	0.20
NS010	17.20	9.77	0.63	0.38	0.21	0.19
NS011	17.30	10.11	0.56	0.29	0.20	0.19
NS012	16.80	9.81	0.51	0.27	0.19	0.17
NS013	15.08	9.40	0.50	0.24	0.20	0.18
NS014	16.35	9.83	0.58	0.24	0.21	0.19
NS015	15.90	9.44	0.48	0.23	0.15	0.14
NS017	31.91	16.36	4.75	2.80	1.84	1.71
NS018	29.47	14.40	3.40	2.12	1.23	1.06
NS020	24.91	13.46	2.42	1.43	0.94	0.85
NS021	23.12	16.58	2.32	1.61	0.63	0.58
NS022	35.85	28.91	10.64	3.65	6.83	6.53
NS024	19.16	14.99	1.34	0.52	0.78	0.75
NS026	15.44	12.31	0.78	0.31	0.45	0.42
NS027	14.06	11.04	0.57	0.23	0.33	0.32
NS028	8.73	7.12	0.12	0.03	0.08	0.07
NS029	19.97	11.86	1.01	0.53	0.40	0.38
NS030	17.12	10.06	0.63	0.35	0.22	0.21
NS031	26.74	20.42	2.87	0.90	1.89	1.81
NS032	18.81	14.81	1.35	0.49	0.84	0.80
NS033	37.08	29.18	11.64	3.80	7.63	7.28

Continued on next page.

Appendix II, continued.

Clam ID No.	Length(mm)	Width(mm)	Wet Weight (g)	Body WWT (g)	Shell WWT (g)	Shell DWT (g)
NS034	19.06	15.49	1.38	-14.11	0.90	0.85
NS035	17.49	14.42	1.48	-12.94	0.93	0.87
NS036	16.85	14.24	1.01	-13.23	0.61	0.59
NS037	17.20	13.85	1.37	-12.48	0.87	0.84
NS038	17.55	13.65	0.72	-12.93	0.47	0.45
NS039	17.12	13.24	1.11	-12.13	0.66	0.64
NS040	14.79	11.97	0.83	-11.14	0.52	0.50
NS041	14.98	12.28	0.77	-11.51	0.45	0.44
NS042	13.55	11.06	0.54	-10.52	0.32	0.31
NS043	12.50	10.01	0.49	-9.52	0.33	0.31
NS046	36.94	19.67	9.32	-10.35	5.85	5.61
NS047	38.07	20.26	6.91	-13.35	3.93	3.77
NS048	41.48	20.43	10.28	-10.15	5.52	5.27
NS049	38.66	18.33	8.19	-10.14	4.57	4.30
NS050	37.66	20.64	8.41	-12.23	5.04	4.78
NS051	32.95	15.90	5.05	-10.85	2.13	1.95
NS052	35.47	27.13	6.19	-20.94	4.33	4.14
NS053	34.69	27.74	8.35	-19.39	5.86	5.66
NS054	26.78	20.88	2.82	-18.06	1.99	1.90
NS055	25.41	18.96	2.43	-16.53	1.61	1.54
NS056	17.94	13.56	1.14	-12.42	0.69	0.67
NS065	24.72	17.90	1.81	0.54	1.16	1.11
NS066	17.45	14.22	1.21	0.34	0.72	0.69
NS067	37.69	19.52	7.62	3.64	3.83	3.59
NS068	18.69	15.01	1.13	-13.88	0.33	
NS069	53.28	42.46	25.00	16.48	8.09	
NS071	26.13	18.89	4.22	-14.67	1.24	1.16
NS072	28.84	22.91	7.26	-15.65	2.48	2.31
NS073	38.20	30.74	12.86	-17.88	8.79	8.51
NS074	19.11	16.13	2.30	-13.83	1.41	1.36
NS075	17.14	13.91	1.19	-12.72	0.68	0.65
NS076	12.98	10.36	0.52	-9.84	0.32	0.30
NS077	12.29	6.79	0.16	-6.63	0.07	0.07

Continued on next page.

Appendix II, continued.

Clam ID No.	Length(mm)	Width(mm)	Wet Weight (g)	Body WWT (g)	Shell WWT (g)	Shell DWT (g)
NS078	26.46	21.54	2.83	-18.71	1.70	1.63
NS079	19.07	14.90	1.31	-13.59	0.81	0.78
NS080	12.17	9.01	0.37	-8.64	0.23	0.22
NS081	7.76	6.54	0.09	-6.45	0.03	0.03
NS087	19.17	15.36	1.96	0.56	1.19	
NS093	20.97	17.62	1.81	1.34	0.44	
NS094	52.59	39.12	33.93	-5.19	12.75	12.22
NS095	32.31	25.94	7.08	-18.86	4.99	
NS096	10.42	8.82	0.28	-8.54	0.09	0.09
NS102	30.04	20.23	3.32	-16.91	1.34	1.26
NS103	24.28	18.25	2.13	-16.12	0.09	0.85
NS104	16.31	10.88	0.51	-10.37	0.21	0.20
NS105	9.46	7.79	0.24	0.08	0.10	0.09
NS106	10.70	5.96	0.13	0.04	0.06	0.05
NS107	32.54	25.29			4.60	
NS108	29.57	25.75	7.04	2.12	4.88	
NS109	29.82	22.89	7.12	2.36	4.66	
NS110	29.22	22.64	4.87	1.78	2.95	
NS111	32.06	25.81	7.92	2.63	5.16	
NS112	25.04	19.52	3.23	1.08	2.05	
NS113	22.59	17.40	2.19	0.76	1.30	
NS114	18.54	14.02	1.01	-13.01	0.63	
NS115	18.61	15.50	1.31	-14.19	0.81	
NS116	22.04	17.71	1.85	-15.86	1.20	
NS117	19.05	15.01	1.08	-13.93	0.67	
NS118	15.25	11.74	0.97	-10.77	0.59	
NS119	16.88	14.48	1.50	-12.98	0.93	
NS120	16.85	12.85	1.09	-11.76	0.64	
NS121	16.93	13.59	0.81	-12.78	0.48	
NS122	16.19	12.62	0.93	-11.69	0.54	
NS123	14.10	12.04	0.85	-11.19	0.53	
NS124	15.86	12.71	1.08	-11.63	0.64	
NS125	14.73	12.29	0.83	-11.46	0.48	

Continued on next page.

Appendix II, continued.

Clam ID No.	Length(mm)	Width(mm)	Wet Weight (g)	Body WWT (g)	Shell WWT (g)	Shell DWT (g)
NS126	15.21	11.70	0.71	-10.99	0.41	
NS127	13.50	10.90			0.32	
NS128	15.14	12.15	0.78	-11.37	0.47	
NS129	14.65	11.73	0.80	-10.93	0.48	
NS130	14.33	11.62	0.75	-10.87	0.44	
NS131	13.93	10.67	0.68	-9.99	0.39	
NS132	13.99	11.99	0.82	-11.17	0.49	
NS133	15.45	12.01	0.95	-11.06	0.58	
NS134	14.87	11.60	0.80	-10.80	0.48	
NS135	13.65	11.50	0.62	-10.88	0.35	
NS136	13.78	10.93	0.57	-10.36	0.33	
NS137	11.49	9.11	0.38	-8.73	0.22	
NS138	13.15	10.70	0.55	-10.15	0.31	
NS139	13.77	10.96	0.60	-10.36	0.35	
NS140	10.74	8.64	0.31	-8.33	0.18	
NS141	9.30	8.11	0.17	-7.94	0.10	
NS142	12.04	9.04	0.39	-8.65	0.23	
NS143	13.42	11.04	0.69	-10.35	0.42	
NS144	12.66	10.20	0.42	-9.78	0.25	
NS145	12.65	9.97	0.46	-9.51	0.27	
NS146	18.68	14.81	1.05	-13.76	0.65	
NS156	11.78	6.57	0.22	-6.35	0.11	0.10
NS157	15.17	10.81	0.45	-10.36	0.16	0.16
NS158	15.48	10.97	0.40	-10.57	0.15	0.15
NS159	12.24	8.61	0.22	-8.39	0.08	0.08
NS160	33.56	25.64	8.17	-17.47	5.23	
NS161	30.27	24.48	6.65	-17.83	4.45	
NS162	28.44	23.61	4.57	-19.04	2.89	
NS163	27.79	21.31	3.99	-17.32	2.66	
NS164	22.99	18.89	2.48	-16.41	1.57	
NS165	22.55	17.84	1.69	-16.15	0.99	
NS166	21.03	17.17	1.63	-15.54	1.02	
NS167	19.67	15.09	1.15	-13.94	0.66	

Continued on next page.

Appendix II, continued.

Clam ID No.	Length(mm)	Width(mm)	Wet Weight (g)	Body WWT (g)	Shell WWT (g)	Shell DWT (g)
NS168	16.51	13.88	1.33	-12.55	0.74	
NS169	16.57	13.87	1.44	-12.43	0.88	
NS170	17.31	14.08	1.28	-12.8	0.73	
NS171	16.51	13.61	1.24	-12.37	0.68	
NS172	16.86	13.06	0.86	-12.20	0.51	
NS173	15.60	12.51	1.16	-11.35	0.70	
NS174	14.60	12.21	1.01	-11.20	0.62	
NS175	14.97	12.56	1.15	-11.41	0.73	
NS176	15.44	12.81	1.05	-11.76	0.60	
NS177	15.86	13.02	0.99	-12.03	0.56	
NS178	14.45	11.24	0.86	-10.38	0.51	
NS179	16.66	12.98			0.55	
NS180	14.16	11.32	0.51	-10.81	0.31	
NS181	15.88	12.34	1.08	-11.26	0.65	
NS182	14.25	11.09	0.64	-10.45	0.38	
NS183	14.68	11.61	0.85	-10.76	0.48	
NS184	14.53	11.89	0.86	-11.03	0.52	
NS185	13.41	11.28	0.69	-10.59	0.42	
NS186	12.89	10.24	0.54	-9.70	0.32	
NS187	12.97	10.67	0.58	-10.09	0.34	
NS188	12.45	10.57	0.53	-10.04	0.32	
NS189	11.92	9.68	0.49	-9.19	0.29	
NS190	13.52	10.76	0.67	-10.09	0.43	
NS191	10.99	8.97	0.35	-8.62	0.23	
NS192	13.29	10.71	0.61	-10.10	0.35	
NS193	11.04	9.29	0.39	-8.90	0.23	
NS194	12.48	10.92	0.66	-10.26	0.41	
NS195	11.54	9.09	0.34	-8.75	0.20	
NS196	10.61	8.23	0.22	-8.01	0.12	
NS197	10.31	8.35	0.25	-8.10	0.15	
NS198	6.59	5.43	0.08	-5.35	0.05	

Appendix III: Measured $\delta^{18}O$ and $\delta^{13}O$ isotopic composition in the youngest sections of shells collected from all stations in Nares Strait. Clam ID No. refers to the stations, depths of collection, and ages identified in Appendices I and II. Gray highlighted rows indicate specimens whose measured $\delta^{18}O$ isotopic compositions are significantly lighter than expected for the measured salinity and temperature range.

Sample Number	Clam ID No. (NS-….)	Species	Species Abreviation	^{13}C PDB (measured)	^{18}O PDB (measured)
1	95	Astarte borealis	AB	0.94	1.87
2	182	Astarte borealis	AB	-0.04	1.8
3	192	Astarte borealis	AB	0.33	2.29
4	193	Astarte borealis	AB	0.14	2.42
5	187	Astarte borealis	AB	0.09	1.89
6	136	Astarte borealis	AB	-0.88	2.14
7	146	Astarte borealis	AB	-0.07	2.12
8	126	Astarte borealis	AB	-0.14	2.24
9	142	Astarte borealis	AB	-0.91	1.78
10	157	Macoma calcarea	MC	0.33	2.14
11	102	Macoma calcarea	MC	0.29	0.95
12	94	Mya truncata	MT	2.93	2.03
13	105	Nucula belloti	NB	3.04	3.22
14	106	Nuculana pernula	NP	0.55	2.17
15	31	Astarte borealis	AB	-0.32	1.76
16	43	Astarte borealis	AB	-0.95	-0.02
17	35	Astarte borealis	AB	-1.24	1.23
18	33	Astarte borealis	AB	-0.68	-1.94
19	65	Astarte borealis	AB	-0.37	-0.23
20	66	Astarte borealis	AB	-0.27	0.62
21	22	Astarte borealis	AB	1.02	2.09
22	24	Astarte borealis	AB	0.26	-4.87
23	52	Astarte borealis	AB	-0.6	0.97
24	54	Astarte borealis	AB	0.81	1.08
25	17	Hiatella arctica	HA	-0.2	0.1
26	18	Hiatella arctica	HA	0.86	1.4
27	46	Hiatella arctica	HA	-0.27	0.32
28	47	Hiatella arctica	HA	-0.7	-1.28
29	48	Hiatella arctica	HA	0.31	-0.23
30	4	Nucula belloti	NB	-0.43	-1.74
31	29	Portlandia arctica	PA	-0.02	-1.05
32	5	Portlandia arctica	PA	0.01	2.42
33	67	Hiatella arctica	HA	1.85	1.91
34	73	Astarte borealis	AB	1.15	1.93

Continued on next page.

Appendix III, continued.

Sample Number	Clam ID No. (NS-….)	Species	Species Abreviation	^{13}C PDB (measured)	^{18}O PDB (measured)
35	74	Astarte borealis	AB	-1.79	1.59
36	75	Astarte borealis	AB	0.33	1.96
37	78	Astarte borealis	AB	-2.21	1.62
38	87	Astarte borealis	AB	-1.06	-0.1
39	71	Mya truncata	MT	2.09	1.98
40	81	Nucula belloti	NB	1.43	1.63
41	77	Nuculana pernula	NP	0.52	1.53
42	68	Serripes groenlandicus	SG	1.15	0.37

NOTE: Thick solid lines indicate the end of a sample set corresponding to a particular site of bivalve collection. The solid line after sample number 14 denotes the end of samples from Alexandra Fjord (Station 5), sample number 32 Bellot Island (Station 2), sample number 33 Offley Island (Station 3), and sample number 42 Scoresby Bay (Station 4).

Appendix IV: Measured $\delta^{18}O$ and $\delta^{13}C$ isotopic composition in whole shells of *Hiatella arctica* and *Astarte borealis* from Bellot Island (Station 2), Scoresby Bay (Station 4), and Alexandra Fjord (Station 5).

Site #	Clam ID No. (NS…)	Species	Age (yrs)	Depth (m)	Increment Sampled (yrs)	^{13}C PDB	^{18}O PDB
2	17	HA	9	13.4-14.3	1	-0.20	0.10
					2	0.47	0.00
					3	0.34	0.19
					4	0.48	1.21
					5	-0.11	-0.31
					6	0.43	1.73
					7	-0.01	1.46
					8-9	1.28	1.75
2	18	HA	9	13.4-14.3	1	0.86	1.40
					2	0.85	0.88
					3	1.02	1.88
					4	1.25	1.28
					5	1.15	1.44
					6	1.72	2.54
					7	1.06	1.72
					8	0.82	2.20
					9	0.87	0.07
2	46	HA	19	21.6-23.2	1	-0.27	0.32
					2	-0.45	0.78
					3	-0.02	-0.11
					4	-0.14	1.43
					5	-0.20	0.71
					6	0.53	1.36
					7	1.00	0.83
					8	0.30	-0.86
					9	0.34	0.10
					10	0.30	0.84
					11	0.78	0.52
					12	0.41	0.08
					13	0.38	1.10
					14	0.41	1.19

Continued on next page.

Appendix IV, continued.

Site #	Clam ID No. (NS…)	Species	Age (yrs)	Depth (m)	Increment Sampled (yrs)	^{13}C PDB	^{18}O PDB
2	46	HA	19	21.6-23.2	15	0.27	1.31
					16	0.37	1.07
					17	0.21	1.11
					18	-0.41	-0.18
					19	-1.95	-1.02
					15	0.27	1.31
					16	0.37	1.07
					17	0.21	1.11
2	47	HA	22	21.6-23.2	1	-0.70	-1.28
					2	-0.65	-0.35
					3	-0.66	-1.71
					4	-0.74	-0.30
					5	-0.51	-0.85
					6	-0.64	-0.26
					7	-0.63	-1.62
					8	-0.75	-0.68
					9	-0.40	-0.33
					10	-0.64	-0.73
					11-12	-0.16	-0.09
					13	-0.25	1.30
					14	-0.08	1.34
					15	0.14	-0.17
					16	0.43	0.04
					17-18	1.42	1.71
					19	1.30	1.69
					20-22	-0.46	1.84
2	48	HA	5	21.6-23.2	1	0.31	-0.23
					2-3	0.37	0.99
					4-5	0.34	1.04
2	22	AB	125	13.4-14.3	1-6	1.02	2.09
					6-9	1.18	1.93
					10-12	1.44	2.09
					13-15	1.87	2.30

Continued on next page.

Appendix IV, continued.

Site #	Clam ID No. (NS…)	Species	Age (yrs)	Depth (m)	Increment Sampled (yrs)	^{13}C PDB	^{18}O PDB
2	22	AB	125	13.4-14.3	16-19	1.93	2.33
					20-25	1.77	2.22
					26-28	2.07	2.40
					29-33	2.01	2.22
					34-40	2.12	2.03
					41-45	1.90	2.19
					46-51	2.01	2.35
					52-62	1.96	2.30
					63-65	1.87	2.30
					66-70	1.51	2.05
					71-90	1.17	1.13
					91-100	0.97	1.27
					101-105	0.60	1.55
					106-110	0.93	2.05
					111-115	0.64	1.64
					116-120	0.93	2.18
					121-125	0.15	1.44
2	24	AB	20	13.4-14.3	1	0.26	-4.87
					2	0.57	-1.85
					3	0.55	-0.77
					4-5	0.90	0.22
					6-7	1.10	1.21
					8	0.83	1.14
					9	0.60	-0.48
					10	1.06	2.12
					11	0.17	-0.50
					12	1.05	0.95
					13	0.94	1.83
					14	0.80	1.52
					15	1.17	1.93
					16-18	1.17	1.72
					19-20	0.53	1.10
2	33	AB	150	18.6	1-5	-0.68	-1.94

Continued on next page.

Appendix IV, continued.

Site #	Clam ID No. (NS…)	Species	Age (yrs)	Depth (m)	Increment Sampled (yrs)	^{13}C PDB	^{18}O PDB
2	33	AB	150	18.6	6-17	0.69	-0.98
					18-29	0.63	-0.91
					30-41	0.61	0.26
					42-51	1.15	1.06
					52-56	1.30	1.06
					57-66	1.55	1.35
					67-76	1.58	1.49
					77-86	1.36	1.61
					87-96	1.20	1.41
					97-116	1.24	1.74
					117-126	0.85	1.36
					127-131	0.55	0.94
					132-150	0.23	0.77
2	35	AB	60	18.6	1	-1.24	1.23
					2	0.51	1.65
					3	-1.02	1.58
					4-6	0.89	1.51
					7-9	1.06	1.93
					10-12	1.17	2.11
					13-15	1.21	2.15
					16-20	1.45	2.15
					21-25	1.12	2.17
					26-30	0.90	1.77
					31-36	1.01	2.07
					37-39	0.88	1.64
					40-45	0.98	1.76
					36-51	0.82	1.87
					52-58	0.78	2.06
					59-60	-0.45	1.54
4	73	AB	75	12.8	1	1.15	1.93
					2	2.07	1.97
					3	1.48	2.07
					4	1.76	2.38

Continued on next page.

Appendix IV, continued.

Site #	Clam ID No. (NS…)	Species	Age (yrs)	Depth (m)	Increment Sampled (yrs)	^{13}C PDB	^{18}O PDB
4	73	AB	75	12.8	5	1.25	2.04
					6-8	1.87	2.22
					9-11	2.20	1.79
					12-14	2.12	1.83
					15-19	1.93	2.00
					20-25	1.80	2.06
					26-31	1.56	1.44
					32-35	1.71	1.61
					36-41	1.62	2.13
					42-45	1.10	1.55
					46-50	1.16	1.91
					51-56	0.96	2.13
					57-61	1.01	2.13
					62-66	0.79	2.18
					67-71	0.80	1.87
					72-80	0.07	1.73
4	74	AB	40	12.8	1	-1.79	1.59
					2	0.80	2.30
					3	0.67	1.48
					4	0.27	1.88
					5-6	1.17	1.72
					7-8	1.14	1.74
					9-10	1.48	2.01
					11-15	0.97	2.09
					16-20	0.92	2.35
					21-30	0.22	2.05
					31-40	-1.50	1.81
4	75	AB	80	12.8	1-12	0.33	1.96
					13-17	1.18	1.89
					18-21	1.47	2.05
					22-25	1.28	2.36
					26-29	0.91	2.32
					30-35	0.84	2.13

Continued on next page.

Appendix IV, continued.

Site #	Clam ID No. (NS…)	Species	Age (yrs)	Depth (m)	Increment Sampled (yrs)	^{13}C PDB	^{18}O PDB
4	75	AB	80	12.8	36-40	1.04	1.92
					41-51	1.09	2.40
					52-61	1.29	1.51
					62-70	1.34	1.57
					71-75	0.94	1.79
					76-80	0.71	2.30
5	126	AB	80	18.9-19.8	1-10	-0.14	2.24
					11-20	0.66	2.58
					21-30	1.40	2.41
					31-40	1.50	2.62
					41-50	1.49	2.26
					51-60	1.37	1.98
					61-70	1.36	1.84
					71-74	1.10	2.16
					75-80	0.87	2.41
5	187	AB	90	22.1	1-12	0.09	1.89
					13-32	0.27	2.19
					33-52	0.44	2.15
					53-67	0.48	2.13
					68-86	0.13	2.00
					87-90	-1.40	1.54
5	142	AB	80	18.9-19.8	1-10	-0.91	1.78
					11-20	0.11	2.28
					21-44	0.71	2.12
					45-55	0.77	2.90
					56-65	0.51	1.83
					66-75	0.20	1.81
					76-80	-0.16	1.61
5	87	AB	80	20.1	1	-1.06	-0.10
					2-6	-0.20	1.10
					7-11	1.07	1.46
					12-16	1.10	1.53
					17-26	1.07	1.75

Continued on next page.

Appendix IV, continued.

Site #	Clam ID No. (NS…)	Species	Age (yrs)	Depth (m)	Increment Sampled (yrs)	^{13}C PDB	^{18}O PDB
5	87	AB	80	20.1	27-36	0.73	1.47
					37-46	0.32	1.02
					47-56	0.50	1.08
					57-76	-0.21	1.23
					77-80	-0.89	1.12